

LITHOSTRATIGRAPHIC UNITS AND TECTONICS OF THE SOUTHWESTERN PART OF DADAY-DEVREKANI MASSIVE, WESTERN PONTIDES, TURKEY

Durmuş BOZTUĞ*

ABSTRACT. - Metamorphic, magmatic and sedimentary rocks, outcropping in the southwestern part of Daday-Devrekani massive, were differentiated in to 12 lithostratigraphic units. The Precambrian Dorukyayla gneiss, comprising high-grade metasediments and dykes of asidic and intermediate composition, constitutes the basement. The Samatlar group, consisting of very low-grade metasediments Lower to Middle Paleozoic in age, unconformably overlies the Precambrian Dorukyayla gneiss. The Samatlar group, with a total thickness of approximately 4000 m , consists, from bottom to top, of the Yayladere (Cambrian), Dotla (Ordovician), Zirze (Silurian) and Kureihadit (Devonian) formations. The Permo-Triassic (?) Kirtulaz formation represents a broken formation structure which is composed of strongly faulted-crushed rocks. The Middle Jurassic Kürek granitoid, a plutonic body from the Kastamonu granitoid belt, is made up of granite, granodiorite, quartz monzonite and dykes of quartzolite, aplite and microdiorite. These units are overlain unconformably by the Yukarıköy and Çatak formations of Yaralıgöz group respectively represented by limestones and flyschoidal sediments with respective ages of Upper Jurassic-Lower Cretaceous and Lower Cretaceous. The Soğanlı formation of Middle Eocene age and the conglomerate-sandstone-siltstone-claystone alternation of the Cemalettin formation, Upper Eocene-Lower Oligocene in age, are unconformable, like the Yaralıgöz group, on the other units. Karabuzey formation of Neogene age, consisting of semi-consolidated and consolidated clastic rocks, is the youngest unit of the consolidated section. The youngest unit in the mapped area is the Quaternary alluvium especially observed in the valleys. As for the structural elements, the foliation planes in the Precambrian Dorukyayla gneiss are interpreted to have been formed in a pre-Alpine period. All other structural elements such as folds, thrust and strike-slip faults are considered to have been formed synchronously with N-S compression after Lower Cretaceous. The main unconformities, also reflecting significant variances of ductile deformation, are observed between the Dorukyayla gneiss and Samatlar group and, between the Samatlar group and Yaralıgöz group.

INTRODUCTION

The studied area takes place in the northern part of Samatlar (İğdir) village, some 20 km. west of Araç town of Kastamonu province in the northern Anatolia (Fig. 1). This paper deals mainly with the lithostratigraphic

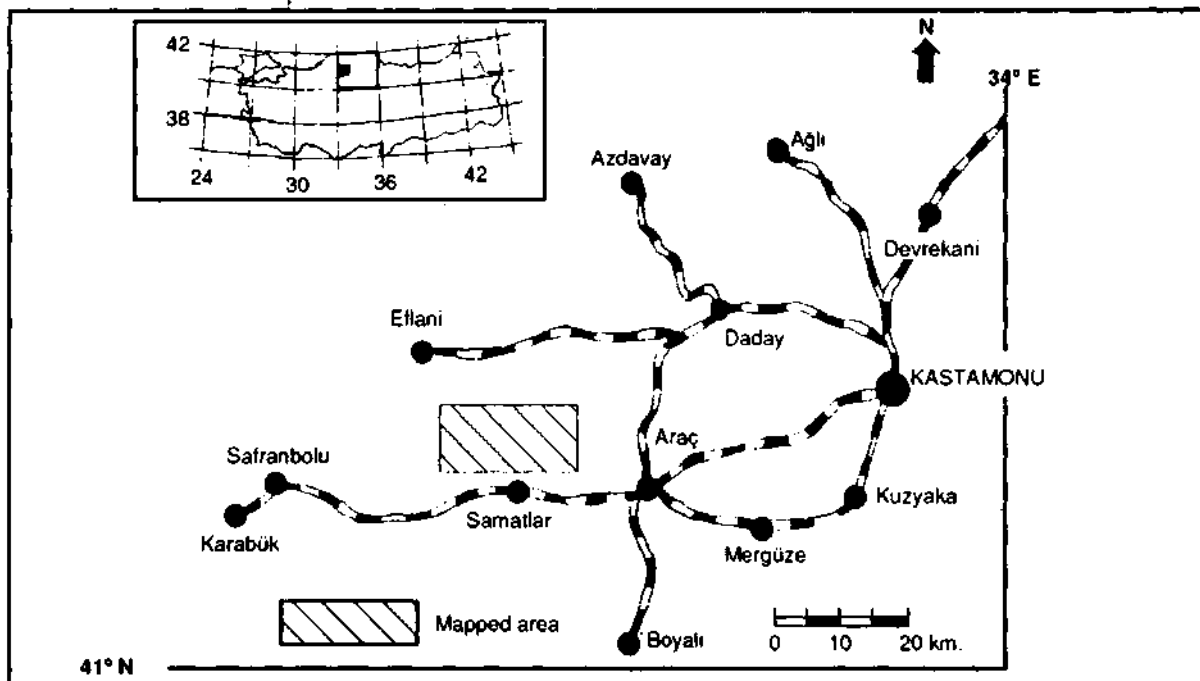


Fig. 1- Location map of studied area.

determination and general structural features of the rock units which have already been studied for the mineralogical-petrographical and geochemical investigation (Boztuğ, 1988). The previous works, in the mapped area, are those of Arpat et al. (1978), Aydın et al., (1986, 1987). On the other hand, some other studies, have been carried out related to basement geology, mineralogy-petrography, geochemistry and geodynamic modelling, by Blumenthal (1948), Yılmaz (1979, 1980, 1981, 1983), Boztuğ (1983), Boztuğ and Yılmaz (1983), Boztuğ et al. (1984), Yılmaz and Boztuğ (1985, 1986, 1987), Yılmaz and Tüysüz (1984), Tüysüz (1985, 1986), Yılmaz and Tüysüz (1988) and Şengün et al. (1990) in the surrounding areas.

Table 1 represents the chronostratigraphic-lithostratigraphic comparison of the Mesozoic and older units from the mapped area and surrounding taking place in the outer zone (Adamia et al., 1980) of the Pontide tectonic unit (Ketin, 1966). In the regional geological setting, The Precambrian Daday-Devrekani metasedimentary group, outcropping in the northeastern and southwestern parts of the Daday-Devrekani massiv, comprises high-grade metasediments and constitutes the basement unit in the mapped area. The Paleozoic very low grade metasediments, positionally overlying the Daday-Devrekani metasedimentary group, show an epicontinental character, whereas the Lower Mesozoic rock units show both of the epicontinental and epiophiolitic features depending on the deposition locations. The pre-Lower Jurassic Çangal metaophiolite typically forms the oceanic crust material. The consuming of this oceanic crust, i.e. subduction zone, has concluded to emplace the Çangal metaophiolite, to induce an Early Alpine regional metamorphism (Bonhomme and Yılmaz, 1984, Yılmaz and Bonhomme, 1991) and to create an arc plutonism called Kastamonu granitoid belt (Boztuğ et al., 1984; Yılmaz and Boztuğ, 1986). The Middle-Upper Jurassic to Lower Cretaceous Yaralıgöz group (Yılmaz, 1980) characterizes the sedimentary rocks deposited in the intermountain basins.

LITHOSTRATIGRAPHIC UNITS

The metamorphic, magmatic and sedimentary rock units, ranging from Precambrian to Neogene, have been mapped as 12 lithostratigraphic units in the southwestern part of the Daday-Devrekani massiv (Fig. 2, 3a, 3b). The common characteristics of these units, from bottom to top, can be summarized as follow:

Dorukyayla gneiss (Precambrian)

Description and typical locality. _ Dorukyayla gneiss has been firstly determined by Boztuğ (1988). It crops out better in the Dorukyayla district and its western prolongation; Soğukçam dere, Çatan dere locations and in the Karadere valley (Fig. 3a).

Lithology. - Dorukyayla gneiss, outcropping in the Karadere valley, consists mainly of the alternation of amphibole/pyroxene gneiss and mica gneiss with a prevailing amphibole/pyroxene gneiss lithology. In the Karadere valley, these rocks also include a lot of pegmatitic-aplitic veins. Just to the east of Karadere valley, namely in the Gökgöl dere district, these amphibole/pyroxene gneisses represent well developed gneissosity due to metamorphic differentiation. The gradational enrichment of biotite minerals can be easily noticed towards the eastern part of the Gökgöl dere district particularly through the Yayladere valley in these gneisses, and even it can be possible to identify the two zones such as amphibole/pyroxene gneiss and amphibole-mica gneiss only in one hand specimen. In the area between the Gökgöl dere and Dögemle yayla, the lowermost, middle and uppermost parts of the Dorukyayla gneiss are composed of biotite gneiss, muscovite-biotite gneiss and muscovite gneiss, respectively. Just in the Dögemle yayla district, however, the main rock type of Dorukyayla gneiss is the quartz-feldspar gneiss. Thus, it can be concluded that the Dorukyayla gneiss consists of, from bottom to top, the amphibole/pyroxene gneiss, mica gneiss and quartz-feldspar gneiss with some acidic and intermediate vein rocks of a few meters in thickness.

Lower and upper boundaries. - The lowermost part of the Dorukyayla gneiss is exposed in the Karadere valley, and it is the basement rock unit of the studied area. As for the upper boundary, it is seen to be positionally overlaid by the Paleozoic Samatlar group (Fig. 2, 3a, 3b).

Age. - The Dorukyayla gneiss has been considered to have a Precambrian age because of covering by the anchimetamorphic-epimetamorphic Lower to Middle Paleozoic units.

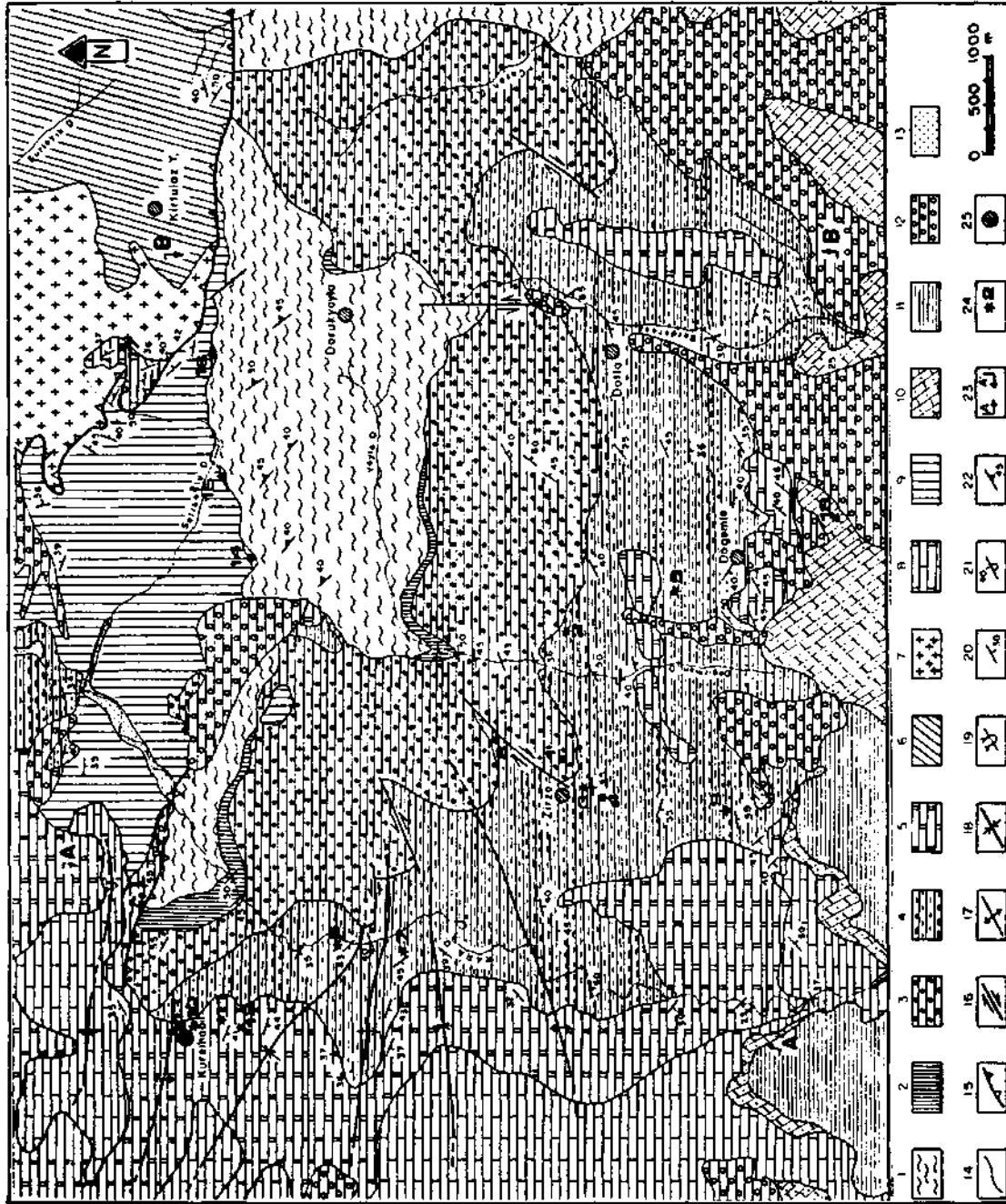


Fig. 3a- Geological map of the SW part of Daday-Devrekani massive.

- 1- Dorukyayla gneiss (Precambrian), 2- YaylADERE formation (Cambrian), 3- DOLTA formation (Ordovician), 4- Zirze formation (Silurian), 5- KÜREHADİT formation (Devonian), 6- Kirtulaz formation (Permo-Triassic?), 7- Kürek granitoid (Middle Jurassic), 8- YUKARIKÖY formation (Upper Jurassic-Lower Cretaceous), 9- ÇATAK formation (Lower Cretaceous), 10- SOĞANLI formation (Middle Eocene), 11- CEMALETTİN formation (Upper Eocene-Lower Oligocene), 12- KARABÜZEY formation (Neogene), 13- Quaternary alluvium, 14- Formation boundary, 15- Thrust, 16- Strike-slip fault, 17- Anticline axis, 18- Syncline axis, 19- Overturned syncline axis, 20- Strike and dip, 21- Overturned bedding, 22- Foliation, 23- Cross section line, 24- Fossil location, 25- Villages.

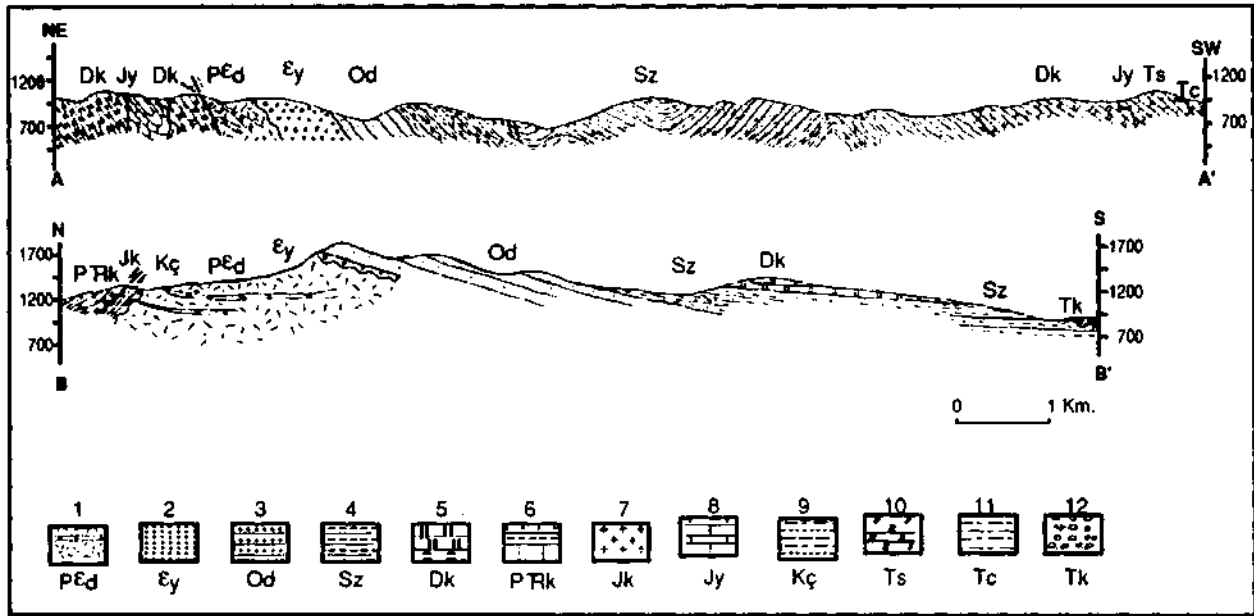


Fig.3b- Geological cross sections (Fig. 3a for the cross section line).

1- Dorukyayla gneiss, 2- Yayladere formation, 3- Dotla formation, 4- Zirze formation, 5- Küreihadit formation, 6- Kirtulaz formation, 7- Kürek granitoid, 8- Yukarıköy formation, 9- Çatak formation, 10- Soğanlı formation, 11- Cemalettin formation, 12- Karabüzey formation.

Regional correlation. - As seen from Table 1, the Dorukyayla gneiss can be evaluated as the equivalent of the Gürleyik gneiss (Yılmaz, 1980) and the Yedigöller formation (Aydın et al., 1986).

SAMATLAR GROUP

The Lower to Middle Paleozoic Samatlar group, firstly described by Boztuğ (1988), is composed of, from bottom to top, the Yayladere (Cambrian), Dotla (Ordovician), Zirze (Silurian), and Kureihadit (Devonian) formations.

Yayladere formation (Cambrian)

Description, type locality and section. - The Yayladere formation, firstly described by Boztuğ (1988) is exposed better in the Karadere valley, Yayladere valley and Geyikoynağı tepe districts of the studied area (Fig. 3a, 3b). Total thickness of the formation, measured within the Yayladere valley, is of some 300 m. (Fig. 4).

Lithology. - The lowermost part of the Yayladere formation, taking unconformably place on top of the amphibole/pyroxene, gneiss and amphibole-biotite gneisses of the Dorukyayla gneiss, is composed of coarse grained metasandstone with a thickness of 30 m. (Fig. 4). The major constituents of these rocks comprise coarse grained (1 to 5 mm. in diameter) sandy materials and they can be misunderstood as the quartz-feldspar gneiss in the first approach. When they have been carefully studied in hand specimen with the aid of handlense, the detrital quartz, feldspars and large flakes of micas can be distinguished in a silky groundmass due to sericite growth. Grain sizes of the constituents of these coarse grained metasandstones, considered as the first depositional products on top of the Dorukyayla gneiss, gradually decreases towards to upper parts of the unit, and then, these coarse grained metasandstones appear as normal metasandstones in grain size. A grayish-greenish quartz argillite and argillite level, with a total thickness of 70 m., takes place on top of these metasandstones (Fig. 4). These greenish argillites are followed by the reddish-purple quartz argillite-argillite level, with a total thickness of 200 m., showing mm.-dm. bedding and including visible mica flakes with unaided eye.

Lower and upper boundaries. - The Yayladere formation unconformably overlies the Precambrian Dorukyayla gneiss, and is conformably covered by the Ordovician Dotla formation (Fig. 2, 3a, 3b, 4).

Age. - There has not been found any fossil in the Yayladere formation in the mapped area, however, Arpat et al. (1978) mentioned something about the existence of Lower Cambrian brachiopods in this formation. The Yayladere formation has been considered to have the Cambrian age, since taking place in the lowermost part of the Samatlar group.

Depositional environment. - The Yayladere formation characterizes the transitional zone between terrestrial and shallow marine environment.

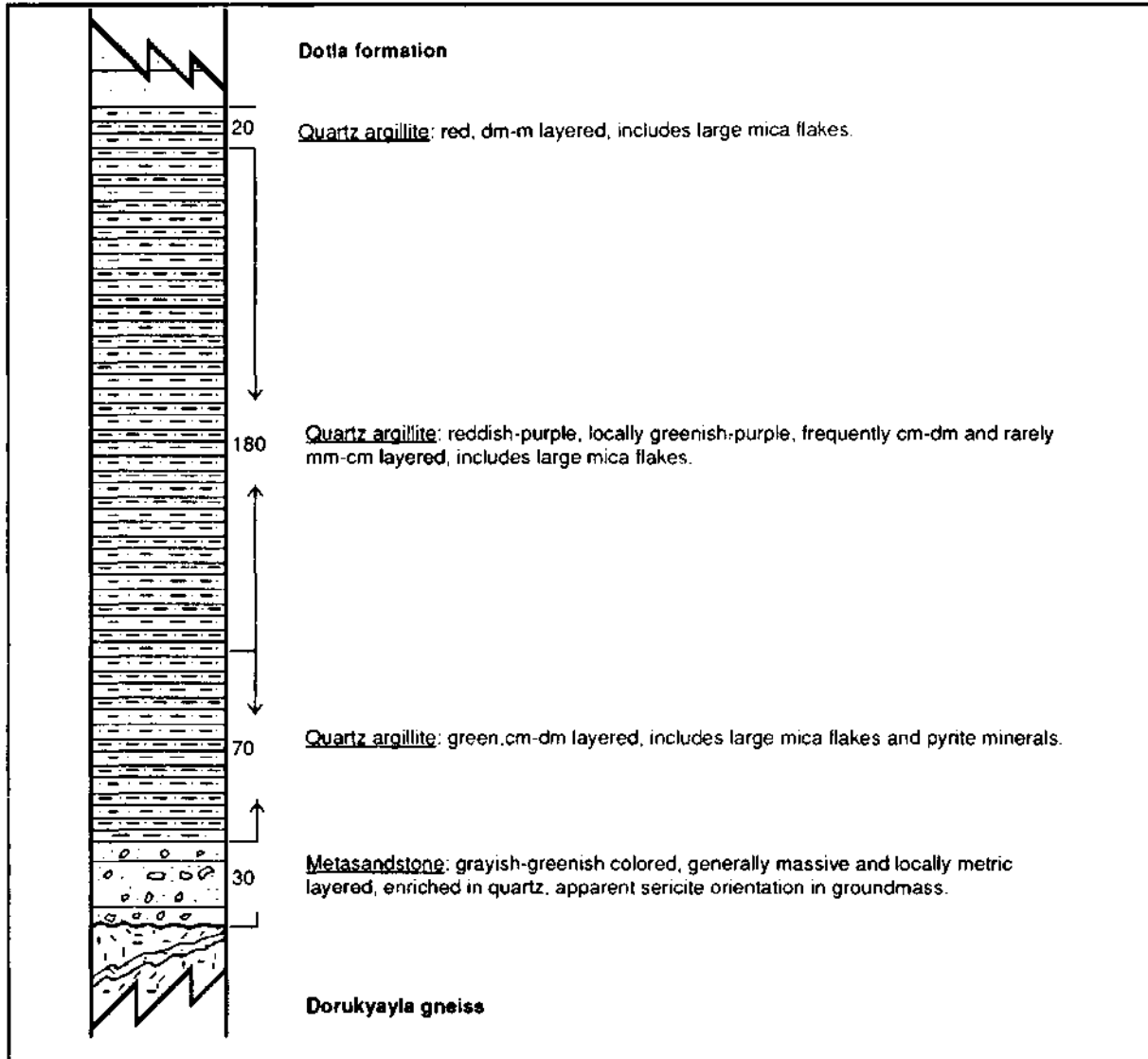


Fig. 4- Type section of the Yayladere formation.

Regional correlation. - The Yayladere formation, considered to have the Cambrian age, is evaluated the equivalent of the Kocatöngel formation (Table 1) described by Aydın et al. (1986).

Dotla formation (Ordovician)

Description, type locality and section. - The Dotla formation firstly described by Boztuğ (1988), is seen to be exposed better around the Dotla village and Yayladere and Karadere valleys. The type section of the Dotla formation has a thickness of 1000 m. in the Yayladere valley (Fig. 5).

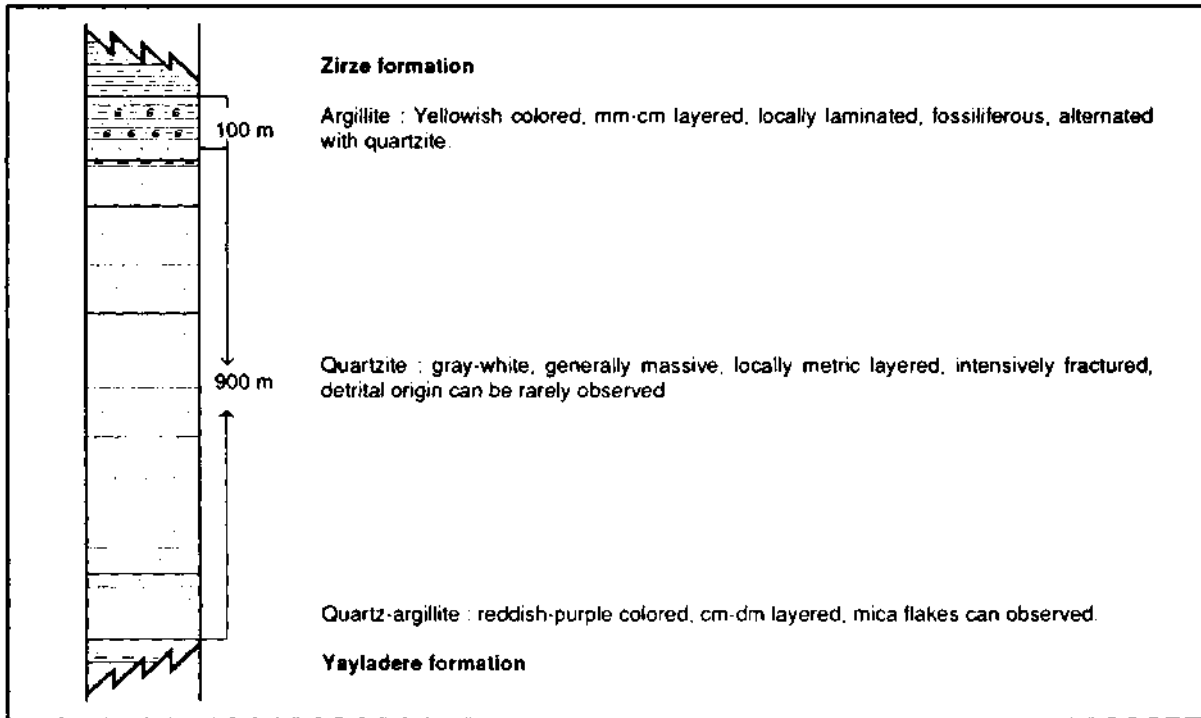


Fig. 5- Type section of the Dotla formation

Lithology. - There is a gray-white colored quartzite level with a thickness of 100 m. total thickness in the lower parts of the formation. This quartzite level shows a well preserved detrital origin in hand specimen. A reddish-purple quartz argillite/argillite band, 20 m. in thickness, takes places on top of this gray-white quartzite. These argillites are followed by another gray-white massive quartzite, with a total thickness of 800 m., representing locally preserved sedimentary bedding of metric thickness (Fig. 4). The uppermost part of the Dotla formation is made up of the alternation of argillite and quartzite with a thickness of 100 m.

Lower and upper boundaries. - The Dotla formation conformably overlies the Yayladere formation and is conformably covered by the Silurian Zirze formation (Fig. 2, 3a, 3b, 5).

Age. - The fossils, found in the ZZ-42A rock sample from the argillite-quartzite alternation in the uppermost part of the Dotla formation, yield the Upper Ordovician-Lower Silurian age, ZZ-42A (Fig. 3a, location number is 1): a brachypoda from-primitive, Orthis group, Trilobite Trinucleid. The age of the Dotla formation has been evaluated as the Ordovician since these fossils have been found in the uppermost part of this formation. Moreover, some other fossils indicating the Lower Ordovician age have been already mentioned by Arpat et al. (1978) in this unit.

Depositional environment. - The Dotla formation seems to be deposited in a beach environment.

Regional correlation. - The Dotla formation is considered to be the equivalent of the Bakacak and Kurtköy formations, and also the equivalent of the lower parts of the Aydos formation (Table 1) described by Aydın et al. (1986).

Zirze formation (Silurian)

Description, type locality and section -Zirze formation has been firstly described by Boztuğ (1988). It is observed to be outcropped better around Zirze village and in the Bahçecik dere to the southeast of the Dotla village. The type section of this formation, measured in the Ketencik dere situated to the southeast of Zirze village, showed that the total thickness of this unit was of approximately 2000 m. (Fig. 6).

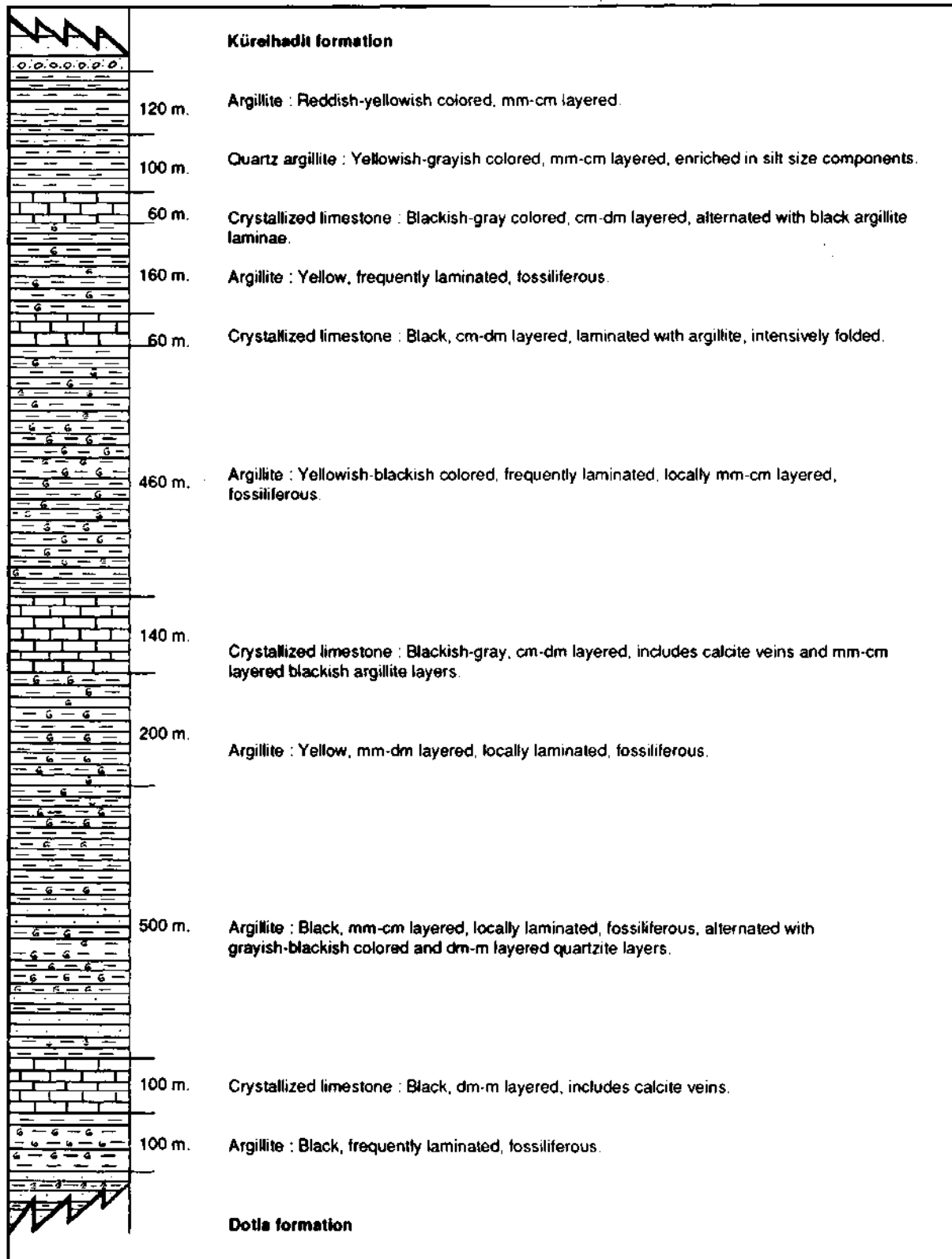


Fig. 6- Type section of the Zirze formation.

Lithology. - The prevailing lithology of the Zirze formation is argillites as seen in Figure 6. However, it locally includes the grayish-white quartzite and blackish-grayish crystallized limestone beds, too. The argillites of Zirze formation represent bedding which is ranging typically from mm. to dm. in thickness. As for the color of these argillites, the blackish, yellowish-brown and yellowish-pinkish colors are dominant in the lower, middle and upper parts of the unit, respectively.

Lower and upper boundaries. - The Zirze formation conformably overlies the Dotla formation and is overlaid by the Küreihadit formation.

Age. - Some fossils have been found in the Zirze formation which yield typically Lower and Upper Silurian ages. The rock samples including the Lower Silurian fossils are as follow:

DG-296A-B (four specimens) (location 2 in Fig. 3a):

Dendograptus sp. (resembling tree branches),

Lingula sp. (an ill-preserved brachiopoda).

ZZ-20 (location 3 in Fig. 3a):

Diplograptus sp.

ZZ-21A, B (two specimens) (location 4 in Fig. 3a):

Didymograptus sp.

Apart from these Lower Silurian fossils, there are some other fossils which may only indicate an age of Silurian rather than the stages of Silurian below:

DG-451 (location 5 in Fig. 3a):

Monograptus sp.

ZZ-67 (location 6 in Fig. 3a):

Monograptus sp.

ZZ-101 (location 7 in Fig. 3a):

Monograptus sp.

On the other hand, the Upper Silurian fossils of the Zirze formation are as follow:

ZZ-180 (location 8 in Fig. 3a):

Monograptus sp.

ZZ-187 (location 9 in Fig. 3a):

Spyrograptus sp.

Depositional environment. - The Zirze formation characterizes a deep marine environment.

Regional correlation. - The Zirze formation can be correlated, as seen in Table 1, with the ferriferous clayey sandstone (Tokay, 1952), the Işığandere formation (Görmüş, 1982), the Fındıklı and upper parts of the Aydos formations (Aydın et al., 1986).

Küreihadit formation (Devonian)

Description, type locality and section. - The Küreihadit formation, firstly described by Boztuğ (1988), outcrops better around Küreihadit village and in the Karadere valley. The type section of Küreihadit formation, measured in the Karadere valley, is of 600 m. in total thickness (Fig. 7).

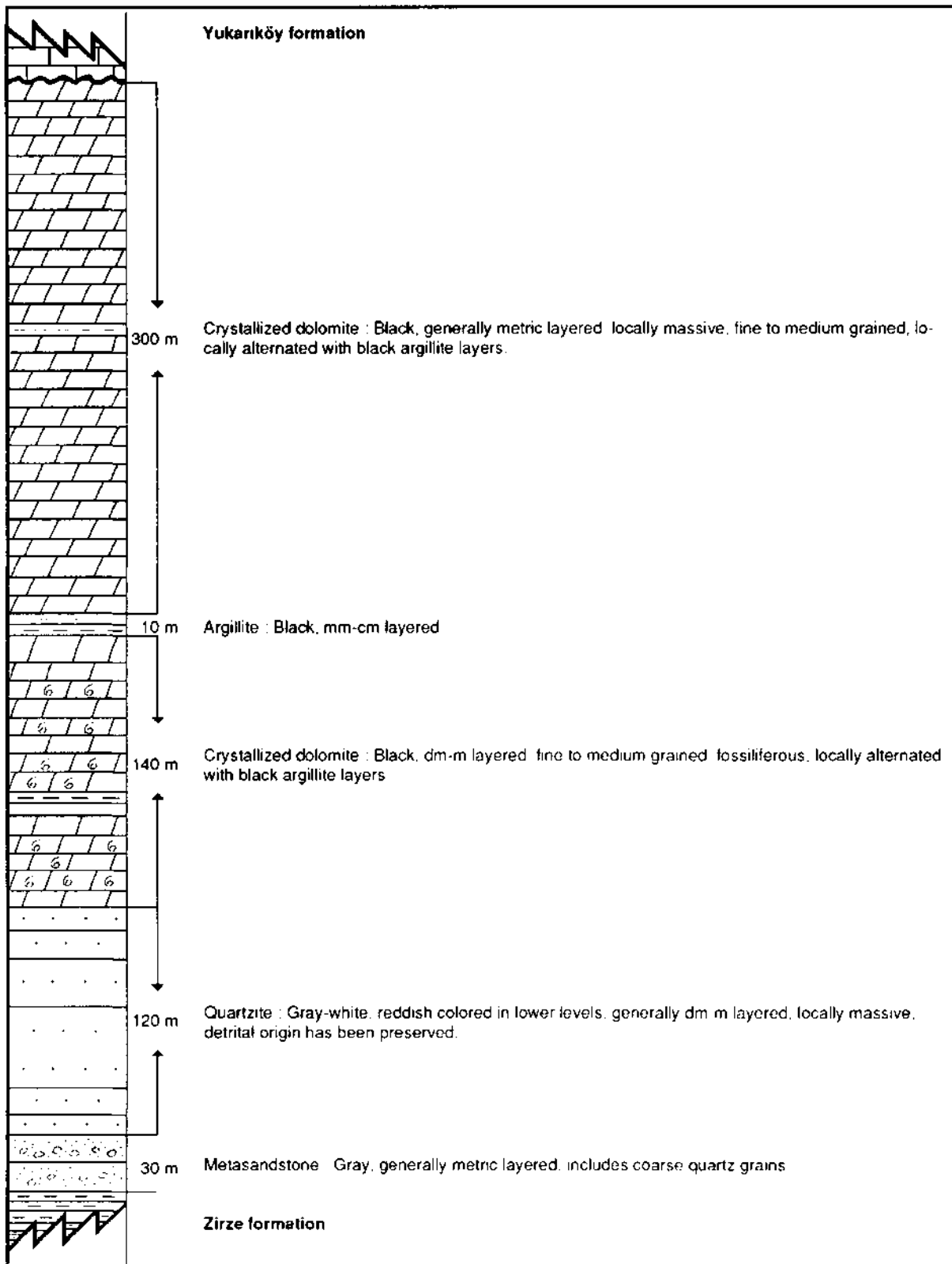


Fig. 7- Type section of the Kurehadit formation

Lithology. -There is a metasandstone level, with a thickness of 30 m., in the lowermost part of Küreihadit formation (Fig. 7). These metasandstones consist mainly of quartz grains, 5 mm. or more in grain sizes, cemented by a siliceous material. On top of these metasandstones, there is a quartzite level representing well preserved sedimentary bedding and detrital origin with a total thickness of 120 m. The lower part of these quartzites show reddish color due to iron enrichment, whereas the upper parts, with a layering dm.-m. in thickness, possess grayish-white color (Fig. 7). This quartzite level is followed by the brownish-black colored and locally bituminous smelling dolomitic rocks with a total thickness of 450 m. Some black colored argillite levels, ranging from 5 to 10 m. in thickness, can also be locally observed within these dolomitic rocks (Fig.7).

Lower and upper limits. - The Küreihadit formation covers the Zirze formation and underlies the Upper Jurassic-Lower Cretaceous Yukarıköy formation.

Age. - Some fossils, characterizing the Middle to Upper Devonian, have been found in the middle and upper parts of the crystallized dolomitic rocks of Küreihadit formation. The Upper Devonian fossils are as follow:

ZZ-91A, B, C (three specimens) (location 10 in Fig. 3a):

Algeas microfossils.

ZZ-94A, B (two specimens) (location 11 in Fig. 3a):

Brachiopoda Meristina.

The fossils indicating Devonian age are as follow:

ZZ-95D, E (two specimens) (location 12 in Fig. 3a):

Devonochonotes.

ZZ-90/1D (location13 in Fig. 3a):

Thamnopora sp.

Rugos soliter fragment.

ZZ-90/1E (location 13 in Fig. 3a):

Alveolites sp.

ZZ-90/1F (location 13 in Fig. 3a): .

Alveolites sp.

ZZ-90/1K (location 13 in Fig. 3a):

Tabular coral fragments.

ZZ-90/1L (location 13 in Fig. 3a):

Alveolites sp.

ZZ-94C (location 11 in Fig. 3a):

Alveolites sp.

Apart from all these fossils, there have also been found some characteristic fossils yielding Kuvinian-Frasnian (Upper-Middle Devonian) age in the Küreihadit formation as follow:

ZZ-90/1G (location 13 in Fig. 3a):

Thamnoporact. reticulata (De Blainville).

ZZ-90/1M (location 13 in Fig. 3a):

Thamnopora cf. reticulata (De Blainville).

Depositional environment. _ The Küreihadit formation characterizes shallow marine environment with a gradational increasing of energy.

Regional correlation. - As seen from Table 1, the Küreihadit formation is considered to be the equivalent of the "quartzitic calcareous rocks" and "dolomitic calcareous rocks" described by Tokay (1952) in Zonguldak area, of the Kocadere, Hacıyardere and Değİzirmendere formations described by Görmüş. (1982) in Bolu region, and the Kartal formation and the lower parts of Yılanlı formation described by Aydın et al. (1986).

Kirtulaz formation (Permo-Triassic?)

Description and type locality. - The Kirtulaz formation, firstly described by Boztuğ (1988) is observed better in the Kirtulaz yayla and surroundings in the NE part of mapped area (Fig. 3a).

Lithology. – The Kirtulaz formation is made up of various rock types such as grayish-blackish crystallized limestones, grayish-white quartzites, red-green argillites, greenish metagraywackes and metaconglomerates composed mainly of white quartzite pebbles and blocks cemented by a red wine colored clayey cement. Most of these rock types show cataclastic features. There is no any regularly continued observable rock type in this unit. All the rocks, mentioned above, are always seen to be fractured and faulted, and they always have tectonic boundaries with each other. For example, when the crystallized limestone, is followed, it suddenly disappears and the argillite appears with a tectonic contact. That is why the Kirtulaz formation is thought to be a broken formation (Hsu, 1968; Berkland et al., 1972) on the basis of these features (oral communication with Dr. B. Batman, Hacettepe Univ., Ankara).

Lower and upper boundaries. - The lower boundary of the Kirtulaz formation is seen to be a faulted contact. Along this E-W faulted contact, this unit is thrust, from north to south, into the Dorukyayla gneiss and Dotla formation (Fig. 3a). As for the upper boundary of the unit, it is out of mapped area, around the Daday region.

Age. - There has not been found any fossil in the rocks of the Kirtulaz formation. However, it is assumed to have an age older than Middle Jurassic because of cutting and thermally metamorphosed by the Middle Jurassic Kürek granitoid. On the other hand, the lithological correlation of the Kirtulaz formation with some units in regional geological framework may suggest an age of Permo-Triassic (?).

Depositional environment. _ The environmental interpretation of Kirtulaz formation seems to be very hard due to intensive and extensive faulting and fracturing of the rocks. However, the rock types of this unit should be deposited in different environments ranging from transitional to shallow and deep marine environments.

Regional correlation. - The Permo-Triassic (?) Kirtulaz formation is thought to be the equivalent of the "Middle Triassic limestone" and partly "Börümce schists" (Blumenthal, 1948), the "Lower Jurassic-Triassic limestone" and partly "old flysch" (Geiss, 1954), the lower parts of Börümce formation (Yılmaz, 1980), Domuzdağ metamorphic complex and partly Akgöl formation, Gümüşoluğu formation and Bekirli metamorphite (Tüysüz, 1986), Çakraz formation and lower parts of Akgöl formation (Aydın et al., 1986), and of the Paleozoic Akılçalman formation (Şengün et al., 1990).

Kürek granitoid (Middle Jurassic)

Description and type locality. - The Kürek granitoid has been firstly described by Yılmaz and Boztuğ (1986), and studied in detail by Boztuğ (1988). The name of this pluton comes from the Kürek village just to the north of mapped area. It outcrops better around Köyveri village in the mapped area (Fig. 3a).

Lithology. - The Kürek pluton consists mainly of granite, granodiorite and quartz monzonite on the basis of chemical-mineralogical nomenclature (Boztuğ, 1988). These medium to coarse grained magmatic rocks can also be determined as granodiorite in hand specimens during fieldworks. The rocks of the Kürek granitoid, possessing fresh exposures in the western and eastern parts of the Köyveri village, are observed to be enriched in the contents of mafic minerals and plagioclases rather than K-feldspars in hand samples. As for the vein rocks of this pluton, they are made up mainly of quartzolites (Streckeisen, 1976), aplites and microdiorites.

Lower and upper boundaries. - The Kürek granitoid intrudes the Permo-Triassic (?). Kirtulaz formation and transforms into contact metamorphic rocks (i.e. forsterite-marble; Boztuğ, 1988) along the contact zone. It is depositionally covered by the Upper Jurassic-Lower Cretaceous Yukarıköy formation in the northeastern part of the Çonlar village.

Age. - The Kürek pluton is considered to be one of the members of the Middle Jurassic Kastamonu granitoid belt, since it is overlaid by the Upper Jurassic-Lower Cretaceous Yukarıköy formation, and it is geologically, mineralogically-petrographically and also geographically associated with the Kastamonu granitoid belt (Boztuğ et al., 1984; Yılmaz and Boztuğ, 1986; Şengün et al., 1990). The Middle Jurassic age of the Kastamonu granitoid belt has also been clarified with the K-Ar radiometric age datings on the Asarcık diorite (Bonhomme and Yılmaz, 1984; Yılmaz and Bonhomme, 1991) and Ahiçay-Elmalıçay granitoid (Boztuğ and Yılmaz, 1991).

Environmental interpretation. - The Kürek granitoid is a member of the Middle Jurassic Kastamonu granitoid belt. The geological, mineralogical-petrographical and geochemical studies, carried out on the Kastamonu granitoid belt, showed that this belt was related to arc magmatism and even some felsic plutons from this belt, were related to crustal thickening towards the end of arc magmatism (Boztuğ et al., 1984; Yılmaz and Boztuğ, 1986).

Regional correlation. - As seen from Table 1, The Kürek granitoid can be correlated with "South Evrenye Intrusive Complex" (Geiss, 1954), Asarcık diorite (Yılmaz, 1980), Çangal granite (Tüysüz, 1986) and Dirgine granite (Aydın et al., 1986). On the other hand, the Kürek granitoid also continues towards the north of mapped area where this pluton has called Jurassic Soğüdek granitoid by Şengün et al. (1990). In their regional geological study Şengün et al. (1990) mention that there are some granitic rocks covered by Lower Jurassic rocks, however, there has not been found any granitic pluton covered by Lower Jurassic rocks in the Araç-Karadere area.

Yukarıköy formation (Upper Jurassic-Lower Cretaceous)

Description and type locality. - The Yukarıköy formation has been firstly described by Yılmaz (1980) around the Yukarıköy village, east of Devrekani town. This unit, also constituting one of the Yaralıgöz group (Yılmaz, 1980), outcrops around the Küreihadit, Küpelik, Saltuklu and Çonlar villages in the studied area.

Lithology. - The typical rock type of Yukarıköy formation is grayish colored limestone. These limestones, with the blackish-gray colors in the lower part of unit, also represents layering dm.-m. in thickness despite karstic erosion.

Lower and upper boundaries. - The Yeniköy formation unconformably overlies the Küreihadit formation, and it is conformably overlaid by the Lower Cretaceous Çatak formation.

Age. - Yılmaz (1980) has found some fossils yielding Upper Jurassic-Lower Cretaceous age in the Yukarıköy formation. The fossils, found in the mapped area, also determine Upper Jurassic-Lower Cretaceous, although, some of them indicate only Malm age (i.e. DG-151 and DG-217 B numbered rock samples). These fossiliferous rocks and their fossil contents are as follow:

DG-59 (location 14 in Fig. 3a):

Valvunidae,

Thaumatoporella sp.

DG-104 (location 15 in Fig. 3a):

Ammobaculites sp.,

Nautiloculina sp.,

Textularidae, Echinoidea, macro shelve sections.

DG-151 (location 16 in Fig. 3a):

Conicospirillina basiliensis Mohler

Nautiloculina sp.,

Pseudocyclammina sp.,

Algeas, Echinoidea, macro shelve sections.

DG-217 B (location 17 in Fig. 3a):

Donacosmilia Corallina de Fromentel.

Depositional environment. -The Yukarıköy formation typically characterizes the shelf carbonates.

Regional correlation. - The Yukarıköy formation is equivalent to the "Yaralığözdağı carbonate" (Blumenthal, 1948), "cover carbonates and basal conglomerate" (Geiss, 1954), and the İnaltı formation (Tüysüz, 1986; Aydın et al., 1986) as seen in Table 1.

Çatak formation (Lower Cretaceous)

Description and type locality. _ The Çatak formation, firstly described by Yılmaz (1980) around Çatak village, east of Devrekani town, is seen to be exposed better in the Salihoğlu dere and around the Aşağıbusup and Köle Hasan villages in the mapped area (Fig. 3a).

Lithology. - The Çatak formation consists typically of flyschoidal rocks comprising the alternation of black colored sandstone-siltstone-claystone and locally marl layers, cm. to dm. in thickness. There is also a calcirudite level, up to 50 m. in total thickness, in the lower parts of the unit in the southern part of Köle Hasan village.

Lower and upper boundaries. - The Çatak formation conformably overlies the Yukarıköy formation, and it is unconformably covered by Middle Eocene Soğanlı formation.

Age. — There has not been found any fossil in the Çatak formation, however, Yılmaz (1980) has found some Lower Cretaceous fossils in this unit.

Table 1 - The comparison of the Mesozoic and older chronostratigraphic-lithostratigraphic units in the studied area and surrounding

	Blumenthal, 1948	Tokay, 1952	Geiss, 1954	Yılmaz, 1980, 1981, 1983	Görmüş, 1982	Tüysüz, 1986	Aydın et al., 1986	Bozluğ, 1988
M E S O Z O I C	C MAASTRICHTIAN	Alaplı marl-İst.	Andesite	Kaygunca fm.	Hızardere fm.	Kargı ophiolite assemblage	Namazlıtepe fm.	
	R CAMPANIAN	Sarıkörmaz bed volcanics	Marl, andesite, limestone	Kirensöküsü fm.			Yemişliçay fm.	
	E SANTONIAN	Liman tuff and volcanics	Young flysch				Kapanboğazi fm.	
	T CONIACIAN	Lower serie					Çağlayan fm.	
	C TURONIAN	Upper blue marl	L. Cretaceous marl				İnalıtı fm.	
	E CENOMANIAN	Sand. glauconite					Burnuk fm.	
	O ALBIAN	Velibey sand.					Dirgine granite	
	S APTIAN	Cretaceous basal. conglom.					Akgöl fm.	
	BARREMIAN						Akgöl fm.	
	HAUTERIVIAN	Yaralıgöz dağı limestone					Yılanlı group Domuzdağ comp.	
	VALANGINIAN							
	BARRIASIAN	Conglomerate						
	MALM	Börümce schist						
DOGGER	M. Triassic. İmsl.							
LIAS								
TRIASSIC								
PERMIAN	Göynükdagi massive	Aritdere İm.	Dikmendağ conglomerate					
CARBONIFEROUS	Daday massive	Karadon, Kozlu, Alacaagazi		Canğal -eophiolite	Değirmendere İm.	Devrekani metamorphite	Karıağaç İm.	
DEVONIAN	1. Serpentinite	Dokomite İst.		1. Karadere metabasite	Hacıyardere İm.	continental assemblage	Yılanlı İm.	
SILURIAN	2. Diabase	Quartzite İst.		2. Dibekele metautramalite	Kocadere İm.		Fındıklı İm.	
ORDOVICIAN	3. Gneiss and mica schist	Ferrous clayey sand.			İşığandere İm.		Aydos İm.	
CAMBRIAN	4. Granite						Kurtköy İm.	
PRECAMBRIAN							Bakacak İm.	
							Kocaelingel İm.	
							Yedigöller İm.	
							metabasite	
							metagranite	
							amphibolite	
							Dorukayla gneiss	
							qtz-feld gneiss	
							mica-gneiss	
							amphibole-pyroxene gneiss	

Depositional environment. - The Çatak formation characterizes an environment which is shallow marine with a high energy at the beginning, and a deep marine environment later.

Regional correlation. - The Çatak formation is seen to be the equivalent, in Table 1, of the "Cretaceous basal conglomerate" (Tokay, 1952) and the lower parts of Çağlayan and upper parts of İnaltı formations (Tüysüz, 1986). On the other hand, this unit may be assumed to be correlated with the Çağlayan formation (Aydın et al., 1986), although, there is no any Albian-Aptian fossils in the Çatak formation.

Soğanlı Formation (Middle Eocene)

Description and type locality. - The Soğanlı formation, firstly described by Aydın et al. (1986), outcrops around the Saltuklu, Döğemle and Mirigürne villages in the studied area (Fig. 3).

Lithology. — The Soğanlı formation is composed up typically of yellowish-orange colored fossiliferous limestones showing layering dm. in thickness.

Lower and upper boundaries. — The Soğanlı formation unconformably overlies the Çatak formation in the north of studied area (out of mapped area), the Yukarıköy formation around the Saltuklu village, and the Küreihadit and Zirze formations around the Döğemle and Mirigürne villages in the mapped area, respectively. As for the upper boundary of Soğanlı formation, it is conformably overlaid by the Cemalettin formation.

Age. - The Soğanlı formation, already aged as Middle Eocene by Aydın et al. (1986), includes some fossils indicating the same age in the mapped area, too.

DG-294 (location 18 in Fig. 3a):

Some forms similar to *N. beaumonti*, *Assilina exponens* (Sowerby),

Operculina sp.,

Rotalia sp.

uepositionalenvironment. -The Soğanlı formation characterizes the shallow marine environment.

Cemalettin formation (Upper Eocene-Lower Oligocene)

Description and type locality. ~ The Cemalettin formation, firstly described by Aydın et al. (1986), outcrops around the Oycalı and Saltuklu villages in the mapped area.

Lithology. - The Cemalettin formation consists of grayish-green conglomerate, coarse sandstone, sandstone, siltstone, claystone and marly rocks. In the southern part of Yukarıkarabüzey village, it is made up essentially of grayish sandstone, siltstone and claystone alternation.

Lower and upper boundaries. - The Cemalettin formation conformably overlies the Soğanlı formation around the Oycalı, Saltuklu and Yukarıkarabüzey villages, and it is unconformably covered by the Karabüzey formation in the studied area.

Age. — There has not been found any fossil in this unit, however, it has been determined to have an age of the Upper Eocene-Lower Oligocene by Aydın et al. (1986).

Depositional environment. _ The Cemalettin formation characterizes locally the fluvatile and locally shallow marine environment with high energy. Aydın et al. (1986) also point out that it includes some braided stream sediments.

Karabüzey formation (Neogene)

Description and type locality. _ The Karabüzey formation has been firstly described by Boztuğ (1988). It is seen to be outcropped better around the Karabüzey, Yeniköy, Harmancık and Süzey villages in the mapped area.

Lithology. - The Karabüzey formation comprises quartzite pebbles and blocks at bottom which are followed by the semi-consolidated and red colored sandy-silty and clayey sediments up to 150 m. in total thickness around Karabüzey village. It is observed to have been formed by unconsolidated quartzite pebbles and blocks around the Yeniköy, Harmancık and Süzey villages. Apart from these lithological characteristics, it is composed of semi-consolidated conglomerates cemented by clayey materials around the Vakıfgürne village. Finally, it is seen to be formed by reddish-yellowish clayey and silty materials around the Kuloğlu village.

Lower and upper boundaries. - The Karabüzey formation takes unconformably place on top of the older units than Neogene in the mapped area. There is no any unit overlying the Karabüzey formation except the Quaternary alluvium which should be stratigraphically on top of this unit.

Age. - The Karabüzey formation, without any fossils, is suggested to have a Neogene age due to stratigraphical setting and lithology.

Depositional environment. - The Karabüzey formation is characterizes by the terrestrial material.

Quaternary alluvium

This occurrence, consisting of recent alluvial materials in the big valleys, is seen better in the northern part of the Karadere valley (Fig. 3). These sandy-pebbly materials have been operating by the native people for concrete materials in constructions.

TECTONICS

The structural elements are distinguished to have been formed in two different stages, i.e. the Alpine and pre-Alpine stages, in the mapped area. The foliation planes due to ductile deformation under the conditions of medium-to highgrade metamorphism (diopside-gneiss; Winkler, 1979) are the products of the pre-Alpine deformation, since they can only be seen in the Dorukyayla gneiss. This ductile deformation in the Dorukyayla gneiss does not affect the Lower to Middle Paleozoic Samatlar group, i.e. neither the mineral paragenesis, nor planar-linear structural elements. Thus, the deformation of the Dorukyayla gneiss is considered to be pre-Alpine age. As for the Alpine deformations, both of the Paleozoic and Mesozoic rocks have been folded and faulted altogether from those deformations. That is the reason why the Paleozoic units are considered to have been also deformed in the Alpine periode.

Folds

The fold axes, with the strikes of approximately E-W, are observed to fold all the Paleozoic and Mesozoic rock units altogether in the northwestern and western parts of the mapped area (Fig. 3a). The Çatak formation, however, possesses many meso-folds which can not be mapped to the scale of 1:25.000 during fieldwork. There is an interesting sycline in the north of Küreihadit village taking place in the western part of studied area. The western part of this sycline is seen to have a normal sycline axe, whereas the eastern part is observed to be an overturned sycline axe due presumably to the reverse fault which is just to the south of this sycline (Fig. 3a, 3b) in the Inciğez village. These Alpine foldings are thought to be formed by N-S compressional forces sometimes around Lower Cretaceous, since they have also folded the Upper Jurassic-Lower Cretaceous Yukarıköy formation, too. .

Faults

The major faults, observed in the studied area, are composed mainly of reverse (thrust) and strike-slip faults. As clearly seen in Figure 3a, both of the Kürek granitoid and Yukarıköy formation have been thrust onto the Çatak formation, from north to south, and the Kirtulaz formation has been thrust onto the Çatak formation, Dorukyayla gneiss and Dotla formation from north to south along the E-W reverse fault zone in the northeastern part of the mapped, area. In the northwestern part of the studied area, the Dorukyayla gneiss, Yayladere and Dotla formations have been altogether thrust onto the Küreihadit formation from south the north along another E-W reverse fault zone (Fig. 3a). However, Dorukyayla gneiss is observed to have been thrust onto the Çatak formation along the eastern prolongation of this reverse fault plane. There are also intensive and extensive cataclastic rocks developed along these reverse fault zones in the mapped area. The youngest unit, affected from these E-W reverse faults, is the Çatak formation as clearly seen from all these observations. Thus, these E-W reverse faults are also thought to be derived from the N-S compressional forces sometimes around Lower Cretaceous as well as E-W fold axes.

As for the strike-slip faults, they have mainly affected the Dotla and Zirze formations (Fig. 3a). These faults are considered to be maximum lateral dilatation planes due to N-S compression.

Unconformities

The unconformities, observed in the mapped area, can be summarized as followed: The most important unconformity is that of between the Precambrian Dorukyayla gneiss and Lower to Middle Paleozoic Samatlar group. This unconformity also indicates a big difference in deformation styles of the Dorukyayla gneiss and Samatlar group (Boztuğ, 1988). In other words, the Dorukyayla gneiss represents a ductile deformation style occurred under the conditions of medium to high-grade metamorphism (Winkler, 1979), whereas the Samatlar group shows a deformation style occurred under the conditions of very low-grade metamorphism (Winkler, 1979). Another unconformity in the mapped area is seen between the Samatlar and Yaralıgöz groups. This unconformity also remarks some differences in the physical conditions of deformations affected these groups, i.e. the Samatlar and Yaralıgöz group represent very low-grade metamorphic and diagenetic mineral assemblages, respectively (Boztuğ, 1988). The Middle Eocene Soğanlı formation unconformably overlies all the pre-Senozoic units as mentioned earlier. Around the Çonlar village situated in the northern part of studied area, the Yukarıköy formation unconformably covers the Kürek granitoid. This unconformity plane between the Yukarıköy formation and Kürek granitoid helps to approach the geological age of the Kürek pluton which could be older than the Yukarıköy formation, i.e. Upper Jurassic. On the other hand, there has not been found any stratigraphical evidence about the lower and upper limit relations of the Permo-Triassic (?) Kirtulaz formation, since it shows a broken formation feature moreover, its lower boundary is already seen to be faulted. However, the Kirtulaz formation may be assumed to take unconformably place on top of the Samatlar group, and affected by the same deformation style of Samatlar group. Illite crystallinity and vitrinite reflectance studies showed that the physical conditions of the deformations affecting these two units were similar to each other, i.e. anchimetamorphism to epimetamorphism.

GEOLOGICAL EVOLUTION

Such an evolution model can be suggested when the geological data, obtained from the southwestern part of Daday-Devrekani Massive by Boztuğ (1988), are evaluated with those of other authors.

The oldest unit of the studied area, the Precambrian Dorukyayla gneiss, consisting of high-grade metasediments, characterizes a typical continental crust material. The Dorukyayla gneiss is considered to constitute the southernmost tip of Eurasian plate (Boztuğ et al., 1984; Yılmaz and Boztuğ, 1986; Koçyiğit, 1989). The Samatlar group, composed of Yayladere (Cambrian), Dotla (Ordovician), Zirze (Silurian) and Kureihadit (Devonian) formations, has been deposited in an epicontinental domain constituted by the Dorukyayla gneiss. The Permo-Triassic (?) Kirtulaz formation may also be thought to be a part of the Samatlar group. Thus, there is

an epicontinental cover of Paleozoic-Lower Mesozoic in age on top of the Dorukyayla gneiss. An oceanic crust, must have been existed at least in Lower Mesozoic, has been developing with its local epiophiolitic cover (i.e. Çangal metaophiolite; Yılmaz, 1980, 1983) during the deposition of such an epicontinental cover mentioned above. For example, the Lower Mesozoic flyshoidal rocks are seen to be epiophiolitic cover on top of the ophiolitic rocks in the Küre region (Bailey et al., 1967; Yılmaz and Tüysüz, 1984; Aydın et al., 1986). From this point of view, the epicontinental cover of the Dorukyayla gneiss has either epicontinental or epiophiolite characters particularly in Lower Mesozoic. The oceanic crust has induced a northward subduction zone (Boztuğ et al., 1984; Yılmaz and Boztuğ, 1986; Şengün et al., 1990; Ustaömer et al., 1991; Robertson et al., 1991) by consuming beneath the Dorukyayla gneiss and its epicontinental cover towards the middle stage of Lower Mesozoic. The Paleozoic-Lower Mesozoic epicontinental cover, taking place next to subduction zone has been metamorphosed in the conditions of low grade facies of this regional metamorphism induced by subduction zone in the active margin (Best, 1982; Fig. 12-21, p. 434) (i.e. Ilgaz metasedimentary group, Yılmaz and Boztuğ, 1986). However, the affects of this regional metamorphism is decreasing towards the north away from the subduction zone and it is remarked to be a very low grade metamorphism in the Samatlar group in the mapped area. Far away from the subduction zone, in other words area. Far away from the subduction zone, in other words in the northernmost parts such a regional metamorphism can not be detected, since the coal bearing Paleozoic rocks in the Zonguldak basin indicate only diagenetic conditions. The first arc plutonism (Best, 1982) product of this subduction zone has formed the Middle Jurassic Kastamonu granitoid belt (Boztuğ et al., 1984; Yılmaz and Boztuğ, 1986). The Kürek pluton, in the studied area, is the part of this granitoid belt. The Middle-Upper Jurassic to Lower Cretaceous Yaralıgöz group has been deposited in intermountains basins developed due presumably to the diapirically rising up and emplacement of the plutons of the Kastamonu granitoid belt. After the deposition of Yaralıgöz group, the Late Alpine structural elements have been created by the N-S compressional forces sometimes around Lower Cretaceous. These Late Alpine deformations can also be observed in the Paleozoic units as the foldings and faultings. The Tertiary units, in the mapped area, have been deposited in the terrestrial and shallow marine environments. The Neogene Karabüzey formation consists of semi-consolidated and terrestrial rocks. As for the Quaternary alluvium, it is only seen in the recent stream valleys.

CONCLUSIONS

The conclusions obtained in the southwestern part of Daday-Devrekani massive can be summarized as follow:

1- The lithostratigraphic units, in the mapped area, consists, from bottom to top, of the Dorukyayla gneiss (Precambrian), Yayladere (Cambrian), Dotla (Ordovician), Zirze (Silurian), Küreihadit (Devonian), Kirtulaz (Permo-Triassic?) formations, Kürek granitoid (Middle Jurassic), Yukarıköy (Upper Jurassic-Lower Cretaceous), Çatak (Lower Cretaceous), Soğanlı (Middle Eocene), Cemalettin (Upper Eocene-Lower Oligocene), Karabüzey (Neogene) formations and of Quaternary alluvium.

2- Dorukyayla gneiss, Yayladere, Dotla, Zirze and Küreihadit formations, constituting the Samatlar group, have been firstly described in this study. On the other hand, it is suggested to study an area between the Daday town and mapped area here by means of geological mapping and mineralogy-petrography and geochemistry for the classification of the stratigraphical setting of Kirtulaz formation.

3- The Paleozoic and Mesozoic units have been folded and faulted by the N-S compressional forces sometimes around Lower Cretaceous in the mapped area. The fold axis and reverse faults possess mainly E-W strikes, whereas the strike-slip faults have mainly NE-SW trends. The reverse faults have also formed some intensive and extensive mylonitic rocks in the studied area.

4- The main unconformities in the area consist of those between the Dorukyayla gneiss and Samatlar group, between the Samatlar and Yaralıgöz groups, and between the Yaralıgöz group and Tertiary units.

ACKNOWLEDGEMENT

This paper is part of the Ph. D. Thesis of author under the advisory of Prof. Dr. O. Yılmaz (İÜ) I am greatly indebted to Dr. Yılmaz for his helps and critics during my studies. MTA and TÜBİTAK have provided financial support. I would like to thank to Prof. Dr. B. Batman (HU) for his improvements in the tectonic features of the area. Also many thanks to the Paleontologists from MTA-namely, A. Salancı, M. Baydar, S. Tuzcu, M. Erkan, S. Örgen and K. Erdoğan.

Manuscript received November 26, 1993

REFERENCES

- Adamia, S.; Bergougnan, H.; Fourquin, C.; Haghipour, A.; Lordkipanidze, M.; Özgül, N.; Ricou, I.E. and Zakariadze, G., 1980, The Alpine Middle East between the Aegean and the Oman traverses: 26th Congr geol. internal. Paris, Coll, C5 Geologie des chaines alpines issues de la Tethys, Mem. BRGM no. 115., 122-136.
- Arpat, E.; Tütüncü, K. and Uysal, S., 1978, Safranbolu yöresinde Kambriyen-Devoniyen istifi: Türkiye Jeol. Kur., 32. Bilimsel Teknik Kurultayı Bildiri Özleri, p. 67.
- Ataman, G.; Yılmaz, O. and Ertürk, O., 1977, Diyajenez-ankimetamorfizma geçişinin illit kristallik derecesi ile araştırılması (Batı Pontidlerde bir deneme): Yerbilimleri, 3, 145-160.
- Aydın, M.; Şahintürk, Ö.; Serdar, H.S.; Özçelik, Y.; Akarsu, İ.; Üngör, A.; Çokuğraş, R. and Kasar, S., 1986, Ballıdağ-Çangaldağ (Kastamonu) arasındaki bölgenin jeolojisi: Bull, of the Geol. Soc of Turkey., 29, 2, 1-16.
- _____; Serdar, H.S.; Şahintürk, Ö.; Yazman, M.; Çokuğraş, R.; Demir, O and Özçelik, Y., 1987, Çamdağ (Sakarya)-Sünnicedağ (Bolu) yöresinin jeolojisi: Bull, of the Geol. Soc. of Turkey ., 30, 1-14.
- Bailey, E.H.; Barnes, J.W. and Kupfer, D.H., 1967, Geology and ore deposits of the Kure district, Kastamonu province, Turkey: Cento Summer Training Program in Geological Mapping Techniques, Küre, Turkey, 1966, Office of United States Economic Coordinator for Cento Affairs, 104 p.
- Berkland, J.O.; Raymond, L.A.; Kramer, J.C.; Moores, EM and O'Day, M., 1972, What is Franciscan? Am. Assoc. Petroleum Geol. Bull., 56, 2295-2302.
- Best, M.G., 1982, Igneous and metamorphic petrology: Freeman and Co., San Francisco, 630 p
- Blumenthal, M., 1948, Bolu civarı ile Aşağı Kızılırmak mecrası arasındaki Kuzey Anadolu silsilelerinin jeolojisi: MTA Publ., B-13, Ankara, Turkey.
- Bonhomme, M.G. and Yılmaz, O., 1984, First K-Ar data from the Daday-Devrekani and Ilgaz massives and the Kastamonu granitoid belt, northern Turkey: Terra Cognita, 4, 199-200
- Boztuğ, D., 1983, Daday-Devrekani masifi kuzeyindeki Büyükçay-Elmalıçay granitik sokulumu: HÜ Yük. Müh. tezi, 149 p., add. 2, (Unpublished), Ankara, Turkey
- _____, 1988, Daday-Devrekani masifi güneybatı kesiminin mineralojik-petrografik ve jeokimyasal incelenmesi: HÜ Doktora tezi, 232 s., 1 ek, (Unpublished), Ankara, Turkey
- _____, and Yılmaz, O., 1983, Büyükçay-Elmalıçay granitoyidi (Kastamonu) ve çevre kayaçlarının mineralojik-petrografik ve jeokimyasal incelenmesi: Yerbilimleri, 10, 71-88
- _____, and _____, 1991, K-Ar geochronology of the fine fractions from the Göynükdagi contact aureole A mixed age due to inherited muscovite, Kastamonu, N Turkey: Mahmut Sayın Kil Mineralleri Sempozyumu, 2-4 Mayıs 1991, Bildiriler kitabı (inpress), Adana, Turkey.
- _____, Debon, F.; Le Fort, P. and Yılmaz, O., 1984, Geochemical characteristics of some plutons from the Kastamonu granitoid belt (northern Anatolia, Turkey): Schweiz Mineral Petrogr Mitt , 64, 389-403

- Geiss, H.P., 1954, Karadeniz taşkömürü prospeksiyon dahilinde İnebolu-Küre-Abana sahasında yapılan jeolojik löve neticeleri: MTA Rep., 2973 (Unpublished), Ankara, Turkey.
- Gömüş, S., 1982, Yiğilca (Bolu KB) yöresinin stratigrafisi: *Yerbilimleri*, 9, 91-110.
- Hsu, K.J., 1968, Principles of melanges and their bearing on the Franciscan-Knoxville paradox. *Geol. Soc. Am. Bull.*, 79, 1063-1074.
- Ketin, I., 1966, Tectonic units of Anatolia: *MTA Bull.*, 66, 23-34, Ankara, Turkey.
- Koçyiğit, A., 1989, Suşehri basin: an active fault-wedge basin on the North Anatolian Fault Zone, Turkey: *Tectonophysics*, 167, 13-29.
- Robertson, A.H.F.; Dixon, J.E.; Aktaş, A.; Clift, P.D.; Degnan, P.; Jones, G.; Morris, A.; Pickett, E.; Sharp, I. and Ustabmer, T., 1991, Tectonic reconstructions of the Eastern Mediterranean region: Controversies, alternatives and possible solutions. *Terra Abstracts*, 3, 322.
- Streckeisen, A., 1976, To each plutonic rock its proper name: *Earth-Sci. Rev.*, 12, 1-33.
- Şengün, M.; Keskin, H.; Akçören, F.; Altun, I.; Sevin, M.; Akat, U.; Armağan, F. and Acar, Ş., 1990, Kastamonu yöresinin jeolojisi and Paleotetisin evrimine ilişkin sınırlamalar: *Bull. of Geol Soc of Turkey.*, 33, 1-16.
- Tokay, M., 1952, Karadeniz Ereğlisi-Alaplı-Kızıltepe-Alacaağzı bölgesi jeolojisi. *MTA Bull.*, 42/43, 35-78, Ankara, Turkey.
- Tüysüz, O., 1985, Kargı masifi ve dolayındaki tektonik birliklerin ayırıcı ve araştırılması (Petrolojik İnceleme): İÜ Doktora tezi, 431 p. (Unpublished), İstanbul.
- _____, 1986, Kuzey Anadolu'da iki farklı ofiyolit topluluğu: Eski ve yeni Tetisin artıkları: *Doğa Tu Müh. ve Çev. D.*, 10, 2, 172-179.
- Ustaömer, T.; Robertson, A.H.F. and Yılmaz, Y., 1991, Paleotethyan tectonic evolution of the central Pontides, northern Turkey: *Terra Abstracts*, 3, 256.
- Winkler, H.G.F., 1979, *Petrogenesis of metamorphic rocks: 5th ed.*, Springer-Verlag, Berlin, 348 p.
- Yılmaz, O., 1979, Daday-Devrekani masifi kuzeydoğu kesimi metamorfileri HÜ Doç. tezi, 243 p., add. 4, (Unpublished), Ankara, Turkey.
- _____, 1980, Daday-Devrekani masifi kuzeydoğu kesimi litostratigrafi birimleri ve tektoniği: *Yerbilimleri*, 5, 6, 101-135.
- _____, 1981, Daday-Devrekani masifi Ebrek metamorfisinin petrografisi ve tumkayac, kimyası: *Yerbilimleri*, 8, 71-82.
- _____, 1983, Çangal metaofiyolitinin mineralojik-petrografik incelenmesi ve metamorfizma koşulları: *Yerbilimleri*, 10, 45-58.
- _____, and Bonhomme, M.G., 1991, K-Ar isotopic age evidence for a Lower to Middle Jurassic low-pressure and a Lower Cretaceous high-pressure metamorphic events in north-central Turkey: *Terra Abstracts*, 3, 501.
- _____, and Boztuğ, D., 1985, Göynükdagi metamorfiti: TÜBİTAK Arş. Projesi Rap., TBAG-569, 121 p., add. 1, (Unpublished), Ankara, Turkey.
- _____, and _____, 1986, Kastamonu granitoid belt of northern Turkey: First arc plutonism product related to the subduction of the paleo-Tethys: *Geology*, 14, 179-183
- _____, and _____, 1987, Göynükdagi (Kastamonu) yöresinin jeolojik ve mineralojik-petrografik incelenmesi: *Doğa Tu Müh. ve Çev.D.*, 11, 1, 91-114.

Yılmaz, Y. and Tüysüz, O., 1984, Kastamonu-Boyabat-Vezirköprü-Tosya arasındaki bölgenin jeolojisi (Ilgaz-Kargı masiflerinin etüdü): MTA Rep , 7838 (Unpublished), Ankara

——— and ———, 1988, Kargı masifi ve dolaylarında Mesozoyik tektonik birliklerinin düzenlenmeleri sorununa bir yaklaşım: TPJD Bült. 1.1.73-86.

NEW DATA ON THE UPPER AGE OF THE INTRA-PONTIDE OCEAN FROM NORTH OF ŞARKÖY (THRACE)

Aral I. OKAY* and İzver TANSEL**

ABSTRACT. - Upper Eocene elastics in the southern part of the Thrace Basin north of Şarköy contain large number of olistoliths. The olistoliths are largely derived from the ophiolitic melange that forms the basement of the Eocene sedimentary sequence in this region. They comprise serpentinite, metadiabase, radiolarian chert and pelagic limestone. Some of the pelagic limestone blocks contain abundant Late Cretaceous and Middle Paleocene foraminifera. The presence of the Middle Paleocene pelagic limestone blocks derived from the ophiolitic melange indicate that the Intra-Pontide ocean was in existence at least until the Middle Paleocene.

INTRODUCTION

An alpine ophiolitic melange constitutes the basement of the southern part of Thrace Basin that is made up of Eocene and younger sediments. The ophiolitic melange outcrops north of Şarköy in the cores of small post-Miocene anticlines and is encountered in the petroleum wells below the Middle Eocene limestones (Kopp and others, 1969; Şentütük and Okay, 1984; Siyako and others, 1989). Şengör and Yılmaz (1981) interpreted this ophiolitic melange as the suture of the Intra-Pontide ocean that separated the Rhodope-Pontide fragment from the Sakarya zone. The Rhodope-Pontide fragment is a composite unit made up of three tectonic units that show distinct lithological, stratigraphic and metamorphic features: the Rhodope-Strandja massif in the west, the Istanbul zone in the centre and the Sakarya zone in the east (Okay, 1989). The Intra-Pontide Suture in Thrace separates the Rhodope-Strandja massif in the north from the Sakarya zone in the south (Fig. 1). There are very little data regarding the age of the opening and closing of the Intra-Pontide Ocean. Data will be presented here to show that the Intra-Pontide Ocean was open until the Middle Paleocene.

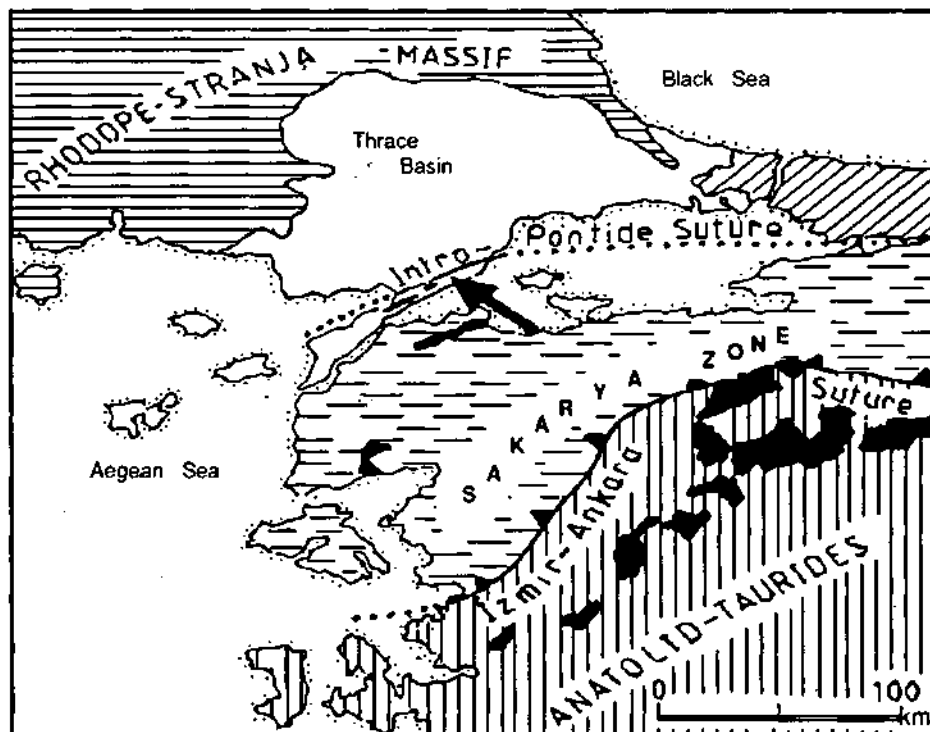


Fig. 1 - Simplified tectonic map of the region around the Marmara Sea. The studied region is indicated by the black arrow. The regions in black show outcrops of alpine ophiolite and ophiolitic melange.

GEOLOGY OF THE REGION NORTH OF ŞARKÖY

The Ganos strike-slip fault, one of the western branches of the North Anatolian Fault, divides the region studied into two geologically distinct parts (Fig. 2). North of the Ganos fault there is a thick Upper Eocene turbiditic clastic sequence called the Keşan group (Turgut and others, 1983). To the south of the Ganos fault there is an over 3 km. thick olistostromal Eocene sequence that is partly overturned to the south (Fig. 2). The lower parts of this sequence is exposed in the north in the vicinity of the Ganos fault and comprises olistostromes and grain flows with large blocks up to 500 m. in size. The blocks are made up of serpentinite, Middle Eocene reefal limestone, metadiabase, diorite and rarely gabbro, recrystallised limestone, Upper Cretaceous and Middle Paleocene pelagic limestone, radiolarian chert and quartzite. The provenance of most of the blocks is the ophiolitic melange that forms the basement in this region and the Middle Eocene limestones that unconformably overlie the ophiolitic melange. Medium to thickly bedded sandstone, calcarenite and shale occur between the olistostromes. The olistostromal sequence passes southwards and upwards through a gradual decrease in the number and size of the blocks to a turbidite sequence of intercalated sandstone and shale. Kopp and others (1969) regard this upper part of the sequence as of Oligocene age. This Eocene-Oligocene sequence can be correlated with the Karaağaç member, an Upper Eocene flysch described from the Gelibolu peninsula by Önal (1986). Variageted sandstones of the Miocene Gazhanedere formation and thickly bedded, yellow sandstone of the Kirazlı formation lie unconformably over the older units.

The ophiolitic melange that has provided blocks to the Eocene sequence outcrops in the cores of the post-Miocene anticlines 5 km. west of the studied region, where it consists of serpentinite, diabase that shows locally blueschist or greenschist facies metamorphism, gabbro, spilite, radiolarian chert and pelagic limestone (Kopp and others, 1969; Şentürk and Okay, 1984). The rocks form a complex of imbricate slices and represent with their lithological and tectonic features a sediment-starved accretionary complex in a subduction zone. Middle Eocene reefal limestones overlie the ophiolitic melange with a pronounced unconformity.

Cretaceous and Paleocene pelagic limestone blocks in the Eocene olistostromal unit

The newly described Late Cretaceous and Middle Paleocene pelagic limestone blocks outcrop along a ridge south of the Harmankaya stream, 500 m. east of the Şarköy-Gölcük road. They are associated with serpentinite, silicified serpentinite, green metadiabase and Eocene reefal limestone blocks. These up to 7 m. large blocks are surrounded by a sandstone matrix. Micritic Upper Cretaceous limestone blocks in Couches Rouges facies form a few small blocks less than one metre in size. A sample (Ş104) collected from one of the blocks contain foraminifera characteristic of Middle-Late Maestrichtian: *Rosita contusa* (Cushman), *Globotruncana* sp., *G. falsostuarti* (Sigal), *Globotruncanella* sp., Heterohelicidae. Another specimen (47) has a slightly different fauna of Maestrichtian age: *Globotruncana* sp., *G. lapparenti* (Brotzen), *G. c. linneiana* (D'Orbigny), *G. cf. area* (Cushman), *Globotruncanita* sp., *G. stuarti* (D' Lapparent), *Rugoglobigerina* sp. A specimen (Ş103) from a different red micritic limestone block contains *Rosita fornicata* (Plummer), *Globotruncana* sp., *G. area* (Cushman), *G. cf. bulbides* (Vogler), *Heterohelix* sp., *Globotruncanita* sp. of probable Campanian age. Kopp and others (1969) describe a similar Campanian-Maestrichtian pelagic fauna from the Upper Eocene grain flows.

Paleocene limestone occurs in the same region as 1-2 m. large, blocks more common than the Late Cretaceous limestones. It consists of greenish grey, thinly to medium bedded (1-5 cm.) micrite and intercalated thinly-medium bedded dark grey calciturbidite. A specimen (Ş100) from the micritic levels contains *Planorotalites* sp., *P. cf. compressa* (Plummer), *Morozovella* sp., *M. angulata* (White), *M. pseudobulloides* (Plummer), *Globigerina* sp., *G. cf. triloculinooides* (Plummer) indicative of Danian-Montian (Early-Middle Paleocene). A specimen (Ş102) from a different block has *Planorotalites* sp., *P. pusilla pusilla*, *Morozovella* sp., *M. cf. angulata* (White), *Globigerina* sp., *G. triloculinooides* (Plummer) of Montian age. Calciturbidite lamella in the same section contain quartz grains, and fragments of echinoid tests, red algae, mollucs, bryozoa, neritic and pelagic foraminifera; the following Late Cretaceous foraminifera were identified in the calciturbidite lamella: *Globotruncana* sp., *Heterohelix* sp., Rotaliidae.

Apart from the Harmankaya ridge, pelagic limestone also occurs as small blocks and pebbles in the Eocene sandstones 100 m. north of the Gölcük-Çengelli road (Fig. 2). A small grey micritic pebble (Ş198) from this

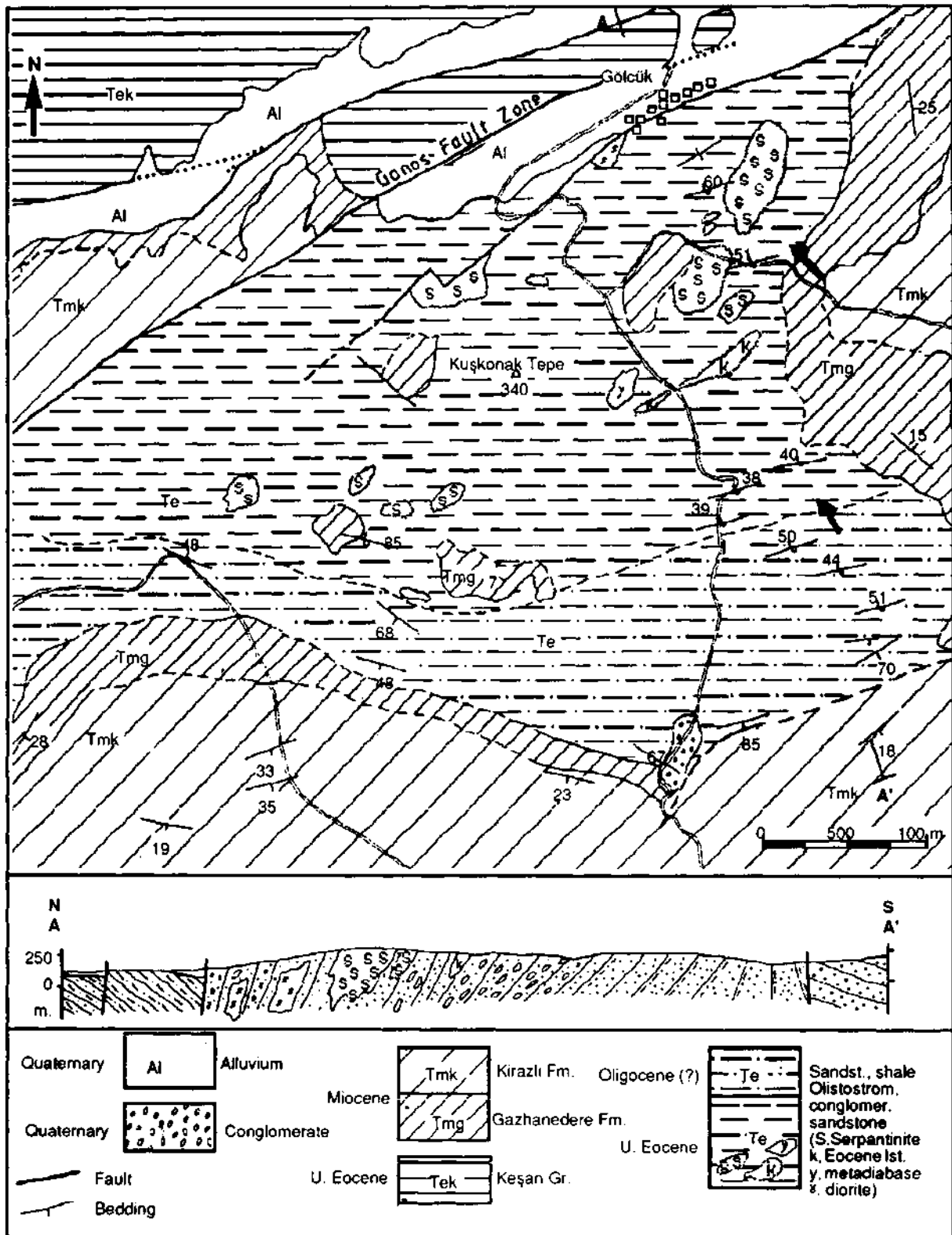


Fig. 2 - Geological map and cross-section of the region north of Şarköy. The black arrows indicate the locations of the Paleocene and Upper Cretaceous limestone blocks.

region contains *Globotruncana area* (Cushman), *G. bulloides* (Vogler), *Globotruncanita stuaiii* (D'Lapparent), *Rosita fornicata* (Plummer), *Gansserina gansseri* (Balli) of Middle Maestrichtian age. Another yellowish grey limestone pebble (Ş199A) has a pelagic fauna indicative of Danian age: *Globigerina triloculinooides* (Plummer), *Globigerina* sp., *Morozovella pseudobulloides* (Plummer) and *Planorotalites* sp.

CONCLUSIONS

The presence of Maestrichtian and Paleocene pelagic limestone blocks, derived from an ophiolitic melange, in an Eocene olistostromal unit north of Şarköy indicates that the Intra-Pontide ocean existed as a deep and most probably oceanic basin at least until the Middle Paleocene. The thinly bedded, micritic character of the Middle Paleocene limestones and the scarcity and the fine grain size of the calciturbidites indicates that the continental collision that would have provided abundant detritus to the basin has not occurred by the Middle Paleocene. The Cretaceous and Paleocene limestones were probably deposited on oceanic crust and then incorporated along a northward dipping subduction zone to the growing accretionary complex. This view is supported by the presence of Late Cretaceous pelagic foraminifera in the Middle Paleocene calciturbidites suggesting subaqueous erosion of the Late Cretaceous limestones already incorporated to the accretionary complex. This also shows that the northward subduction was active at least during the Campanian-Montian interval. The closure of the ocean occurred after the Middle Paleocene, probably during the Eocene.

Middle Paleocene pelagic limestone, similar to that described here, are reported from the Gelibolu peninsula under the name of Lort Limestone (Önal, 1986). The Upper Cretaceous-Paleocene Lort Limestone outcrops in a very small area south of the Saros Bay and is regarded by Önal (1986) as the stratigraphic basement of the Gelibolu Tertiary sequence. The observations north of Şarköy suggest that the Lort Limestone is not a coherent formation but forms a large block in the ophiolitic melange or in the Eocene elastics, wells drilled in the Gelibolu peninsula has encountered below the Eocene sequence not the Lort Limestone but various lithologies that could be assigned to an ophiolitic melange.

ACKNOWLEDGEMENTS

We thank Hasan Güner, Fazıl Kıran and Niyazi Şennazlı for help with the field work, and Naci Görür who helped with the petrography of the calciturbidites.

Manuscript received January 20, 1992

REFERENCES

- Kopp, K.O.; Pavoni, N. and Schindler, C., 1969, Das Ergene Becken: Beihefte Geol. Jahrbuch, Heft 76, 136 p.
- Okay, A.I., 1989, Tectonic units and sutures in the Pontides, northern Turkey: ed. A.M.C. Şengör, Tectonic Evolution of the Tethyan Region, Kluwer Academic Publ., 109-116
- Önal, M., 1986, Gelibolu Yarımadası orta bölümünün sedimenter fasiyesleri ve tektonik evrimi, KB Anadolu, Türkiye: Jeoloji Müh. 29, 37-46.
- Siyako, M.; Bürkan, K.A. and Okay, A.I., 1989, Tertiary geology and hydrocarbon potential of the Biga and Gelibolu peninsulas. Turkish Assoc. Petrol. Geol. Bull , 1, 183-200.
- Şengör, A.M.C. and Yılmaz, Y., 1981, Tethyan evolution of Turkey: a plate tectonic approach: Tectonophysics, 75, 181-241.
- Şentürk, K. and Okay, A.I., 1984, Blueschists discovered east of Saros Bay in Thrace: MTA Bull., 97/98, 72-75, Ankara.
- Turgut, S.; Siyako, M. and Dilki, A., 1983, Trakya havzasının jeolojisi ve hidrokarbon olanakları: Türk. Jeol. Kongr. Bull., 4, 35-46.

ABSTRACTS OF THE PAPERS PUBLISHED ONLY IN THE TURKISH EDITION OF THIS BULLETIN

GEOLOGY OF THE NIKSAR-ERBAA AND DESTEK REGION

H. Tahsin AKTİMUR*; Şerafettin ATEŞ*; M. Emin YURDAKUL*; M. Ender TEKİRLİ* and Mustafa KEÇER*

ABSTRACT.- The basement rocks of the investigated area, situated near Niksar, Erbaa and Destek are crossed by the North Anatolian Fault they comprise Turhal group metamorphic rocks of Permo-Triassic age. It is unconformably overlain by consisting of a sedimentary sequence of Liassic-Upper Eocene age deposited in the fore-arc basin of the Eurasian continent. The study area is in the suture zone between Eurasian and Anatolian plates. Thus it is affected by a north-south compression resulting in east-west trending thrusts in relation to formation of the North Anatolian Fault in the neotectonic period. Continental sedimentation took place in basins during Pliocene. Later activity of the North Anatolian Fault caused formation of pull-apart basins of Niksar, Erbaa-Taşova regions.

PETROGRAPHY AND ORIGINE OF THE MIDDLE DEVONIAN DOLOMITES (ŞAFAKTEPE FM.) IN THE GEYİKDAĞI UNIT (EAST TAURUS), TUFANBEYLİ-SAİMBEYLİ

BakiVAROL**

ABSTRACTS.- The middle Devonian dolomites exposed in the Autochthonous Geyikdağı unit (East Taurus) had resulted in dolomitization of Amphipora-bearing reefal limestones along with ostracod-algal laminated limestones. The dolomitic unit is composed of homogenous, mottled, laminated and banded (zebroid) types of dolomites. Dolomitization took place in the different timing, namely early and late diagenetic. The early diagenetic ones underwent mixing-water diagenesis (marine-fresh water) on a tidal flat environment. Their isotopic signature ($\delta^{18}\text{O} = -2.48$ to 0.039‰ ; $\delta^{13}\text{C} = 0.079$ to 3.18‰) also fits this dolomitization model. The second type, late diagenetic dolomites (epigenetic dolomite) are coarser crystalline than the earlier ones, and their isotopic composition became more negative or greatly diminished ($\delta^{18}\text{O} = -10.75$ to -8.36‰ ; $\delta^{13}\text{C} = -0.63$ to 1.45‰), this suggests increasing temperature during dolomitization. The late diagenetic dolomitization invoked recrystallization and dissolution of the early diagenetic dolomites. Additionally, coarsely crystalline white dolomites (saddle dolomites) precipitated in the dissolution vugs, and subsequently some ore deposits emplaced within the late diagenetic dolomites.

AN APPROACH TO THE ORIGIN OF KEBAN LEAD-ZINC MINERALIZATIONS, ELAZIĞ, TURKEY: A PRELIMINARY STUDY

Ayhan YILMAZ*; Taner ÜNLÜ** and İ. Sönmez SAYILI**

ABSTRACT. _ Mineralizations at Keban and its surroundings are generally observed at the contacts of granitoids and epimetamorphic rocks, in Nimri formation and in Keban marbles. Lead-zinc mineralizations in this region are previously interpreted as skarn type occurrences associated with granitoids. In this study, predominantly carbonate mineralizations in the carbonate rocks of Nimri formation and sulphide and carbonate ores within the Keban marbles are investigated. As a result of mineralogical, petrographical and geochemical studies, some significant evidences indicate that the mineralizations are not directly related with the skarn type associated with granitoids. According to the limited data collected during this study, the view that the mineralizations, present in Nimri formation and Keban marble, are mobilized with the influence of granitoids becomes significant. Mineralizations taking place earlier than mobilization are discussed by exhalative sedimentary (SEDEX) type and Mississippi Valley Type (MVT) relying on the present data. Some evidence is found for SEDEX type. While primary occurrences are getting their new positions by means of secondary processes, metallic contents of primary occurrences are enriched. Mobilizations related with metamorphism and/or granitoid impact and enrichment processes caused by weathering are out of the study. The main result of this study is the necessity of new other revitalization of discussions about the origin of primary occurrences for contribution to science and economy.

INTRODUCTION

The Keban region has been subjected to a number of investigations and studies of many geologists because of copper-molybdenum-fluorite-tungsten-vanadium ores known since the 18. century and engineering problems with Keban dam located at the north of Keban town.

Lithologies in the studied area have been investigated and the regional stratigraphy is attempted to be constructed by various geologists at different times. The approaches by those geologists for lithostratigraphic sequence are correlatively illustrated in Figure 1. Studies about the basement are represented by Özgül, 1981 and Özgül and Turşucu, 1984.

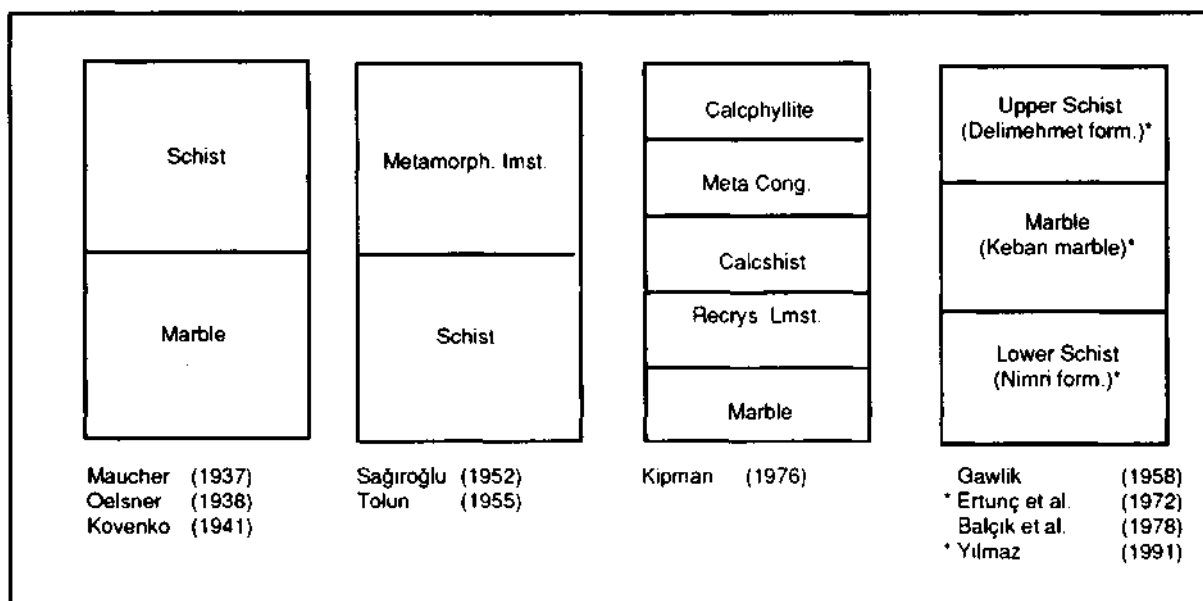


Fig. 1 - Lithostratigraphic sequences around Keban schematized according to various authors.

The major mining geological studies made in this region are as follows: Fishbach, 1900; Ami, 1937; Maucher, 1937; Kovenko, 1941; Kumbasar, 1964; Ziserman, 1969; Kineş, 1971; Köksoy, 1972; Balçık et al., 1978; Balçık, 1979; İTÜ, 1981; Yılmaz et al., 1983; Çağlayan, 1984; Öztunalı, 1985-1989.

Main technological studies are: Canbazoğlu, 1986; Demirocak et al., 1986 and Göktekin and Önal, 1986.

Two different views about the ore formation are introduced with previous mining geological studies. The first view about mineralization suggests that the origin of ore elements are related with granitic rocks based on the position of mineralizations at the contact between syenite porphyry and Keban marble and/or schists, which tend to develop into the Keban marbles. Meanwhile, accompaniment of pirometasomatic, pneumatolitic, hydrothermal stages and skarn minerals with the mineralizations form additional evidence for contact type occurrences (Fig. 2). In contrast, the second view puts forward the view that the mineralization must have originated from host rock and granitoidic intrusions into the above mentioned units and played an effective role for today's position of mineralizations mobilizing the low metal concentrations from the units (Fig. 3).-

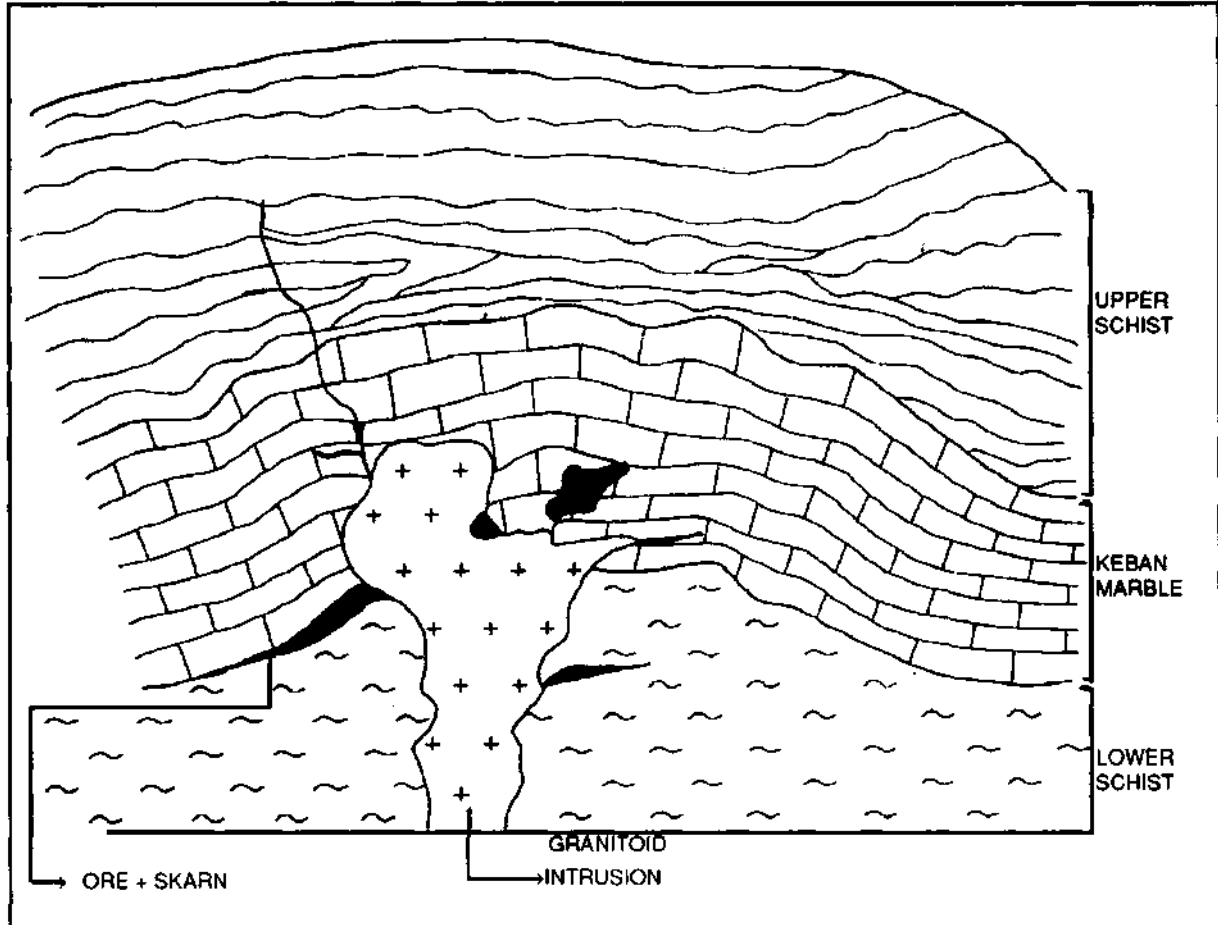


Fig. 2 - Ore forming model directly related with granitoids (schematized after Arni 1937, Köksoy, 1972 and Çağlayan, 1984).

In previous studies, mining geological data pectuar to ore occurrences described as skarn type are discussed in detail. In this study, primary occurrences, belonging to the pre-stage described as skarn, are investigated by means of mineralogical, petrographical, geochemical, and geostatistical methods and the findings obtained are discovered.

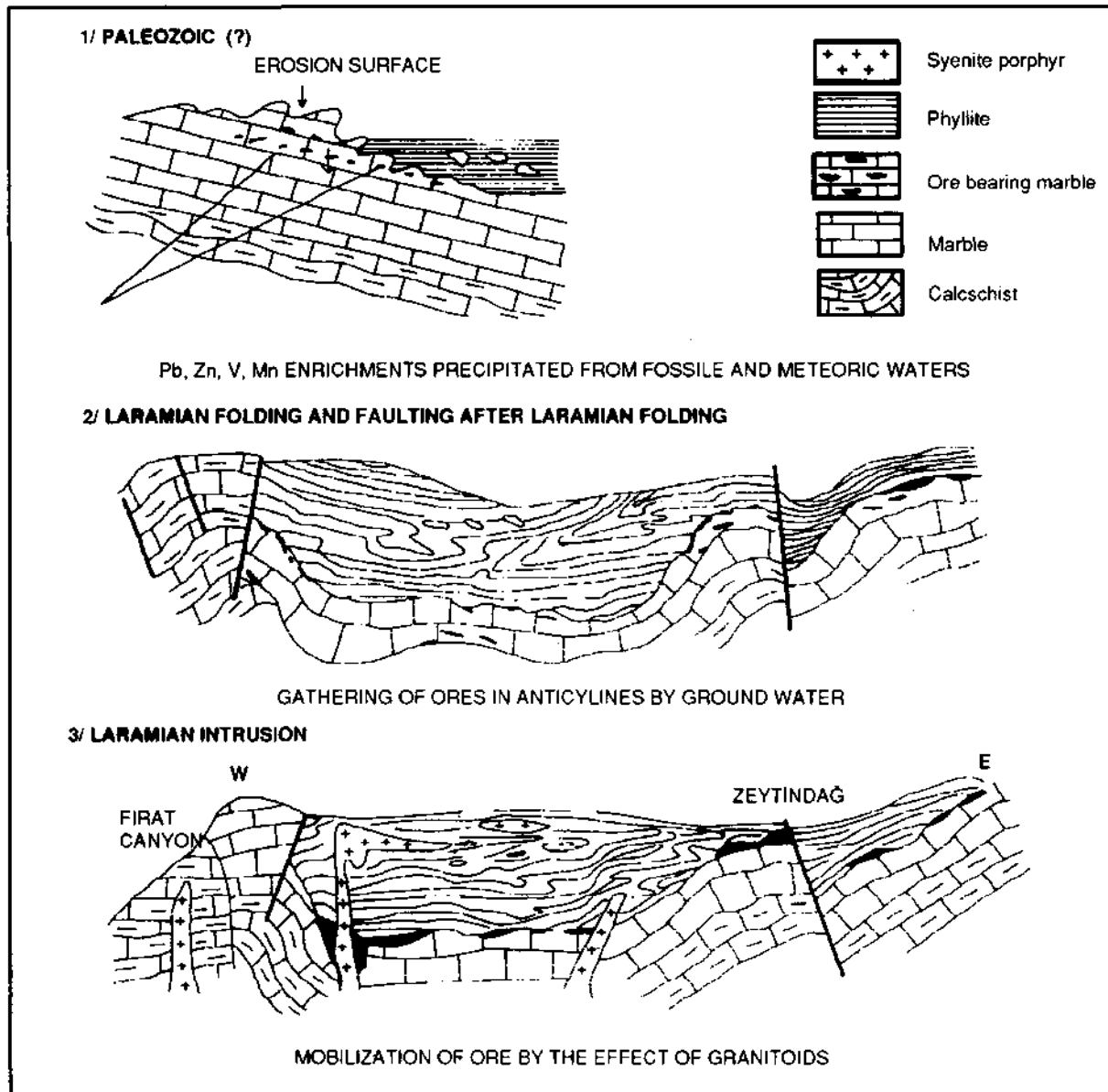


Fig. 3- Ore forming model indicating that the mineralizations in country rocks are mobilized by granitoid intrusions (after Ziserman, 1969).

GEOLOGICAL SETTING, FIELD RELATIONS AND PETROGRAPHY

The Keban area is located at the Eastern Taurus region of Tauride tectonic belt which is one of the tectonic units of Anatolia. The stratigraphic sequence of the studied area can be summarized from older to younger as Nimri formation, Keban marbles and Delimehmet formation. Low angle unconformities are seen between these units (Fig. 4 and 5). These Paleozoic (Permocarbonifer) aged units are influenced by low grade metamorphism (epimetamorphism) and are intruded by syenite porphyries which are the products of magmatic activity that occurred at the beginning of the upper Cretaceous or Eocene (Ertunç et al., 1972; Yılmaz, 1991).

At the bottom of Nimri formation crops out gray colored, porous Arapkir limestones which are made of fine grained, equigranular calcites and accessory xenomorph quartz. This unit is overlain by calcschists, a domi-

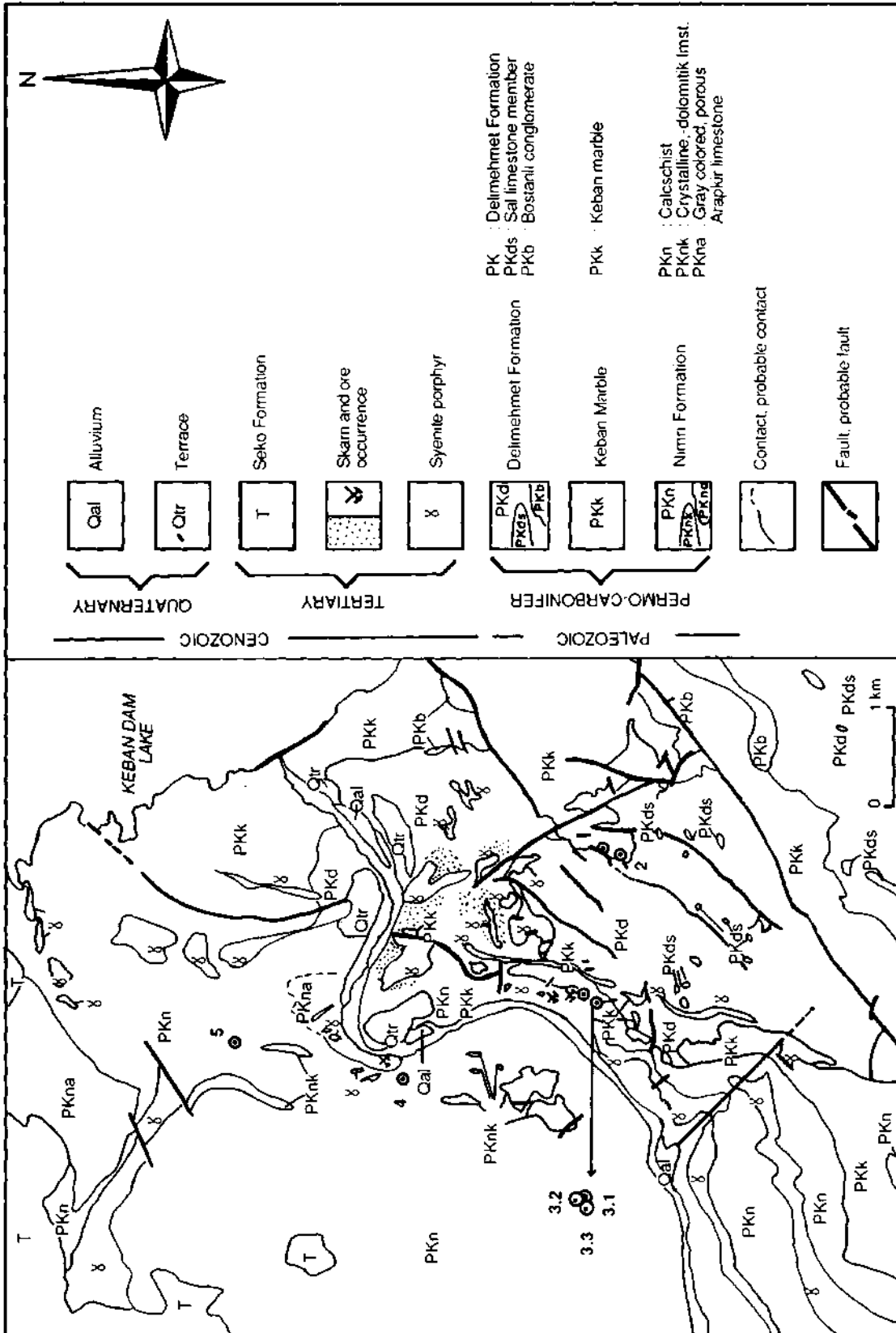


Fig. 4. Geological map of Keban and its environs and location map of sample groups which are chemically analysed [sample groups and their numbers: 1. Group: AKY. 5, 7; 1. Group: AKF. 1, 2. Group: AKY. 39; 3. 1. Group: AKF. 19, 21, 22; 3. 2. Group: AKF. 8, 9, 12, 14, 16; 3. 3. Group: AKF. 17, 4. Group: AKY. 30, 31, 34, 35; 5. Group: AKB 4, 5, 8].

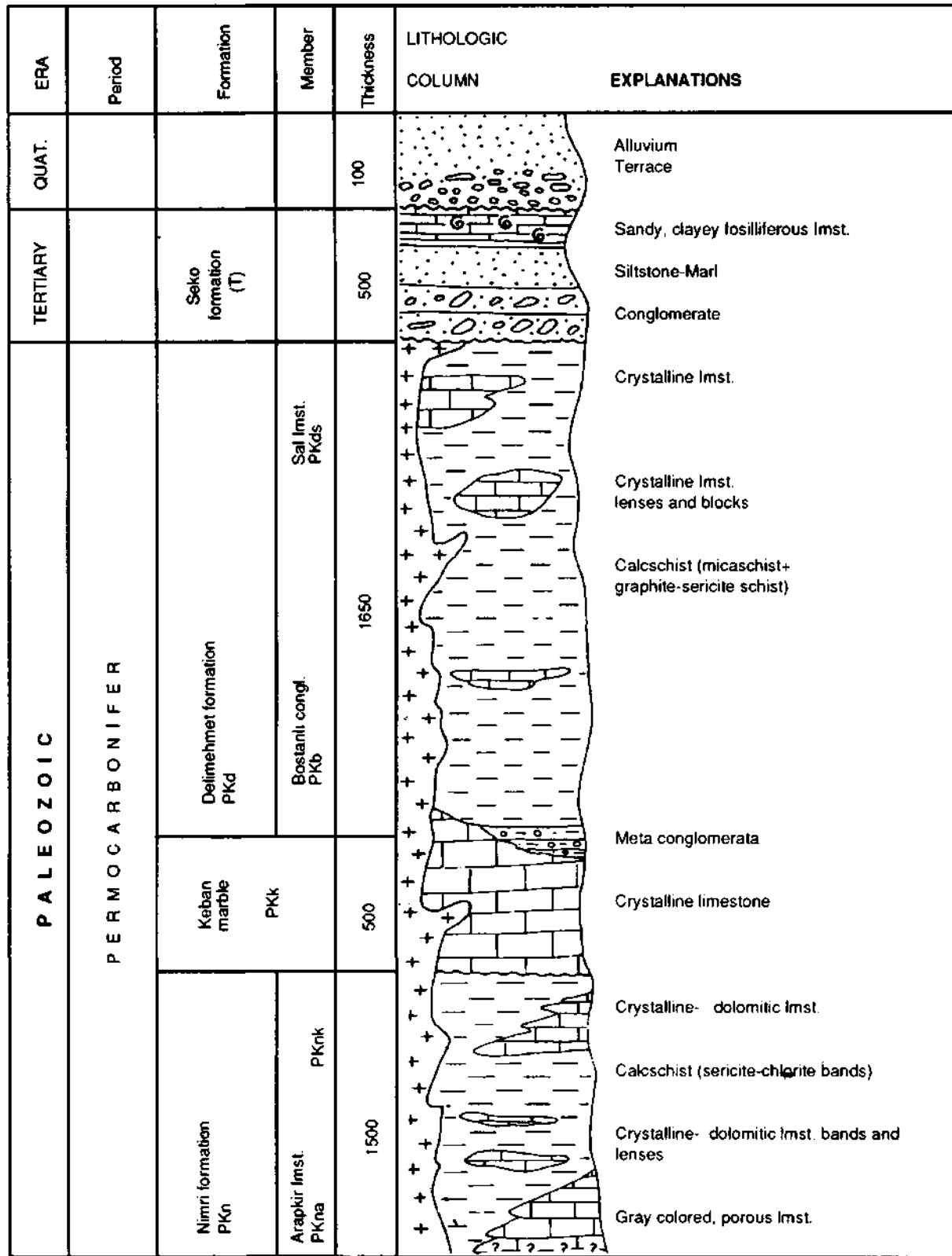


Fig. 5 - Generalized column section of studied area.

nant lithology of Nimri formation, composed predominantly of carbonate minerals, plagioclases, quartz and, at some horizons, of sericite, graphite, chlorite and opaque minerals. Showing lateral and vertical transitions to calcschists, crystalline limestones with decreasing amounts of dolomite crystals towards their upper outcrops in Nimri formation. In some places, sericite flakes, quartz, plagioclase and opaque minerals and also enrichments with iron and manganese minerals are observed within this lithology. Crystalline limestones display the characteristics of spatially dolomite bearing crystalline limestones or dolomitic limestones.

Keban marbles are pinkish-white colored, fractured and cracked, brecciated looking and composed of equigranular, medium grained calcite crystals with deformation twinnings. At the contacts of Keban marbles formed with Delimehmet formation, increasing amounts of feldspar, quartz, chlorite, sericite and, in some places, graphite minerals, are determined.

Delimehmet formation, which is characterized by calcschists, lies above the Keban marbles, while in some places, Bostanlı conglomerate lies between those lithologies. Calc schists are represented by graphite, sericite, quartz, feldspar and chlorite. Lens shaped Sal limestone member is separated from this formation and contains fine grained quartz minerals spatially.

Magmatic rocks, which intrude all these units, consist of porphyric syenite porphyry dominated by sanidines and orthoclases. Contact metamorphic minerals of garnets and epidotes are observed at the contacts between syenite porphyries and calc schists and marbles. Additionally, syenite porphyries are subjected to the sericitic, argillic and chloritic type of alteration.

POSITION AND MINERALOGY OF ORE

Ore horizons in a thickness of 0,5 to 2 meters are observed concordant to the layers of crystalline and dolomitic limestones of Nimri formations. These horizons are scattered on an approximately 8 km² region within the studied area and are found in underground mining activities especially between the elevations of 730-795 meters. Primary ore mineral occurrences, which are transformed from rhodochrosite, of psilomelane and pyrolusite and, in addition, fine grained pyrites are located in ore bearing horizons (Photos 1, 2 and 3). Psilomelane is also found as kidneylike, gel textured open fillings in the cracks. Pyrites constitute fine grained or medium grained, zoned pseudomorphs in the rocks. Both types of pyrite are replaced by limonite which can also be observed as gel textures in the cracks. Chalcocopyrite, pyrite, sphalerite, pyrrhotite and molybdenite representing the late stages are determined in addition to the above mentioned minerals.

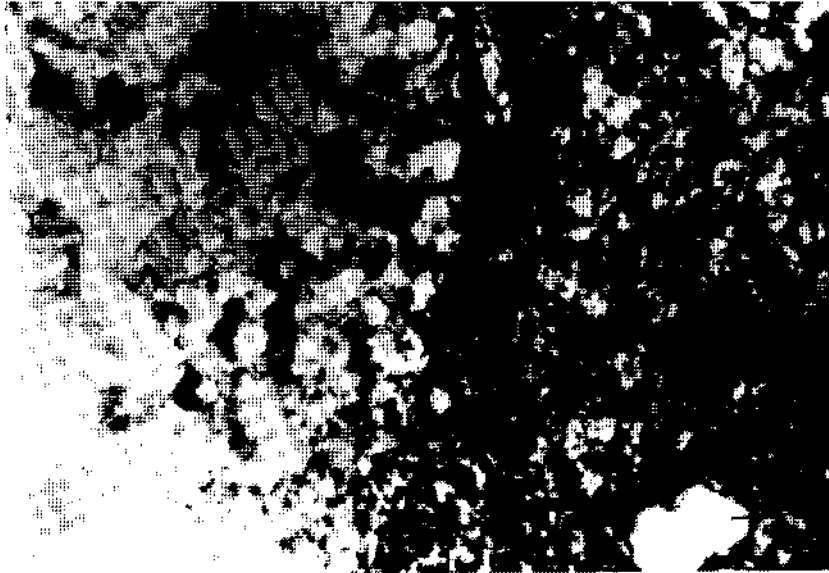
Mineralizations within Keban marbles form either small lenses in thicknesses of 2-20 meters or big lenses in a thickness of 20-50 meters. White, gray and brown colored sections caused by different mineral assemblages are distinguished in the mineralizations. Carbonaceous, sulphidic and oxidic ore mineral varieties representing different mineral paragenesis are determined in these sections.

Predominantly zinc carbonates (smithsonite) and lead carbonates (cerucite) form carbonaceous ore minerals within the carbonate rocks. A very small amount of galenite and sphalerite is also found in these rocks. Grinoid and sphalerite inclusions are determined in kidney, grape-like textured smithsonites. Limonites are developed in the cracks of smithsonites (Photos 4, 5, 6).

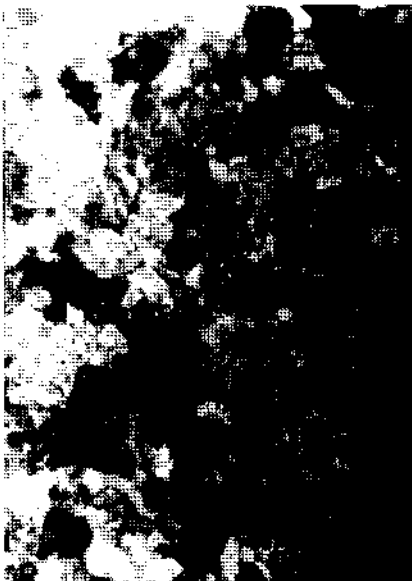
Galenite, sphalerite, pyrite, Chalcocopyrite, marcasite and arsenopyrite constitute the main sulfidic ore minerals in the Keban marbles. While pyrites and arsenopyrites accumulate in the same places, it is determined that the chalcocopyrites are converted into bornite, neodigenite, chalcocite and covellite. High and low temperature types are observed in galenites and sphalerites. Low temperature types of those are characterized by gelled textures.

Goethite and lepidocrocite with pyrite relicts are determined as oxidic ore minerals in the Keban marbles. In addition, Chalcocopyrite, hematite, magnetite, rutile, anatase and chloritized augite are found in small amounts of detritic constituents in the grayish, brownish sections of Keban marbles.

a



b



c



Photo 1 - Sections in crystalline, dolomitic limestone
a) rich in calcite and manganese minerals, b) filled by calcite, c) filled by dolomite, mangan oxide minerals and a small amount of quartz
(cross nicols, X 63)

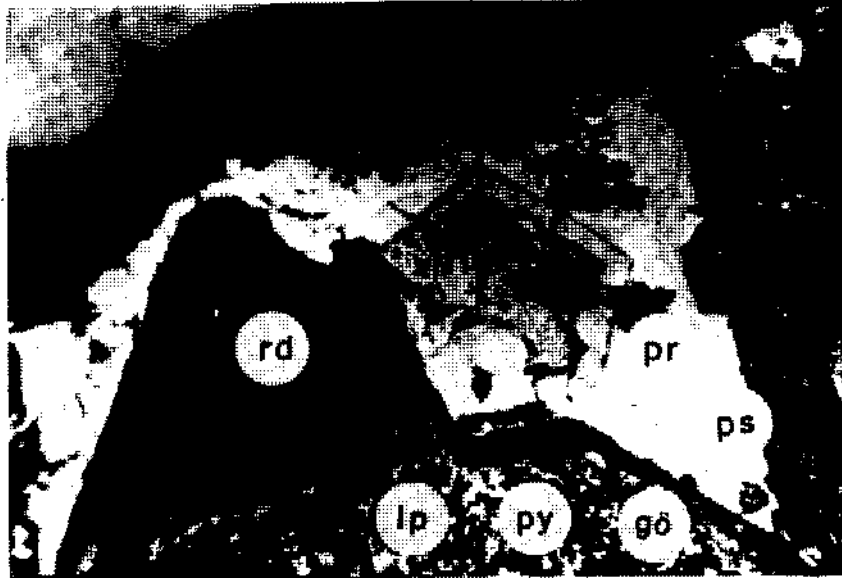


Photo 2 - Rhodocrocite (rd) replaced by pyroluzite (pr) and psilomelane (ps), pyrite (py) replaced by lepidocrocite (lp) and goethite (go) occurrences in crystalline, dolomitic limestone, (X 420, in oil).

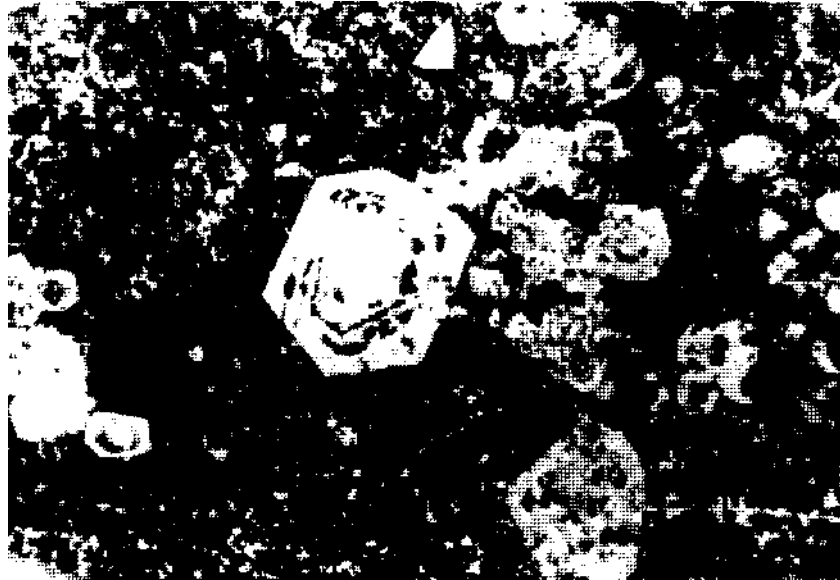


Photo 3 - Pyrite pseudomorphs replaced by limonite in crystalline, dolomitic limestone (X 420, in oil).

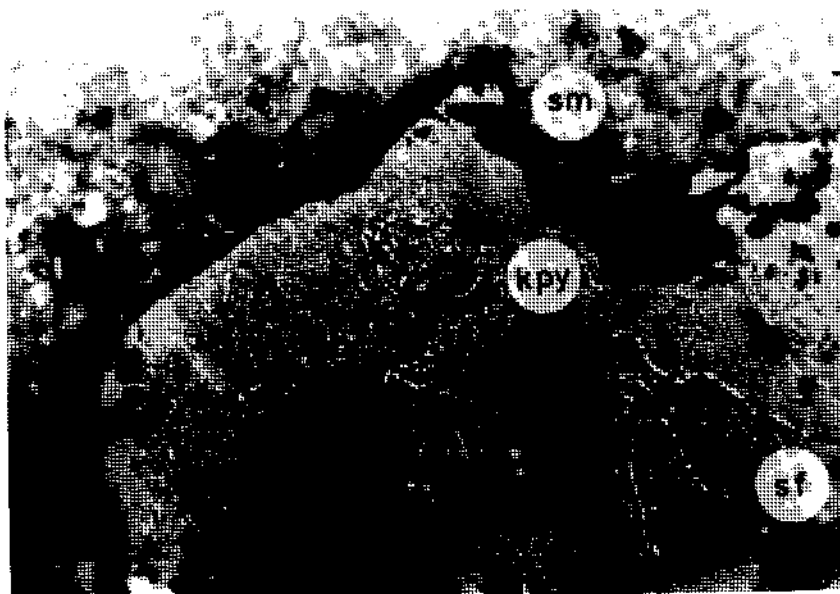


Photo 4 - Carbonate ores in Keban marbles. Smithsonite (sm), sphalerite (sf) and chalcopyrite (kpy) exolutions in sphalerite (X 420, in oil).

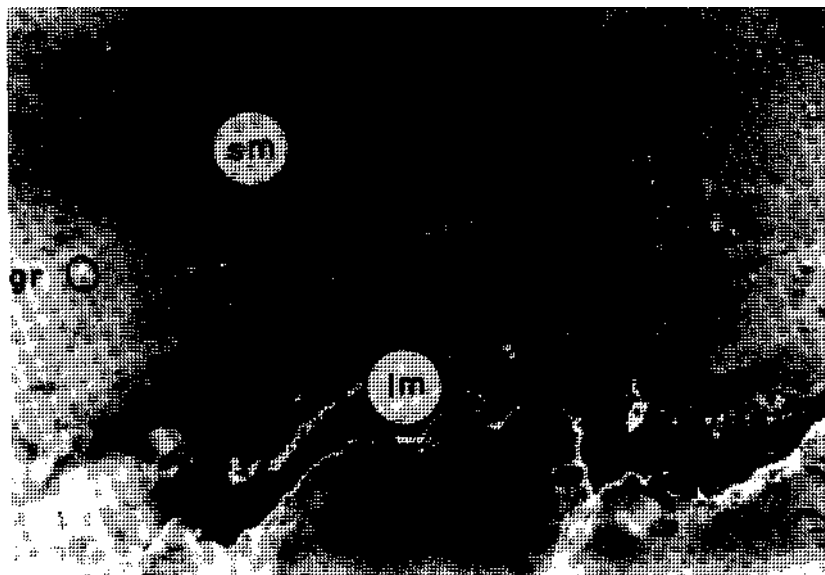


Photo 5 - Carbonate ores in Keban marbles. Grinocoid (gr) drops bearing smithsonite (sm) and limonite (lm) occurrences (X 420, in oil).

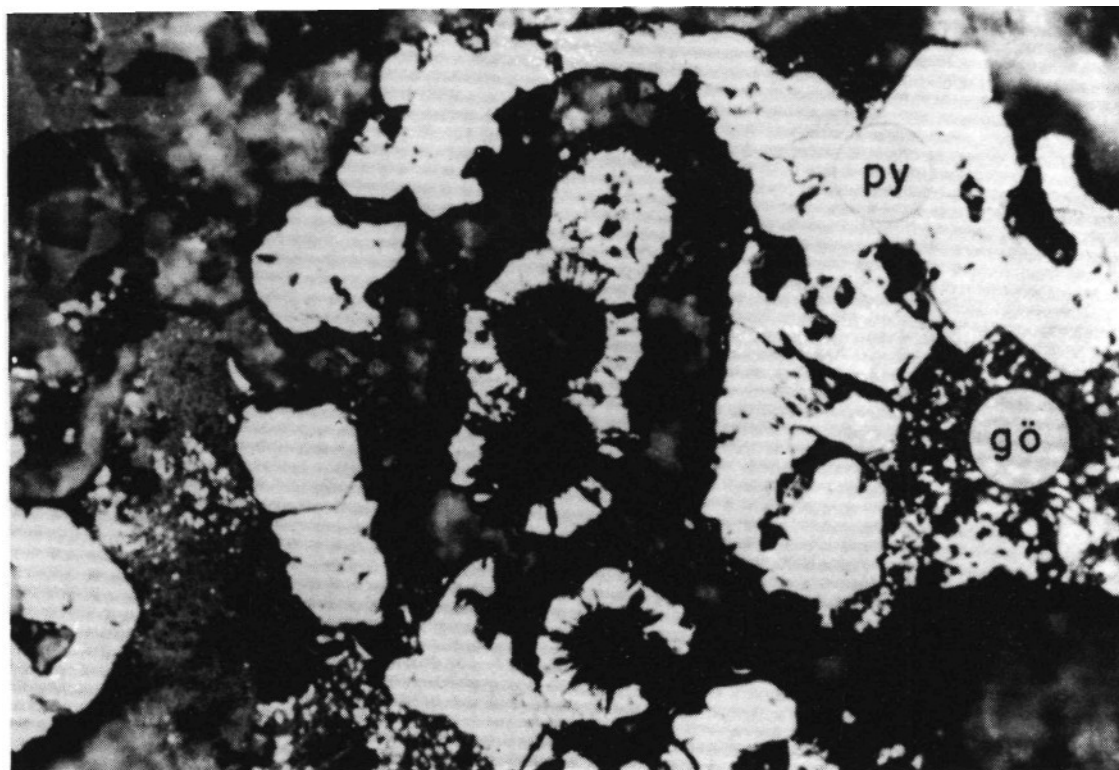


Photo 6 - Carbonate ores in Keban marbles. Goethite (go) and gel-radial pyrite (py) occurrences (X 420, in oil).

Delimehmet formation is rather poor for ore minerals and only pyrites and limonites occur in this formation.

Enrichments with ore minerals are spatially observed at the contacts of syenite porphyries with the country rocks.

GEOCHEMISTRY AND GEOSTATISTICS

Ore and host rock samples, collected from Keban area, are chemically analyzed at Etibank laboratories. The results of these chemical analyses are shown in Table 1 and the lower and upper limits of all geochemical data are listed in Table 2.

Dolomitic limestone levels of Nimri formation are the oldest units in the area, which contain Pb-and Zn concentrations. However, low PbO and ZnO values are characteristics of these units.

Carbonate type ores within the Keban marbles are Ca, Mg, Mn, Fe, Pb and Zn carbonate minerals, which are later replaced by oxide minerals. Sulphide ores in Keban marbles are characterized by high Mn, Fe, Pb and Zn rates and high clay contents. Iron cap formations of Keban marbles show Fe and Al enrichments of surficial oxidation conditions.

Hydrothermal formations in Nimri formation, which show different features from all above mentioned mineralization bearing levels, are represented by phlogopite and quartz and high K_2O rates are evident.

Relations of various elements with each other in all samples are graphically represented in Figure 6 and distribution relationships of Pb and Zn elements versus Ca, Mg, Al and Si are shown at Table 3. In this table Ca and Mg are the main components of carbonate minerals and Al and Si of clay minerals. Pb and Zn elements exhibit decreasing relationships with carbonate minerals (i.e. Ca and Mg components) and increasing relationships with clay minerals (i. e. Al components). Variable distribution relationship of Pb and Zn elements with Si of clay minerals is caused by the mobile character of Si element against secondary events. According to these results, the decrease of Pb and Zn element contents with the increase of carbonates, and increase of the same contents with the increase of clays on the one hand, and on the other the increase of carbonates against decreasing clays in the environment, all suggest a gradationally sedimentation of Pb and Zn elements with clays and carbonates.

Table 1 - The results of chemical analyses of ore and country rock samples collected around Keban, realized at Ettbank Laboratories (Yilmaz, 1991 for analytical methods)

UNIT	SAMPLE NR. MARK	% SiO ₂	% Al ₂ O ₃	% CaO	% FeO*	% K ₂ O	% MgO	% MnO	% Na ₂ O	% ZnO	% PbO	% KK	TOTAL	Ba (ppm)	Sr (ppm)	Ag (ppm)	Cd (ppm)	Cu (ppm)	Ni (ppm)	Co (ppm)	EXPLANATIONS
K E B A N	1 AKF- 1	1.86	1.98	41.66	0.77	0.040	9.14	1.12	0.168	0.31	0.19	39.80	97.038	2000	400	ND	ND	ND	60	40	KEBAN MARBLE
	13 AKY- 5	1.79	2.85	41.90	0.14	0.030	9.75	0.24	0.138	0.09	0.03	40.33	97.288	900	700	ND	ND	ND	ND	ND	
	16 AKY- 7	1.92	0.96	48.80	0.18	0.043	3.35	0.61	0.837	0.06	0.05	42.00	98.81	2000	400	ND	ND	100	ND	ND	
M A R B L E S	15 AKY- 39'	6.80	12.41	0.04	70.29	0.063	0.56	0.76	0.174	0.06	0.88	7.20	99.237	400	600	103	ND	1100	60	100	IRON CAP OF KEBAN MARBLE
	7 AKF- 19	1.76	13.43	11.28	23.31	0.042	1.67	1.86	0.208	39.41	4.49	1.28	98.74	300	100	290	1600	300	ND	ND	CARBONATE TYPE ORE
	8 AKF- 21	1.86	10.22	12.36	19.15	0.045	1.91	1.78	0.140	44.08	0.74	3.57	95.855	900	800	ND	200	ND	ND	ND	
	9 AKF- 22	2.00	9.69	10.44	22.78	0.025	1.41	1.51	0.101	43.04	0.71	3.15	94.856	700	200	10	800	100	ND	ND	
	2 AKF- 8	12.40	14.75	0.64	36.98	0.054	2.75	0.43	0.220	3.73	2.88	18.59	93.424	400	700	2850	ND	7100	80	60	SULPHIDE TYPE ORE
	3 AKF- 9	14.75	12.27	1.48	41.01	0.049	0.20	2.36	0.140	0.62	4.13	17.43	94.439	700	300	395	ND	1900	80	60	
	4 AKF- 12	17.84	32.56	1.68	9.11	0.051	0.07	0.46	0.202	7.47	13.62	9.91	92.973	800	400	2050	200	1000	ND	ND	
5 AKF- 14	21.70	22.91	1.30	20.63	0.024	0.07	0.83	0.119	7.26	15.62	6.77	97.233	500	300	1575	200	1100	ND	ND		
6 AKF- 16	16.40	21.45	1.20	21.50	0.052	0.20	1.29	0.216	15.25	5.74	8.39	91.688	400	600	1250	400	1100	ND	ND	COMPLEX TYPE ORE	
14 AKF- 17	0.50	20.96	7.70	12.32	0.027	1.31	3.24	0.163	23.85	27.47	0.72	98.26	800	800	2000	400	1600	ND	ND		
N I M R I F O R M.	10 AKB- 4	2.70	6.77	38.02	2.15	1.255	8.19	1.64	0.321	0.16	0.68	29.97	91.856	800	300	10	ND	200	ND	ND	HYDROTHERMAL OC- CURRENCES IN NIMRI FORM.
	11 AKB- 5	10.96	8.40	35.84	2.79	1.265	0.73	1.41	0.168	0.15	0.09	29.36	91.163	900	600	ND	ND	300	ND	ND	
	12 AKB- 8	3.18	6.51	42.64	1.34	1.305	1.21	1.38	0.410	0.14	0.40	32.93	91.445	1000	1000	ND	ND	100	ND	ND	
FORM.	18 AKY- 30	N.A.	N.A.	30.92	15.87	N.A.	N.A.	7.49	N.A.	0.24	0.04	40.98	95.539	ND	N.A.	N.A.	N.A.	N.A.	N.A.	N.A.	DOLOMITIC LMST. IN NIMRI FORM.
	17 AKY- 31	N.A.	N.A.	52.91	5.43	N.A.	N.A.	1.07	N.A.	0.01	ND	42.63	102.05	ND	N.A.	N.A.	N.A.	N.A.	N.A.	N.A.	

Fe O*: Total iron, ND: Below detection limit, N.A.: Not analysed
Chemical analyses are performed on samples dried at 105° C.

Table 2 - Lower and upper limits of the results of chemical analysis given in Table 1

EXPLANATIONS		NUMBER OF SAMPLES	Pb O %	Zn O %	Ca O %	Mg O %	Fe O* %	Mn O %	KK %	Al ₂ O ₃ %	Si O ₂ %	Na ₂ O %	K ₂ O %	Ba ppm	Sr ppm	Ag ppm	Cd ppm	Cu ppm
K E B A N M A R B L E	KEBAN MARBLE IRON CAP	1	8800 ppm	600 ppm	0.0	0.6	70.3	0.8	7.2	12.4	6.8	0.2	0.1	400	600	103	ND	1100
	KEBAN MARBLE COMPLEX TYPE ORE	1	27.5	23.9	7.7	1.3	12.3	3.2	0.7	21.0	0.5	0.2	0.0	800	800	2000	400	1600
	KEBAN MARBLE SULPHIDE TYPE ORE	5	2.9-15.6	0.6-15.3	0.6-1.7	0.1-2.8	9.1-41.0	0.4-2.4	6.8-18.6	12.3-32.6	12.4-21.7	0.1-0.2	0.1	400-800	300-700	395-2850	200-400	1000-7100
	KEBAN MARBLE CARBONATE TYPE ORE	3	0.7-4.5	39.4-44.1	10.4-12.4	1.4-1.9	19.2-23.3	1.5-1.9	1.3-3.6	9.7-13.4	1.8-2.0	0.1-0.2	0.0-0.1	300-900	100-800	10-290	200-1600	100-300
	KEBAN MARBLE	3	300-1900 ppm	600-3100 ppm	41.7-48.8	3.4-9.8	0.1-0.8	0.2-1.1	39.8-42.0	1.0-2.9	1.8-1.9	0.1-0.8	0.0	900-2000	400-700	ND	ND	ND-100
N I M R I F O R M.	NIMRI FORMATION DOLOMITIC LIMESTONE	2	400 ppm	100-2400 ppm	30.9-52.9	N.A.	5.4-15.9	1.1-7.5	41.0-42.6	N.A.	N.A.	N.A.	N.A.	N.A.	N.A.	N.A.	N.A.	N.A.
	NIMRI FORMATION HYDROTHERMAL OCCURRENCES	3	900-6800 ppm	1400-1600 ppm	35.8-42.6	0.7-8.2	1.3-2.8	1.4-1.6	29.4-32.9	6.5-8.4	2.7-11.0	0.2-0.4	1.3	800-1000	300-1000	ND-10	ND	100-300

Abbreviations like in Table 1.

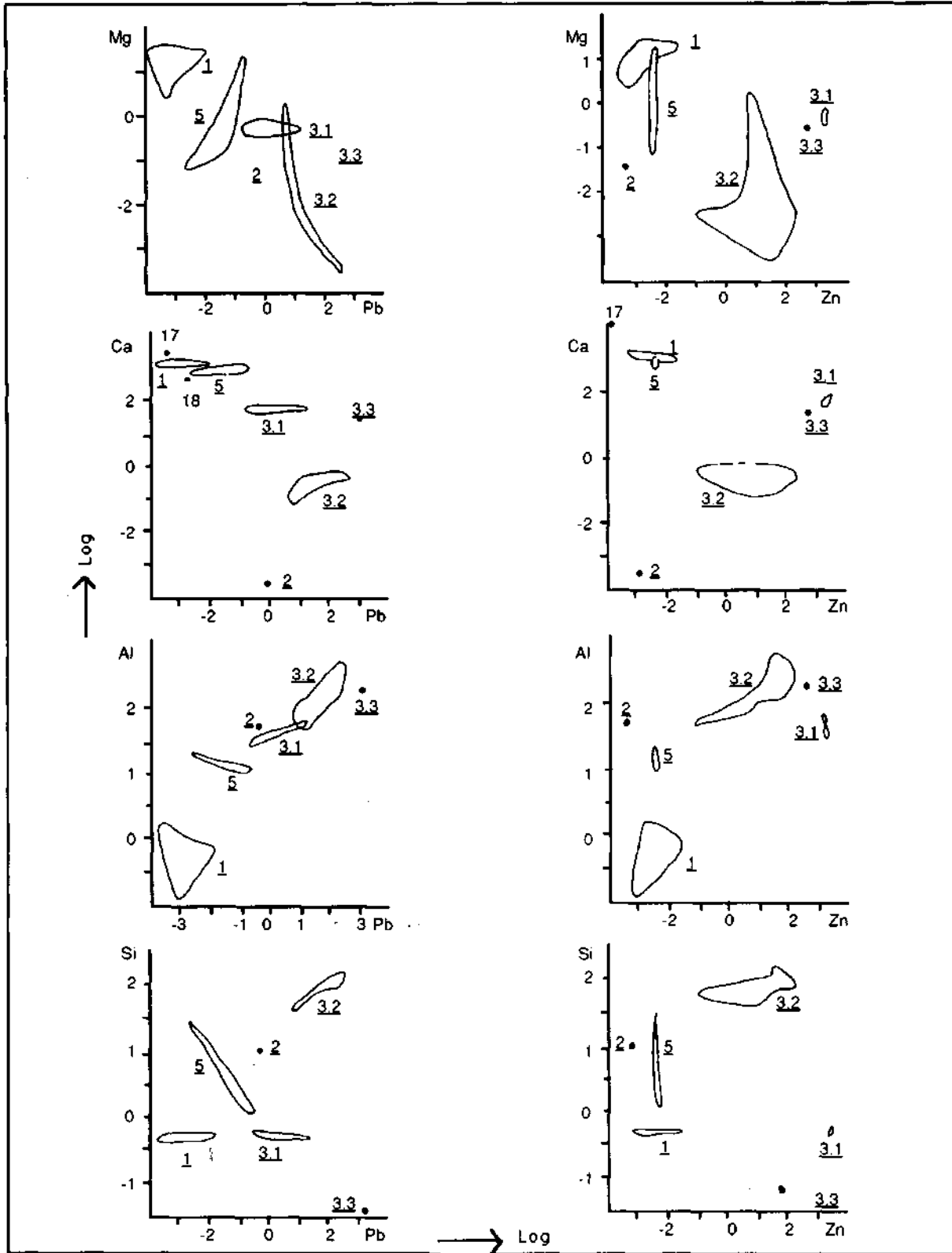


Fig. 6 - Logarithmic distribution relationship of Pb and Zn elements versus Mg, Ca, Al and Si in all groups. (see figure-4 for sample groups and Table 6 for 17. and 18. samples).

Table 3 - Relationship of Pb and Zn elements versus Ca, Mg, Al and Si in all groups

METALS	CARBONATE		CLAY	
	Ca	Mg	Al	Si
Pb	decreasing relationship	decreasing relationship	increasing relationship	variable relationship
Zn	decreasing relationship	decreasing relationship	increasing relationship	variable relationship

Keban marbles and two group of carbonate ores within them are summarized as one group under the name of carbonate samples and sulphide samples in Keban marbles as one group under the name of sulphide samples and these new two groups are subjected to correlation analyses (i.e. cluster and factor analyses). Element associations are listed in Table 4 and Table 5.

1. Group with high positive correlation (Al, Fe, Mn, Zn, Pb, Cd and Ag) observed in total rock analyses (Table 4) belonging to carbonate samples exhibits association of metals with clay minerals. Nonexistence of Si element in this group is supposed to be caused by decomposition of aluminum silicates and thus, while Si is removed from the environment, aluminium hydroxide becomes enriched. 2. Group with high positive correlation belonging to carbonate samples (Ca, Mg) is a result of existence of dolomite formation in the environment and necessity of dolomite formation in the environment and necessity of dolomite during ore formation process.

1. Group with medium positive correlation (Al, Fe, Mn, Zn, Pb, Cd, Ag and Cu) belonging to carbonate samples differ from 1. Group of high positive correlation with the addition of only Cu element to the same association. On the contrary, 2. Group with medium positive correlation (Ca, Mg, Sr, Ba, Co, Ni, Si, Na and K) contains Ca, Mg, Sr, and Ba elements, which are expected to take place in carbonates, and Co and Ni elements (probably in pyrite), which are expected to be enriched in clay minerals and Si element, which becomes free during the process of aluminium hydroxide from clay minerals. Na and K, here, are probably related with clay composition.

Table 4 - Element groups and associations determined from carbonate samples of Keban marbles

CARBONATE SAMPLES																					
High Positive Correlation ($r > + 0.75$)																					
1. Group:	Al,	Fe,	Mn,	Zn,	Pb,	Cd,	Ag														
2. Group:	Ca,	Mg																			
Middle Positive Correlation ($+ 0.34 < r < + 0.75$)																					
1. Group:	Al,	Fe,	Mn,	Zn,	Pb,	Cd,	Ag,	Cu													
2. Group:	Ca,	Mg,	Sr,	Ba,	Co,	Ni,	Si,	Na,	K												
High Negative Correlation ($r < - 0.70$)																					
Al,	Fe,	Mn,	Zn,	Pb,	Cd,	Ag,	Cu							Ca,	Mg,	Sr,	Ba				
1. Group								2. Group													
Middle Negative Correlation ($- 0.35 > r > - 0.70$)																					
Al,	Fe,	Mn,	Zn,	Pb,	Cd,	Ag,	Cu							Ca,	Mg,	Sr,	Ba,	Co,	Ni,	Si,	Na
1. Group									2. Group												

Table 5 - Element groups and associations determined from sulphide samples of Keban marbles

SULPHIDE SAMPLES																
High Positive Correlation ($r > + 0.75$)																
1. Group:	Al,	Zn,	Pb,	Cd,	Ca,	Si,	Ba									
2. Group:	Mg,	Sr,	Co,	Ni,	Na,	K,	Cu									
Middle Positive Correlation ($+ 0.34 < r < + 0.75$)																
1. Group:	Al,	Zn,	Pb,	Cd,	Ca,	Si,	Ba,	Mn								
2. Group:	Mg,	Sr,	Co,	Ni,	Na,	K,	Cu,	Fe,	Ag							
High Negative Correlation ($r < - 0.70$)																
Al,	Pb,	Cd,	Ca,	Si				Mg,	Sr,	Co,	Ni,	K,	Cu,	Fe,		
1. Group:								2. Group								
Middle Negative Correlation ($- 0.40 > r > - 0.70$)																
Al,	Pb,	Cd,	Ca,	Si,	Zn,	Ba,	Mn	Mg,	Sr,	Co,	Ni,	K,	Cu,	Fe,	Na,	Ag
1. Group								2. Group								

High negative correlation are determined in two groups of carbonate samples. 1. Group consisting of Al, Fe, Mn, Zn, Pb, Cd, Ag and Cu, points out metals and aluminium hydroxide, 2. Group, consisting of Ca, Mg, Sr and Ba elements, indicates dolomite formation.

What is important here is that these two groups show a highly positive correlation in themselves but a highly negative correlation between each other. The elements of the first and second groups represent a highly positive correlation both in and between each other but the elements of these two groups show a highly negative correlation reciprocally. This situation displays that the elements of both groups exhibit two different behavioural features separately. On the other hand, a highly negative correlation (relationship) between two groups expresses that these two different geological events are in the necessity of being the products of developments which belong to the same environment and are directly related with each other (This geological event here is expressed with the word, association). Under the light of these opinions, high negative correlation relationship of carbonate samples suggests that the clays accompany metals on the one hand and on the other, for the sedimentation or crystallization (i.e. stabilization) of metal ions, dolomite (and/or dissolution of calcite) is needed for the equilibrium of the environment from the physicochemical point of view.

A medium negative correlation (relationship) of carbonate samples shows Al, Fe, Mn, Zn, Pb, Cd, Ag and Cu association versus Ca, Mg, Sr, Ba, Si, Na, Co and Ni association. The first association (group) reflects metals and aluminium hydroxide and second one, most heavily, dolomite and silica occurrences. As a result of decomposition of clays, aluminium hydroxide and silica become free and these two components take their place in different physicochemical environments, it means that aluminium hydroxide and metals are enriched and dissolved Si separates from the environment or with a different-geostatistical expression, Si supplies association with the elements of second group.

The above explanation of carbonate samples in Table 4 puts forward the below interpretation:

Metal rich carbonate samples in Keban marbles are the isochronal components of an environment in which clay and carbonates precipitate together. Metal concentrations together with clay components in the envi-

ronment become enriched probably with the dissolution of carbonates rich in metal ions. It is suggested that the dolomitization of dissolved carbonates are closely related with separation processes of metals from dissolved carbonates.

Original results observed from total rock analyses of sulphide samples (Table 5), symbolize the complex and hard interpretable associations observed in the formation, of sulphide mineralizations.

The results of the interpretation efforts of elements of two different group, which correlate positively with each other, and element associations of two groups, which correlate negatively with each other, can be summarized as follows:

The difficulty in the interpretation of association of both Al, Pb, Cd, Ca, Si versus Mg, Sr, Co, Ni, K, Cu and Fe with high negative correlation of sulphides necessitates the cointerpretation of associations of medium negative correlation (Al, Pb, Cd, Ca, Si, Ba, Mn versus Mg, Sr, Co, Ni, K, Cu, Fe, Na and Ag). Therefore, with the useful of elements of coexisting minerals, which accompany to ore minerals and are expected to reflect the environmental conditions, it can be realized that they will interpretate together with ore minerals as a whole.

At the association of Al, Pb, Cd, Ca, Si, Zn, Ba and Mn comprising of the first group, Pb, Zn and Ca are used for the formation of galenite and sphalerite, Al and Si for clay minerals and Ca, Ba and Mn for relatively low amounts of carbonate minerals which are associated with clay minerals.

To the contrary of the association of Ca to Mg in carbonate samples, in this group Ca is not accompanied by Mg and so Mg takes place in the second group. Again, Al and Si observed in carbonate samples are localized in different groups. These elements, found together in the first in sulphides, exhibit another difference. That is, an environment occurs, which differs from the one that is formed probably dissolution of metal carbonates and observed in carbonate samples, in this environment, conditions of almost no dissolution of carbonates, no dolomitization and destabilization of clay minerals become important.

Thus, an occurrence form of sulphides in the compositions of directly primary formation of galenite and sphalerite becomes more and more visible.

Fe, Cu, Co, Ni, Ag indicate particularly pyrite and chalcopyrite as sulphide minerals in the association of Mg, Sr, Co, Ni, K, Cu, Fe, Na and Ag which consist of the second group. Very low amount of Mg, Sr, Na and K point out probably the sea water (?). Thus, the second group element association suggests that particularly pyrite and chalcopyrite rich sulphide mineralizations are most probably affected by seawater.

The above explanation of sulphide samples in Table 5 suggests the below interpretation:

Studies, carried out on sulphide samples in Keban marbles, point out that galenite and sphalerite and also pyrite and chalcopyrite are the main constituents of sulphides and these two mineral associations occurred successively. The occurrences of less carbonate but abundant clay components and probably effects of seawater can not be ignored in such an environment where an occurrence form expressed by different mineral phases may become original.

SYNTHESIS

Different genetic interpretation basing on the analyses carried out on ore and host rocks of Keban and its mineralizations around, which are classified as directly related with granitoids in earlier studies, and especially geochemical-geostatistical studies, urges detailed evaluation of this subject. For this reason, four samples (AKY-30, 31, 34 and 35) taken from the carbonate levels which are observed concordant to the schists basing on field observation and which take place in Nimri formation, which is the oldest unit in this region, are analyzed at MTA laboratories.

Chemical analyses, XRD and DTA results of these samples are totally listed in Table 6.

Table 6 - The results of chemical, X-ray diffraction and DTA analyses of four samples in Nimri formation made in MTA Laboratories. (Yılmaz, 1991 for analytical methods)

RATIOS	ELEMENTS	AKY. 31	AKY. 30	AKY. 34	AKY. 35	
%	Si O ₂	1.40	5.00	1.00	2.40	
	Al ₂ O ₃	1.20	3.15	4.60	3.55	
	Fe ₂ O ₃	1.55	12.63	14.61	34.48	
	MnO	2.03	10.04	30.19	26.05	
	TiO ₂	0.07	0.07	0.03	0.02	
	CaO	49.50	29.90	14.40	8.10	
	MgO	1.90	6.00	0.15	0.55	
	Na ₂ O	< 0.10	0.20	0.15	0.10	
	K ₂ O	0.15	0.20	0.15	0.15	
	P ₂ O ₅	0.10	0.10	0.10	0.10	
	A.Z.	41.70	31.45		16.50	
				BaO	2.40	1.10
				SO ₃	20.00	
				H ₂ O	11.94	
		S	0.03	0.17		0.41
		Pb	0.06	0.02	0.26	3.34
		Zn	0.05	0.03	1.13	2.35
	TOTAL	99.74	98.96	101.11	99.20	
	BaO	< 0.02	< 0.02			
	Zr	< 0.01	< 0.01	< 0.01	< 0.01	
	Sr	< 0.10	< 0.10	< 0.10	< 0.10	
ppb	Au	11	150	17	11	
ppm	Ag	6.2	5.4	28.2	162	
	As	37	380	150	173	
	Sn	< 50	< 50	< 50	< 50	
	Co	< 10	< 10	< 10	< 10	
	Cr	< 10	13	22	25	
	Cu	< 10	24	33	33	
	Ni	< 10	< 10	< 10	< 10	
	V	< 10	15	19	20	
	Cd	< 10	< 10	57	10	
	Sb	< 20	< 20	31	200	
	Bi	< 50	< 50	< 50	< 50	
	Rb					
XRD RESULTS	Calcite (abundant)	Manganocalcite ? - Dolomite (abund.)	Gypsum (abundant)	Goethite ? (abund. ?)		
	Dolomite (rare)	Calcite (less)	Clay min. (rare)	Quartz (very rare ?)		
	Rhodocrocite? (rare)	Quartz (very rare)	Dolomite (rare)	Hematite ? (abund. ?)		
	Quartz (rare)		Calcite (very rare)	Clay min. (very rare) (sericite ?)		
	Clay minerals (rare)		Barite ? (very rare)	Amorph. substance in diffractogram		
DTA RESULTS	Calcite	Dolomite	Gypsum	Goethite ?		
		Calcite	Calcite ?	Calcite ?		
			Clay min (Kaolinite ?)	Clay min. ?		
			Gypsite ? or Goethite			

The sample AKY-31 displays a lot of similarities to those samples which are collected mineralogically from crystalline-dolomitic limestone lithologies of Nimri formation. Micro photographs of those samples are illustrated in Photo-1a in general and Photo 1b in detail. For example, carbonate part is formed by totally recrystallized, clamped calcite mosaic.

The sample AKY-30 shows a great similarity to those samples which are collected again from crystalline-, dolomitic limestones of Nimri formation. Those samples represent transition character between the samples in Photo 1 a in general and Photo 1 c in detail, and Photo 7.



Photo 7 - Solution breccia observed in crystalline-, dolomitic limestone (cross nicols, X 40).

In general sense, the sample AKY-30 has brecciated texture and coarse and medium grained dolomitic crystals are observed in less fine dolomite and ore mineral matrix. In thin sections made at the other parts of this sample, clamped, recrystallized calcite mosaic with transition to brecciated texture in some places (solution breccia) are also observed like sample AKY-31. The latter case can be schematized, like in Figure 7, in micro size.

Some feldspar (alkali feldspar?) and quartz (volcanic quartz?) mineral particles are also found in some places of solution breccia. Dolomite particles as fine dolomite sand become rich in this breccia and brecciated structure exhibit transition to fractured structure. Dolomite particles together with sericite flakes consist weak laminations in ores.

The sample AKY-34 displays another composition different from the two samples mentioned above. In this sample, gypsum minerals are widespread. Calcites in dissolved sections show radial growth structures in abundance. These structures are heavily developed in spaces and gypsum crystals accompany them. Thus, calcite and gypsum phases are met repeatedly in these spaces. Ore emplacement are also accompany to those phases.

The sample AKY-35 is microscopically characterized by enrichment of ore phases with the rock fragments represented by sericite, very rare gypsum crystals and calcite fillings in some places.

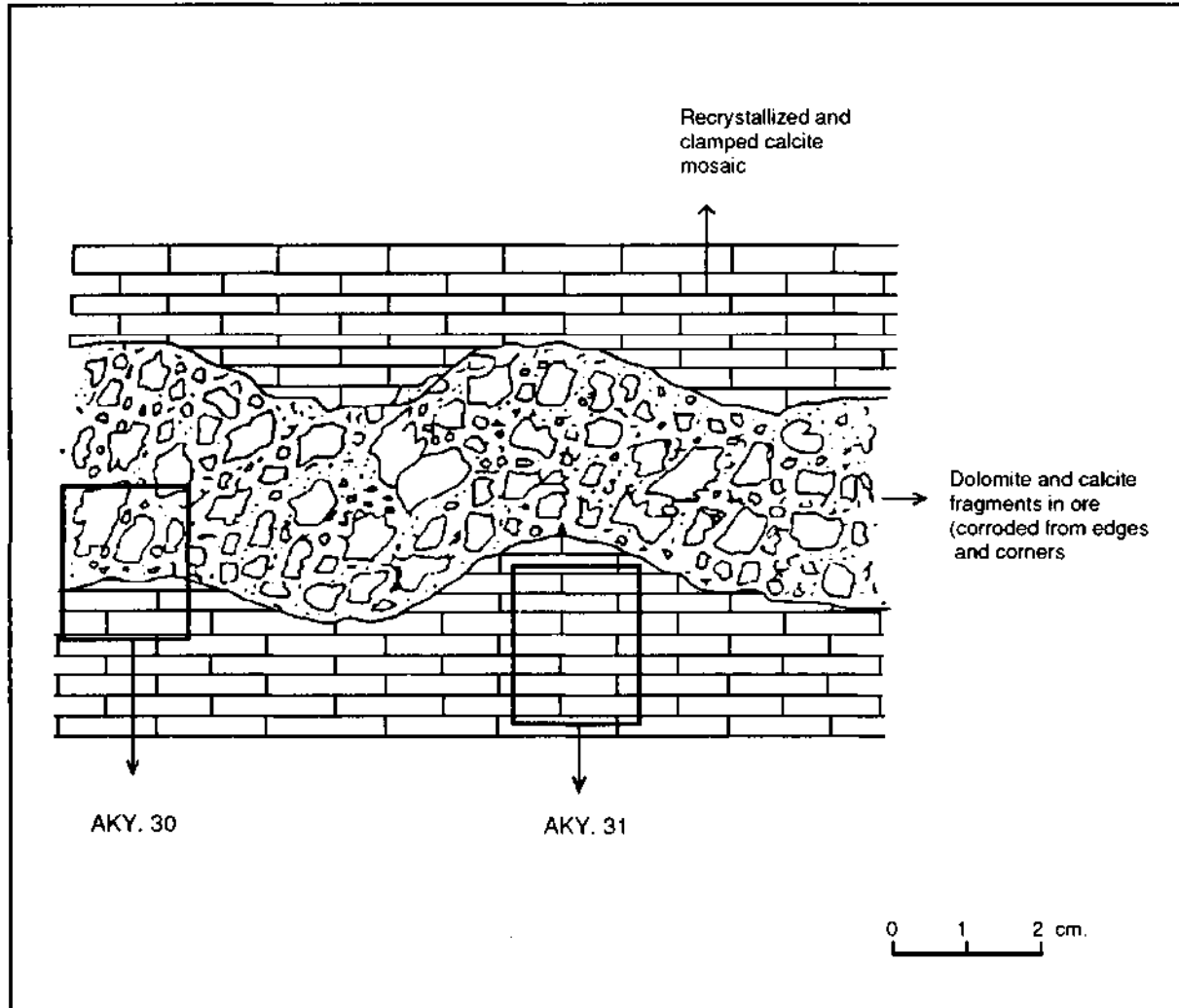


Fig. 7- Schematized transition from massive structure to breccious structure in crystalline, dolomitic limestone (symbolized places of studied two samples: AKY. 30, 31).

The sample AKY-31 formed totally calcite minerals with 49.50 % CaO and 41.70 % ignition loss rates shows very close coincident with the carbonates of Nimri formation. MgO ratio is 1.90 % and dolomitization is almost absent. The interesting point of this sample is that it contains 500 ppm Zn and 600 ppm Pb. MnO and Fe₂O₃ draw attention with high rates of 10.04 % and 12.63 % respectively, in the analyses of the sample AKY-30. MgO ratio is 6.00 %. Secondary psilomelane and pyrolusite minerals are often observed on the rhodochrosite minerals at the microscopic investigations of this sample (like in photo 1 a, c and photo 2). 200 ppm Pb and 300 ppm Zn are found in the same sample.

In the samples AKY-34 and AKY-35, Pb rates range from 2600 ppm to 3.34 % and Zn rates from 1.13 % to 2.35 %. Fe and Mn rates are quite high in these samples. Metal contents of these samples are enriched by secondary processes, which is verified by thin- and ore section studies. It is observed in the samples taken from levels concordant to the schists in Nimri formation as a result of detailed geochemical studies that carbonate phases which contain Pb, Zn, Fe and Mn metals are replaced by metal rich phases by late secondary processes. As an original result, the existence of Fe and Mn elements in high ratios in carbonate facies must be emphasized.

DISCUSSION

In order to introduce a discussion on the origin of lead-zinc mineralizations of Keban and its environs, a short compilation of general features for Mississippi Valley Type (MVT) and Exhalative Sedimentary Type (SEDEX) deposits, based on literature, appears to be useful.

MVT deposits are characterized by nonexistence of magmatic rocks at their vicinity, lateral extension over hundreds of square kilometers, thicknesses of less than 100 meters and quite simple mineralogy. Especially, galenite with low silver and sphalerite with low iron content, fluorite, barite, rare pyrite and marcasite are the main components. Although vein type mineralizations, fracture fillings related with folding and solution and collapse breccia fillings generally form the important type of deposition, mineralizations show developments as unconformities of layered, stratabound replacement type in sedimentary host rocks which are consisted of generally dolomite or dolomitized limestones. Solution activities are widespread. Most of the mineralizations occur as open space fillings in solution breccias, however some are certainly as replacements. Mineralizations are settled at the sides of large sedimentary basins, shallow depth and structurally passive, anorogenic regions. Although, these mineralizations are discussed as syngenetic, diagenetic and epigenetic occurrences from genetical point of view (Ohle, 1959; Synder, 1967; Anderson, 1975; Roedder, 1976; Vaughan and Craig, 1978; Giordano and Barnes, 1981; Sverjensky, 1984; Guilbert and Park, 1986 and Pratt, 1990), they are considered in the class of "suspicious deposits related with magmatism" according to the criteris of Synder, 1967 (Guilbert and Park, 1986).

SEDEX type deposits usually occur in sedimentary host rocks of Precambrian and Paleozoic age. The mineralogy with pervasive galenite and sphalerite and abundant of pyrite and pyrotite are typical. Silver and iron contents are high. Mineral zoning is their typical characteristic. Deposition both in deep sea and in shallow water sediments is possible. Syngenetic and diagenetic Pb-Zn mineralizations in carbonate and shale host rocks are especially investigated. Although no direct relation is established between mineralizations and volcanism, most of the deposits occur either at the same age of some regional volcanic activities or in basins in which significant amounts of volcanic material are located especially at the lower parts of stratigraphic sequence. Sediment hosted stratiform Cu-Pb-Zn deposits differ from volcanogenic massive sulphide deposits in nonexistence of associating volcanism. Compared by MVT deposits, these stratiform deposits have significant differences as early mineralization time due to basic sediment deposition, more conformity with the basic sediments, higher iron sulphides and Ag ratios and contents (Gustafson and Williams, 1981; Large, 1981; Lydon, 1983; Edwards and Atkinson, 1986).

Important parameters related with both types are given in Table 7.

Table 7 - Significant parameters of MVT and SEDEX-Type deposits (Generalized after Pratt, 1990)

PARAMETERS	MVT	SEDEX
Temperature	~ 100 - 150° C	~ 100 - 300° C
Salinity	1 - 3 m.	0.5 - 3 m.
pH	4 - 7	3.5 - 6
ϵS	10^{-3} - 10^{-2} m.	10^{-3} - 10^{-2} m.
fO_2	10^{-58} - 10^{-46}	10^{-50} - 10^{-38}
Metals	Zn, Pb, Fe, Cu, Ba	Zn, Fe, Pb, Cu, Ba, Ag
Tonnage	< 10^6 - > 10^6 t	> 10^7 t
Grade	4 - 6 % Zn + Pb	10 - 15 % Zn + Pb

In general sense, genetical critic between SEDEX and MVT deposits includes the discussion of syngenetic and epigenetic formation type. Ore bearing solutions (metals and/or sulphides) enter the environment, whether during the formation of primary minerals of rocks or after their formation, constitute the focus of the genetic interpretation problems. According to the recent studies, modern findings lead to the opinions that the feeding channels of syngenetic occurrences (SEDEX) characterize the epigenetic occurrences (MVT). Thus, these two type occurrence are related with each other and a combination of continuity due to both formation mechanisms and characteristics are presented by various authors (Gustafson and Williams, 1981; Pratt, 1990).

Some basic features determined related with Pb-Zn mineralizations of Keban and its vicinity and are given as follows:

- a) According to the field observations, mineralizations are stratiform type deposits concordant to the host rocks in Nimri formation.
- b) Existence of abundant primary rhodocrocite minerals in concordant mineralizations of Nimri formation.
- c) In the calcites of primary carbonate minerals of Nimri formation, 500 and 600 ppm Zn and Pb, respectively, are determined due to the geochemical studies (Table 6).
- d) As a result of geostatistical evaluations, metals belonging to the mineralizations of Nimri formation and Keban marbles show strong evidence for the associations of gradationally precipitation and zoning between carbonates and clays (Table 3, 4 and 5).
- e) Ore formation as matrix of solution breccias and breccias especially in ore bearing level of Nimri formation.

Thus, some of the above mentioned important criteria related with Pb-Zn mineralizations of Keban and its environs exhibits similar and/or common character with SEDEX type, though the others with MVT deposits.

INTERPRETATION

Most of the samples are distributed in exhalative sedimentary (SEDEX) type field, when the chemical analyses are plotted on Fe, Pb, Zn diagram illustrated in Figure 8. If the same analytical results are transported on Cu, Ag, Pb+Zn diagram (Figure 9), again most of them are located very close to the SEDEX field, but their character of high Ag contents predominates.

Carbonate samples in Keban marbles (Number 7, 8 and 9 in Figure 8) show attractive similarities to those of Cafana (Malatya) Zn-Fe-Pb-Ba mineralizations of sedimentary type. Although Cafana mineralizations have a transition type feature between exhalative sedimentary (SEDEX) type and Mississippi Valley Type (MVT) (Pratt, 1990), Keban occurrence exhibit a great tendency toward SEDEX type.

The most important geochemical characteristic, observed in Keban mineralizations, is high amounts of Fe, Mn and Ag which emphasize close similarities to SEDEX type.

It is a fact that genetically related volcanism in field studies, which is expected to form source rock for ore development, doesn't exist locally, and this isn't handled sufficiently. But, being aware of the existence of volcanism (metadiabase) within the Permian units in a large regional geology will be able to create important evidence for the establishment and further strengthening of the relation between the data to be gained from further studies, and the above interpretation.

CONCLUSIONS

Primary ores of Keban Pb-Zn mineralizations in Nimri formation, whether they are classified as SEDEX type or MVT, are not skarn type mineralizations directly related with granitoids.

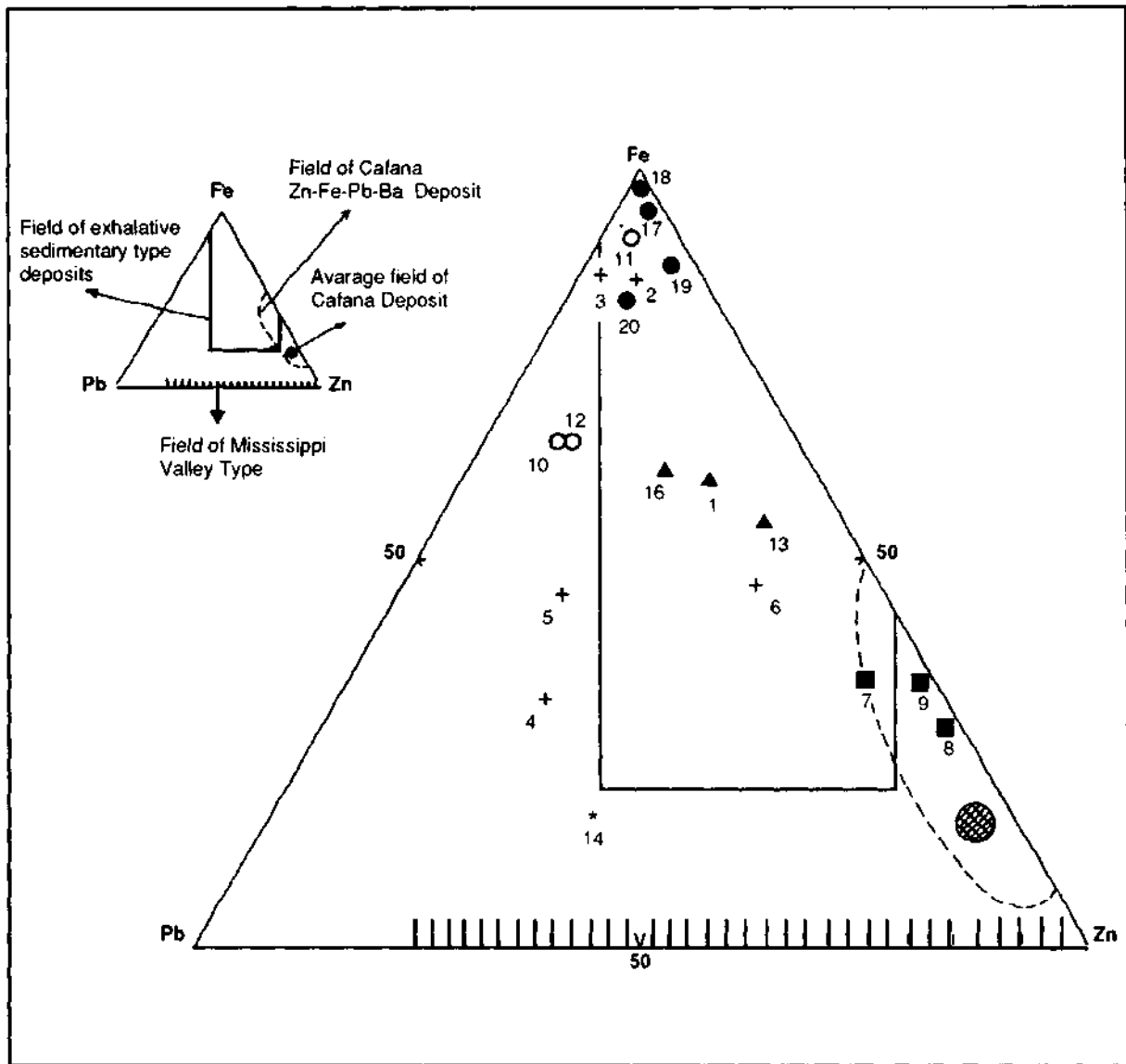


Fig. 8 - Locations in Pb-Fe-Zn triangle diagram of Keban (Elazığ) lead-zinc occurrences. (Numbers like in Table-1, but samples 17, 18, 19 and 20 are equal to AKY 31, 30, 34 and 35 in Table- 6, respectively. Related fields are taken from Gustafson and Williams, 1981; Lydon, 1983; Sangster, 1983 and Pratt, 1990).

Metals, belonging to primary ores, could be more enriched later as a result of mobilization with the effect of granitoids. On the other hand, minerals, formed by mobilizing metal bearing solutions, are located together with skarn minerals in some places and, on the other, minerals, belonging to granitoids, are added to the primary ore minerals. Primary ores contain different mineral paragenesis with lower temperatures than skarn type mineralizations.

Mobilizations related with metamorphism and/or granitoid impact and enrichment processes caused by weathering are out of the study. The emphasize has been given on the origin of primary ores which constitute source for mineralizations in the region.

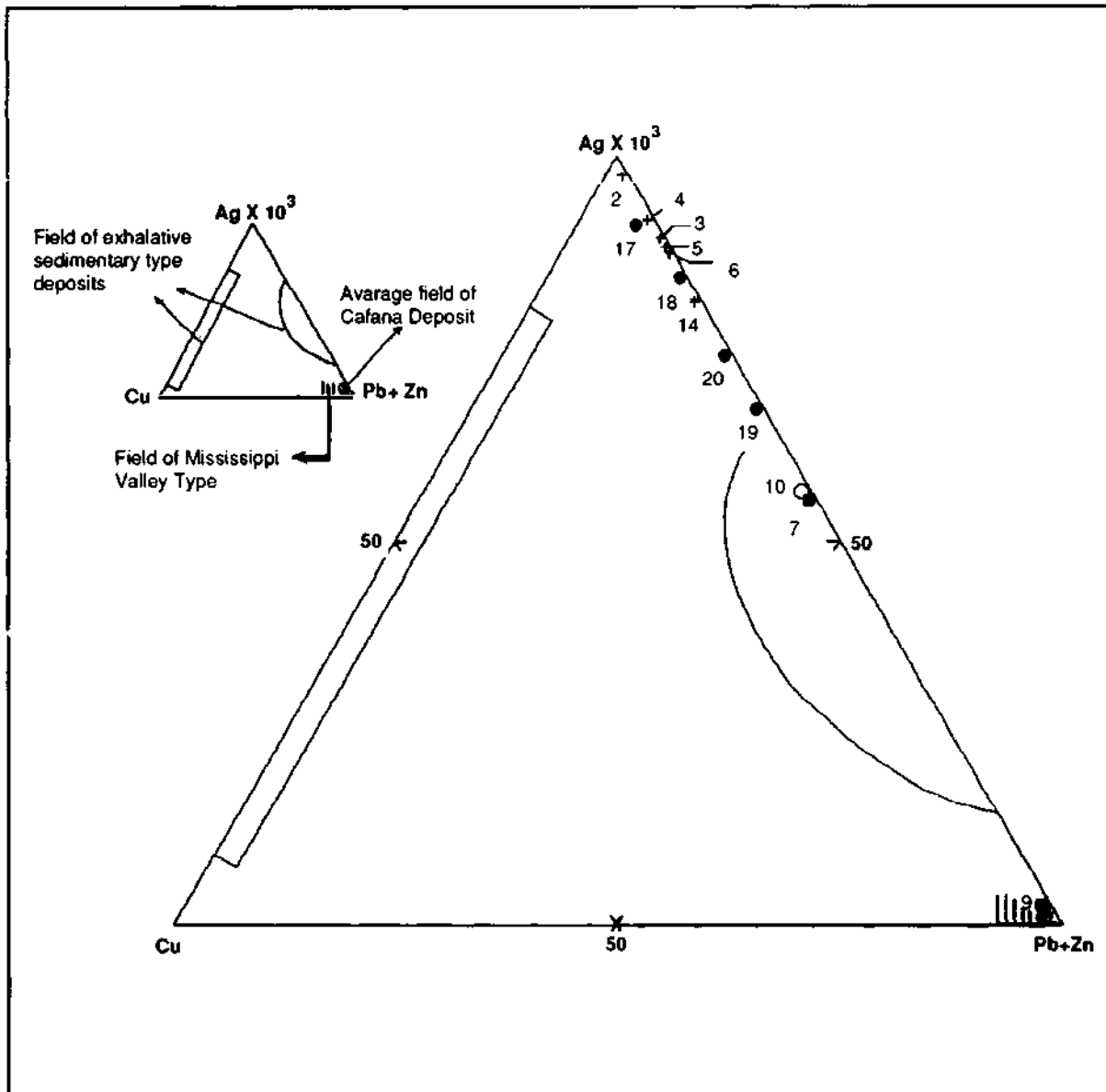


Fig. 9 - Locations in Cu, $Ag \times 10^3$ and Pb+Zn triangle diagram of Keban (Elazığ) lead-zinc occurrences (symbols and references are like in Figure 8).

Investigation and separation of mineralizations, belonging to granitoids, which accompany to primary ores, with detailed efforts during next field studies are very important in order to avoid the complexity of planned studies.

The subject of the-origin of the lithologies in the Nimri formation and their relations to Keban marble are left open as an important problem which should later be taken into account.

This paper presents a preliminary study of the understanding of the primary origin of ores at Keban district with the discussion of the problems related with this subject. The insufficient data basis of this study leads to the necessity of much more data in order to understand the problems. This type of studies may result in the highlighting of the agenda of the revitalization of mining activities again, which are gradually terminating at present.

ACKNOWLEDGEMENT

This study is prepared basing on master of thesis realized by the first author at Geological Engineering Department of Ankara University under the control of second and third authors. Authors thank to Dr. Tank Tuğal and Orhan Uzluk from General Directorate of Etibank for the permission of work, to the authorities of chemistry Laboratory of Etibank Research and Development Department for the realization of chemical analyses. For the permission of the contribution of detailed chemical analyses, we express our gratitude first to the general director of MTA Dr. M. Ziya Gözler and Dr. Jerf Asutay, Rükzan Teşrekli and all MTA laboratory staff.

And in addition, we are greatly indepted to Prof. Dr. Ayhan Erler, Assoc. Prof. Dr. Baki Varol and Dr. Ahmet Çağatay for their scientific contributions to each stage of the study.

Manuscript received March 31, 1992

REFERENCES

- Anderson, G.M., 1975, Precipitation of Mississippi Valley Type Ores Econ. Geol , 70, p. 937-942
- Asutay, H.J. and Turan, M., 1986, Doğu Toroslar-Keban Baskil (Elazığ) dolaylarının jeolojisi: MTA Rep., 8007 (unpublished), Ankara.
- Ami, P., 1937, Keban madeni jeolojisi hakkında muvakkat rapor: MTA Rep., 564 (unpublished), Ankara
- Balçık, A., 1979, Keban Nalliziyaret Tepe ve Karamağara Dere (Bamaş) cevherleşmesi: MTA Rep , 6675 (unpublished), Ankara.
- _____; Tüfekçi, Ş.; Koyuncu, M. and Ulutürk, Y , 1978, Keban Madeni ve Fırat Ocağı geliştirme raporu: MTA Mineral Exploration Department Rep. 1518, (unpublished), Ankara
- Canbazoğlu, M., 1986, Etibank-Keban manganlı gümüş cevherinden mangan ve gümüş kazanılması laboratuvar çalışmaları: Etibank Archives No: 1099, 26p., Ankara.
- Çağlayan, H., 1984, Die Vererzung der Fluorit-Molybdanglanzführenden Blei-Zink-Lagerstätten von Keban-Elazığ im Sudost-Taurus (Turkei): Ph. D. Thesis Univ Vienna
- Demirocak, Y.; Ertem, M.; Kumru, C. and Ünal, S , 1986, Keban simli kurşun cevherinin zenginleştirme çalışmaları: Etibank Archives No. 1090, 22p., Ankara.
- Edwards, R. and Atkinson, K., 1986, Ore deposit geology and its influence on mineral exploration: Chapman and Hall, London-NewYork., 466p.
- Ertunç, A.; Ural, Y.; Baysak, M. and Eser, N., 1972, Keban projesi rezervuar sol sahili muhtemel su kaçak yollarının araştırılması: Etibank Archives No: 85, 48p., Ankara.
- Fischbach, W., 1900, Keban gümüş madeni hakkında rapor: MTA Rep , 384 (unpublished), Ankara
- Gawlik, J., 1958, Keban (Elazığ) prospeksiyon raporu: MTA Rep , 3096 (unpublished), Ankara
- Giordano, T.H. and Barnes, H.L., 1981, Lead transport in Mississippi Valley type ore solutions Econ, Geol , 76, 2200-2211
- Göktekin, A. and Önal, G., 1986, Keban gümüşlü mangan cevherinin değerlendirilmesine ilişkin teknolojik ön etütler: Etibank Archives No. 1098, 11 p., Ankara
- Guilbert, J M and Park, C.F., 1986, The geology of ore deposits W H Freeman and Company, New York , 985 p

- Gustafson, L. B. and Williams, N., 1981, Sediment-hosted stratiform deposits of copper, lead and zinc: Skinner, B.J. (ed.): Econ. Geol. Seventy-fifth anniversary volume, p. 139-178, Amsterdam
- ITU, 1981, Etibank Elazığ-Keban ruhsat sahaları içinde yer alan cevherleşmelerin on değerlendirme raporu: Etibank Archives No. 965, 52p., Ankara.
- Kineş, T., 1971, The geology and ore mineralization in the Keban area, E Turkey: Ph. D. Thesis, Durham Univ. 213p., (unpublished), İngiltere.
- Kıpman, E., 1976, Keban'ın jeolojisi ve volkanitlerinin petrolojisi: 92p., (unpublished), Ankara.
- Kovenko, V., 1941, Keban madeni etüdü hakkında rapor: MTA Rep. 1255 (unpublished), Ankara.
- Köksoy, M., 1972, Keban madeni civarında cevherleşmeyle ilgili elementlerin dağılımları: Etibank Archives No. 983, 88p., Ankara.
- Kumbasar, I., 1964, Keban bölgesindeki cevherleşmelerin petrografik ve metalojenik etüdü: Ph. D Thesis, ITU, 113p., (unpublished), İstanbul.
- Large, D.E., 1981, Sediment-hosted submarine exhalative lead-zinc deposits-a review of their geological characteristics and genesis. In: Wolf, K.H. (ed.): Handbook of strata-bound and stratiform ore deposits, 9, 469-507.
- Lydon, J.W., 1983, Chemical parameters controlling the origin and deposition of sediment-hosted stratiform lead-zinc deposits: Min. Assoc. Can., Short course, p. 8., 175-245
- Maucher, A., 1937, Keban maden zuhuratu hakkında mineralojik rapor: MTA Rep 406 (unpublished), Ankara.
- Oelsner, O., 1938, Keban madeni hakkında rapor: MTA Rep. 279 (unpublished), Ankara.
- Ohle, E.L., 1959, Some considerations in determining the origin of ore deposits of the Mississippi Valley type: Econ. Geol. 54, 769-789.
- Özgül, N., 1981, Munzur dağlarının jeolojisi: MTA Rep. 6995 (unpublished), Ankara.
- and Turşucu, A., 1984, Stratigraphy of the Mesozoic carbonate sequence of the Munzur Mountains (Eastern Taurides) In: Tekeli, O. and Gönçüoğlu, M.C. (ed.): Geology of the Taurus Belt, 173-180, Ankara.
- Öztunalı, Ö., 1985-1989, Etibank-Keban maden sahaları durum tespit raporları: Etibank Archives, 85., Ankara.
- Pratt, A.D., 1990, The geology, geochemistry and mineralogy of the sedimentary Cafana Zn-Fe-Pb-Ba deposit, SE Turkey: Ph. D. Thesis, Vol: 2, 116p., Copenhagen, Danimarka.
- Roedder, E., 1976, Fluid inclusion evidence on the genesis of ores in sedimentary and volcanic rocks: In: Wolf, K.H. (ed.): Handbook of strata-bound and stratiform ore deposits, 2, 67-110. Elsevier, Amsterdam.
- Sağiroğlu, G., 1952, Keban volfram zuhuratu hakkında rapor: MTA Rep. 1942 (unpublished), Ankara.
- Sangster, D.F., 1983, Mississippi Valley-Type deposits: a geological melange: Program, Int. Conf. on MVT lead-zinc deposits, Univ. of Rolla, Misfeori-Rolla, p. 7-18.
- Snyder, F.G., 1967, Criteria for origin of stratiform orebodies: Econ. Geol. Mon. 3, 1-13
- Sverjensky, D.A., 1984, Oil,field brines as ore-forming solutions: Econ Geol , 79, 23-37
- Tolun, N., 1955, Elazığ; Keban, Çemişgezek ve Pertek bölgesinin jeolojik etüdü: MTA Rep. 2227 (unpublished), Ankara.

Vaughan, D.J. and Craig, J.R., 1978, Mineral chemistry of metal sulphides Cambridge University Press, London 493p.

Yılmaz, A., 1991, Keban (Elazığ) kurşun-çinko cevherleşmelerinin maden jeolojisi incelenmesi AÜFF Jeo. Müh. Bölümü, Masters Thesis, 134p , (unpublished), Ankara

———; Ünsal, A., Savcı, C. and İskit, M., 1983, Keban simli kurşun işletmesinde yapılan arama çalışmalarına ait ara rapor: Etibank Archives No. 938, 4p., Ankara

Ziserman, A., 1969, Geological and mining study of Keban Maden Etibank Archives No 123, 70p . Ankara

GEOLOGY, MINERALOGY AND GENESIS OF YENİDOĞAN (SİVRİHİSAR) SEPIOLITE DEPOSIT

Mefail YENİYOL*

ABSTRACT. - In addition to the lump sepiolite known as the meerschaum, it has been known that there also exist some layered sepiolite deposits in the Eskişehir Neogene basin since 1960's. Sepiolite deposit, which is found nearby the Yenidoğan village, southern Sivrihisar is one of the most important one among them. Here, sepiolite occurs as two separate beds in the upper part of the Pliocene sequence, which is made up of the alternation of dolomites and dolomitic marls. The lower sepiolite bed is up to 3 m. thick and consists of sepiolite clay and dolomitic sepiolite. The upper one has maximum thickness of 10m. and it regularly extends over 750 000 square meters. It is made up of the alternation of sepiolite clay and sepiolite-rich layers and lenses. Sepiolite clay consists of over 90 % sepiolite mineral and also organic material in varying proportions but not exceeding 10 %. It may also contain quartz, feldspar, illite, dolomite and pumice grains less than 5 %. Dolomitic sepiolite is the most abundant sepiolite-rich material in the upper bed. Its dolomite content is less than 50 %, and in some cases, illite and quartz grains may also be found in trace amounts. Sepiolite has been deposited at the shallow margins of alkaline lake, short-living ponds and marshlands. Si^{4+} and Mg^{2+} -rich solutions with 8-8.5 pH values have probably favoured sepiolite formation. Under these conditions, sepiolite was formed by direct crystallization and precipitation from the lake water. It was also formed from the solutions circulating through the intergranular space and along the desiccation cracks during and after diagenesis.

INTRODUCTION

Meerschaum occurred near Eskişehir, has been used to make pipes and ornamental goods for centuries owing to convenient physical features. The meerschaum exists as lumps in Neogene aged conglomerates, has been known as the only kind of commercially valuable sepiolite. The existence of sedimentary and layered sepiolites was discovered in this region by MTA researches in 1960's. Technical reports of MTA investigations on economical evaluation mention these sepiolites as "layered meerschaums". First published study on this subject belongs to Akıncı (1967). The sepiolite occurrence located in southwest of Eskişehir was investigated in this work. The position of sepiolite in the sequence was described along a section and some mineralogical information was given. In 1960's, few amount of sepiolite from the sepiolite deposits in the south of Sivrihisar country which is the subject of this text, was exported in order to use as drilling mud. Later, any exploitation or exploration on these sepiolites has not been done.

Layered sepiolites form deposit which presents economic reserve due to their occurring manner. Owing to their physicochemical features, the sepiolites have become on interesting industrial mineral which is served increasing number of usages during last several decades. The study of the subject of this text is one of works based on deposition, mineralogical and original characteristics of this kind of sepiolites which has not been sufficiently investigated and has not been submitted for industrial usage yet. The sepiolite deposit in the south of Sivrihisar which is considered as one of the most important occurrences owing to its reserve, is described in this article (Fig. 1).

GENERAL GEOLOGY

Pre-Tertiary and Neogene aged rocks outcropped in investigated and surroundings area. Pre-Tertiary rocks form morphological heights which extend in northwest-southeast trend. In a field about 25 km. southwest of investigated area, this old lithology is mostly represented by recrystallized limestones and serpentinites that are occasionally in dolomitic character and contain schist layers (Yenişol, 1982). Marbles, recrystallized limestones, gneiss, schist and granodiorites are located in about 12 km. northwest of the area, and ultramafics are outcropped in an island shape about 30 km. northwest of the area due to erosion of Neogene aged cover. Limestones, marbles, schist and gneiss are in Mesozoic(probably Cretaceous) age (Niehoff, 1964). The emplacement age of ultramafics mostly represented by serpentinites and intrusive rocks in which granodiorites are dominant, is Upper Cretaceous (Erentöz, 1975; Yenişol, 1982).

The region has been affected by structural movements in uplift and subsidence character between Lute-tian and Neogene (Erentöz, 1975). The morphology which is almost today's morphology has been exposed by

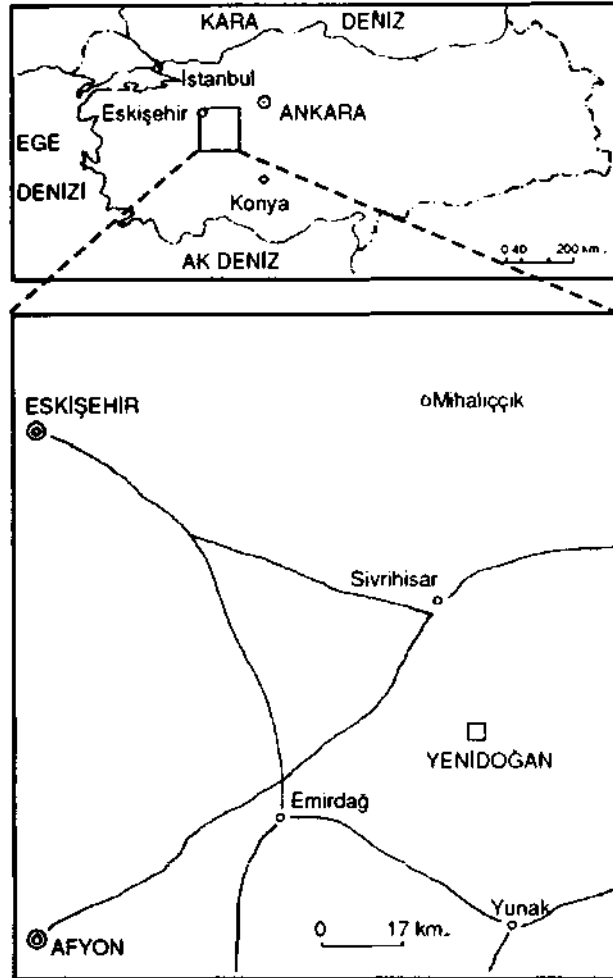


Fig. 1 - Location map.

these movements of initial regional gravity faultings which extend in northwest-southeast trend and subsequent tectonic lines extending in northeast-southwest trend. Neogene sedimentary rocks have been deposited in subsidence areas bounded by the morphologic heights of peneplanated old lithology, and coarse-grained material has been deposited in especially marginal sections, and the thin, clastic material has been deposited in inner sections during the first period of sedimentation in which tectonics was active. Rocks produced by chemical precipitation have been deposited at upper part of the sequence during the subsequent period of slow and quiet tectonic activity. Volcanic products which have been occasionally developed in Miocene and have been increased in Pliocene (Erentöz, 1975), were also added to sedimentation.

Entire investigated area is covered by Neogene sedimentary rocks (Fig. 2). These rocks form a 200 m. thick sequence from the valley floor of Sakarya River which runs nearby the east boundary of the area. Stratigraphic sequence may almost be described as three rock assemblages according to sedimentation environments and some lithologic differences.

First section of the sequence from the basement is approximately 80 m. thick and consists of dolomite, dolomitic marl, tuff, sandstone and alternation of silty and clayey rocks. Hard and micritic dolomites are occasionally loose. Some dolomite beds contain abundant freshwater gastropoda fossils. Numerous dolomite beds are sili-cified probably due to volcanic activities. The dolomite beds are located in 5-10 m. intervals and their maximum

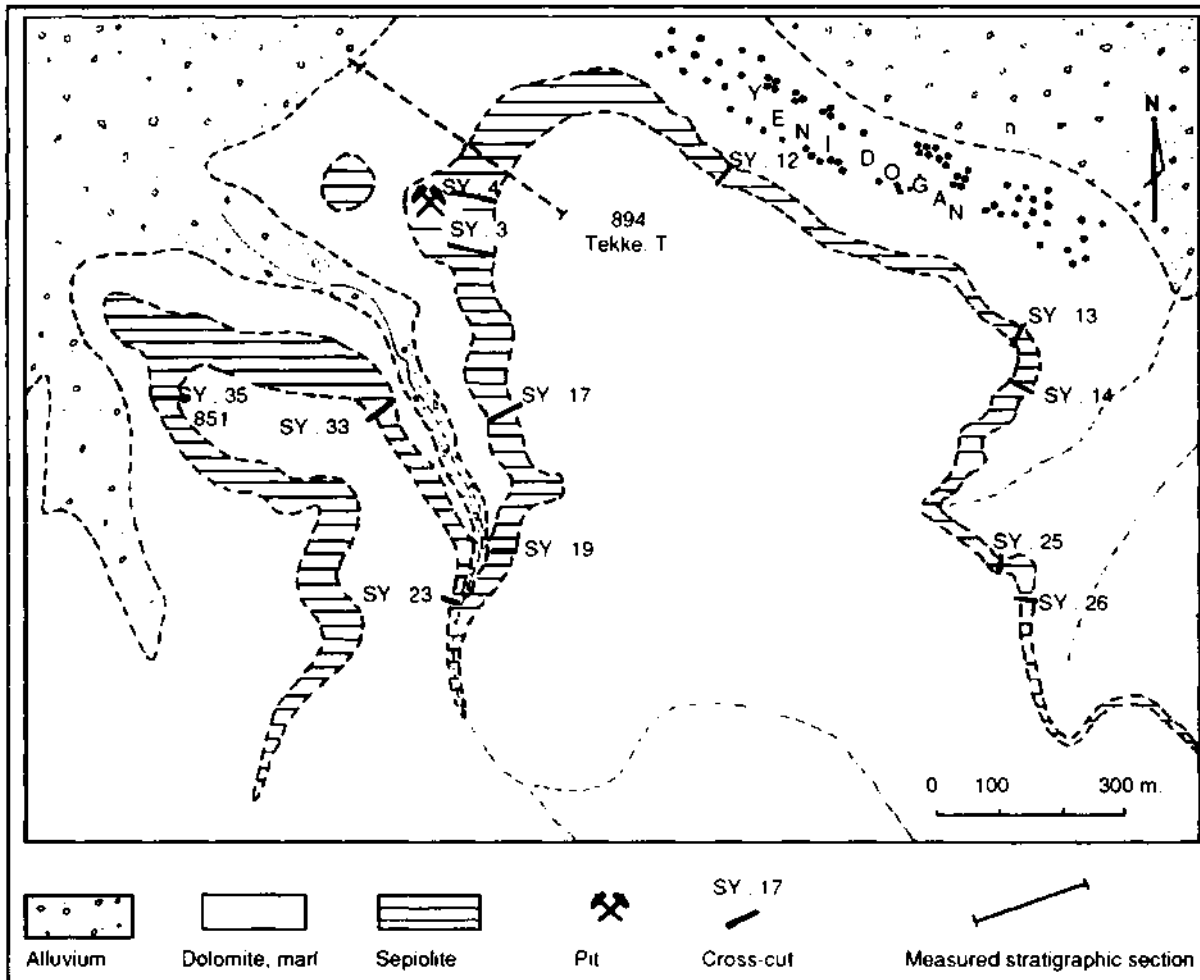


Fig. 2 - Geological map of Yenidoğan (Sivrihisar) sepiolite occurrence.

thickness is 10m. in some places. Acidic tuff and volcanic material-bearing sandstone are frequently alternated with dolomites in this section of sequence. Dolomitic marl, detrital sandstone and silty-clayey beds are added this alternation in the upper section of sequence, and 1-1,5 m. thick, hard, silicified dolomite bed is located at the top (Fig. 3).

The following rock assemblage which is dominated by dolomitic sedimentation, is approximately 40 m. thick and comprises of dolomite and dolomitic marl alternation. The base of the assemblage is 1-2 m. thick crystalline gypsum. Green and brown chlorite-corrensites clays deposited in brackish environment are added the dolomite-marl alternation in the middle and upper sections.

Rock assemblages described above are formed a dome structure in the outside and in the east of the studied area by vertical movements occurred after sedimentation. Rocks outcropped in southwest of studied area have dips to north and northwest as continuation of this structure. The uppermost rock assemblage which conformably overlies the others, has dips to the same directions. It is thin in southwest of investigated area. The dip decreases in north, in west and in northwest of the area, and the layers become almost horizontal layers. The thickness exceeds up to 70 m.

The observable succession of this assemblage starts with a light green-white coloured, loose, over 2 m. thick magnesite mudstone bed (Fig. 3; YD-1). Dolomite and dolomitic marl alternation that contains two main sepiolite beds, overlies the magnesite mudstone. The uppermost bed is a hard, over 3,5 m. thick micritic dolomite.

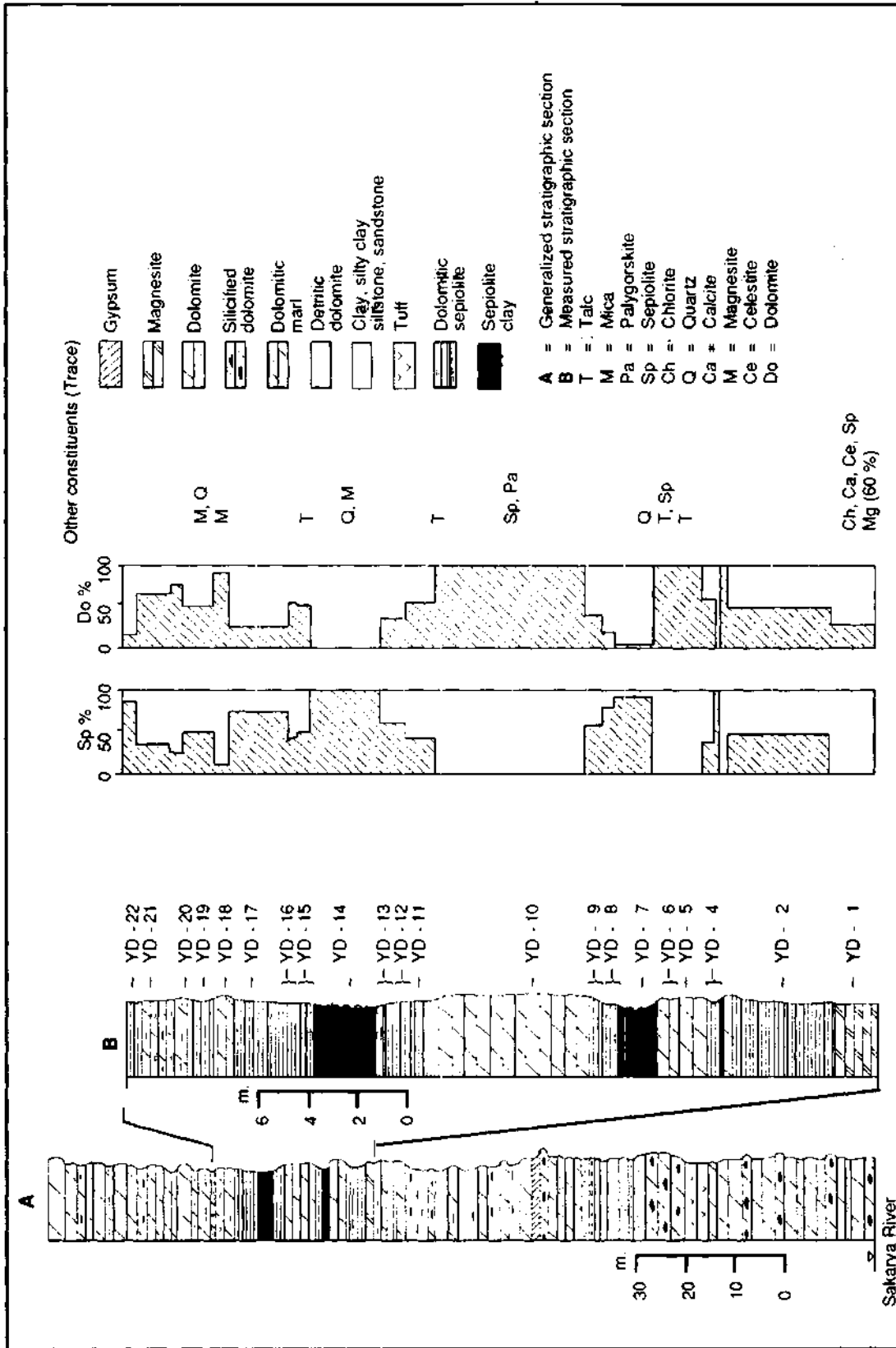


Fig. 3 - Stratigraphic section and diagrams that show lithologic sequence and mineral compositions.

Dolomites are dark white-beige coloured, usually hard, tight and micritic, and occasionally are loose and chalky and in detrital texture. Main mineral in composition is dolomite. Besides trace amounts of talc mineral is located in some beds as a product of chemical precipitation (Isphording, 1984).

Dolomitic marls comprise 50 % dolomite and 50 % clay minerals. Accompanying clay mineral is sepiolite in lower sections. It is possible to classify that composition of marls as "sepiolitic marls". Trioctahedral smectite (Stevensite ?) ± sepiolite in the upper sections, smectite and chlorite in the uppermost sections of assemblage are located as clay components of marls.

Both dolomites and marls contain very few amount of thin, angular quartz, muscovite and rounded volcanic glass grains. Moreover there may be sparse and having maximum 1 mm. diameter reworked material grains such as rounded dolomite, sepiolite and smectite in some beds. They have been added to sedimentation probably during arid periods.

Frequent or sparse organism burrows that indicate shallow sedimentation environment are secondary structures which are observed in many beds. Fenestra and boxwork structures are formed by desiccation cracks with secondary dolomite fillings are also observed in some beds (Fig. 3; YD-3, 19, 20). They are developed vertical or parallel to bedding and indicate that sedimentary materials were occasionally exposed above the water level during extremely arid periods.

SEPIOLITE

Sepiolite formations as in two separate beds outcropped at the lower half of uppermost rock assemblage (Fig. 3). 3 m. thick lower sepiolite bed is observed along the "measured stratigraphic section". Lower and upper sections of this bed are dolomitic sepiolite in detrital character (YD-8). It is composed of sepiolite matrix and dolomite grains. Laminated and 50-60 cm. thick sepiolite clay is situated in the middle section (YD-8). This sepiolite-rich bed is definitely bordered by dolomites at bottom and top of it. The thickness laterally decreases, and the composition grades to dolomitic sepiolite.

The upper sepiolite-rich bed regularly extends and can be observed along the slopes in entire investigated area. Maximum thickness is 10m. in southwest-and northwest of Tekke Tepe (Fig. 3, 4). Thickness regularly decreases southwards and southwestwards, and finally the bed disappears. It comprises sepiolite clay, sepiolitic marl and the alternation of layers and lenses composed of sepiolite and dolomite at various rates.

Sepiolite clay is as lower and upper separate layers (Fig. 4). It has been occurred that small size lenses came together and above each other. Lateral continuity of lower sepiolite layer is shorter than the other, and maximum thickness is 2,5 m. in some places. Upper layer continues in entire area except an interruption is observed at the morphologic defile in south of Tekke Tepe. Maximum thickness is 3,5 m.

Sepiolite clay in soft wax characters when it is wet. The colour is beige or brown in general, and is dark brown or even is black when it includes organic matter. Dry sepiolite clay is too light and its colour is light beige or beige. Sepiolite clay in some places has homogeneous appearance, and is laminated or thin bedded. It is splitted into thin sheets parallel to lamination when it gets dry. These sheets resemble mountain leather. Rounded intra-clasts composed of sepiolite may occasionally be located in sepiolite texture at varying rates. Sepiolite clay in some places has massive structure and detrital character that the bedding is not developed well like on the quarry in west of Tekke Tepe.

Thin tuff, diatomite and chert intercalations located in sepiolite clay are observed at some trenches in southwest of Tekke Tepe (Fig. 2, 4; 13, 14, 25, 26). Tuff consists of white acidic glass (pumice), vermicular biotite in 1 - 2 mm. size and accessory muscovite. Tuff is situated as thin beds of 0.5-10 cm. in thick, as alternated with sepiolite or as disseminated angular detrital material in sepiolite. Diatomite is located close to tuff material and as disseminated diatom tests in sepiolite or as a few cm. thick beds that have been formed by intensive diatom test aggregate. Chert is as nodules in a few cm. size or as thin bands.

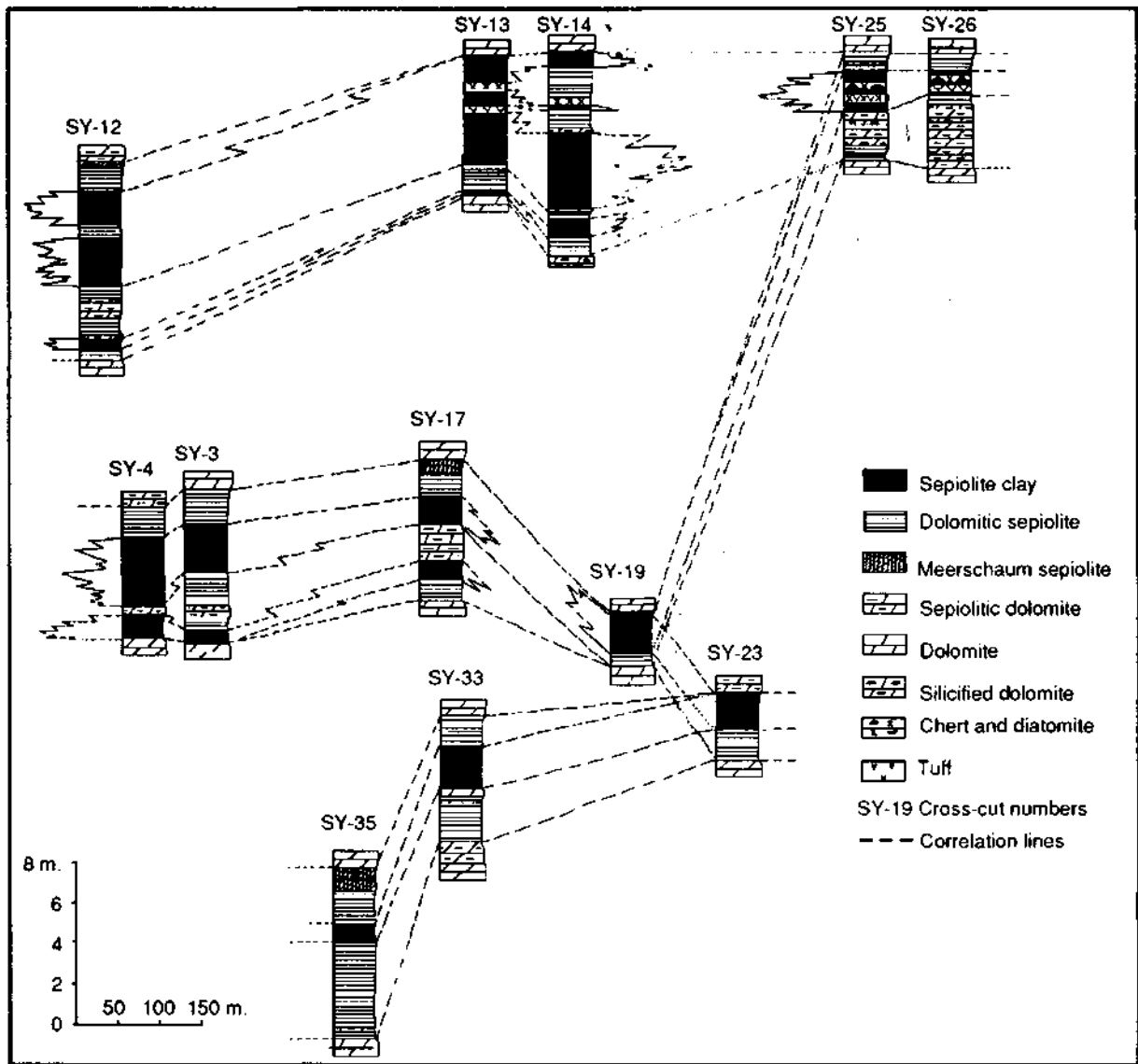


Fig. 4 - Diagram of lithologic correlation.

The material described as "dolomitic sepiolite" which contains over 50 % sepiolite, constitutes the biggest portion of the volume in upper sepiolite bed. The colour of dolomitic sepiolites varies from white to light beige and beige according to sepiolite content in composition, and their unit volume weights decrease.

Dolomitic sepiolites have massive structure, their beddings are not developed well in general. Some of them are produced by chemical precipitation and are fine-grained. They occasionally have detrital structure and contain intraclasts which their maximum size is 1 cm. in some places but generally in sand size or finer. These intraclasts are sepiolites and dolomites belong to same aged sediments. When dolomitic sepiolites get dry, form columnar desiccation cracks that have been developed in various dimensions at outcrops. These cracks are occasionally vertical to beddings.

Dolomitic sepiolites are occasionally in meerschaum character at upper sections of the main sepiolite-rich bed that described above. This white or occasionally light beige coloured matter is not dispersed in water. It can easily be chiseled and be treated. Meerschaum has detrital texture and porcelain appearance, and is fine-

grained. Sparse and 1-2 cm. opened polygonal desiccation cracks have been formed in wet condition at outcrops. This maximum 1.4 m. thick and roughly lense shaped meerschaum has a specific economic importance among the other sepiolite-rich materials in the deposit.

Young sepiolite formations as thin veins and the tracks of plants and organism burrows which indicate the depositional environment are observed in both dolomitic sepiolites and sepiolite clay. Besides fenestras and box-works that have been occurred concerning arid periods are observed. (Fig. 3; YD-12, 16, 9, 20).

Sepiolite clay and dolomitic sepiolites laterally grade to each other. This gradation vertically lasts a short distance. There is also a sharp boundary relation between them in some places.

The upper sepiolite bed described above, is bounded at the base by a hard, varying thick dolomite layer (YD-10). A hard dolomite bed with relief which is occasionally in dolomitic sepiolite composition overlies the upper sepiolite bed (Fig. 3; YD-18, 19, 20). This bed in which detrital character and fenestra structure are observed, is occasionally overlain by thin magnesite and magnesite-rich clay formations. Dolomitic sepiolite with lateral continuity in some places and the beds composed of sepiolite+trioctedral smectite (probably stevensite) which occasionally have fenestra structure and paleosol character are also located.

MATERIAL AND METHODS

Measured stratigraphic section of the upper of the sequence in which sepiolite formations are located, is prepared in order to detailly observe and to describe the superposition manner and the textural features, mineral composition and its variation. Furthermore, 34 trenches in sepiolite-rich beds vertical to bedding are opened. 170 samples are collected from various lithologic units, from the stratigraphic section and trenches, from wells and the quarry for investigations at laboratory. These samples are firstly examined under binocular microscope. Later XRD analysis of 38 required samples, microprobe analysis and scanning electron microscope (SEM) analysis of 5 samples and the chemical analysis of 46 samples are carried out.

Qualitative mineral determination are also carried out by Philips XRD equipment. Analysis are created on non-oriented powder preparatories that are prepared by grinding the samples in natural state. In the same records, integral field of the first pique (110) belongs to sepiolite and the maximum pique heights of the other minerals are compared and the semiquantitative composition is estimated.

As an approach, estimation of the quantitative composition on dolomitic sepiolites are carried out by means of a prepared working curve. Both CaO analysis and the XRD records of the samples taken from sepiolite occurrences in Eskişehir area, are carried out. These samples have different dolomite/sepiolite ratios. CaO percentage values which are calculated from chemical analysis, are accepted as abscissa and the ratios of the most severe piques of XRD records belong to dolomite and sepiolite minerals (DO/ASp) are accepted as ordinate (Fig. 5), and a curve is prepared in this way. During the routine works about to determine the composition of the only samples which are taken the XRD records, this curve is used.

Samples in different composition and textural features are used on electron microscope investigations. Samples are firstly plated by a thin gold film. Later, analysis are carried out by using JEOL-733 electron microprobe and JSM-T330 scanning electron microscope.

Only the CaO analysis is carried out in order to calculate the dolomite percentage in dolomite-bearing samples. For this purpose, carbonate in samples is solved with 1M HCl solution. Later, CaO percentage is determined by atomic absorption. Dolomite percentage in composition is calculated from these values. Entire rock analysis is carried out to define the chemical composition of sepiolite clay. Firstly, sample in natural state is roasted at 1000°C for two hours. Later chemical analysis is carried out by combination of atomic absorption and the wet method. Oxide percentage values that are turned into normal temperature according to total water loss and the analysis results of a classical meerschaum type sepiolite are given in Table 1 for comparison. Oxide percentages in Table 1 are usual values for sepiolite mineral. However, Al_2O_3 and Fe_2O_3 values of sepiolite clay are higher and MgO value is lower than meerschaum. This indicated that octahedral Mg is substituted with more amount of Al and Fe in sepiolite clay.

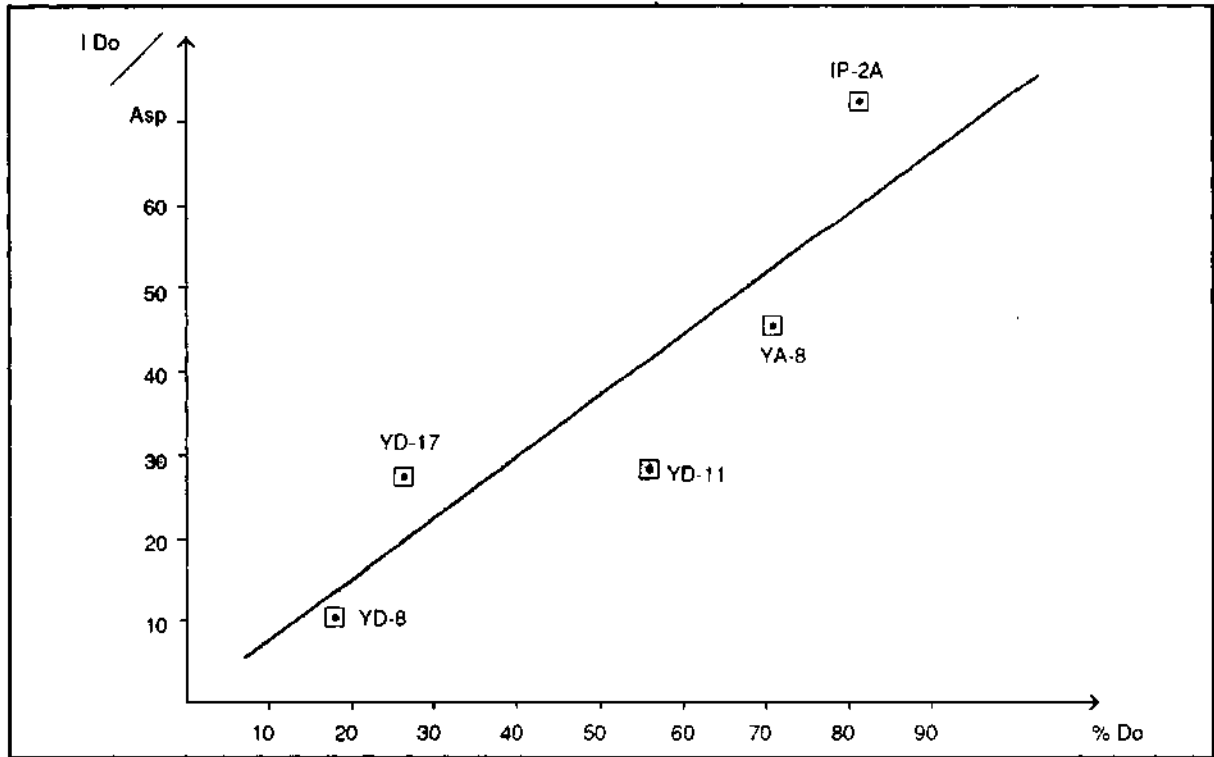


Fig. 5 - Diagram that shows the relation between the dolomite/sepiolite pique ratios at X-ray powder diffraction patterns of the samples and the dolomite content. YD: Yenidoğan. YA: Yörükakçayır. IP: Ilyaspaşa

Table 1 - Chemical composition of sepiolite clay

	(1)	(2)
SiO ₂	54.04	54.02
Al ₂ O ₃	2.85	0.19
Fe ₂ O ₃ *	1.08	0.51
MgO	20.69	23.13
MnO	0.01	-
CaO	0.19	0.06
Na ₂ O	0.11	0.02
K ₂ O	0.69	0.02
A.Z.	20.07	21.63
Total	99.74	99.58

* Total iron.

(1) Massive sepiolite clay

(2) Meerschaum (Yeniyoğal and Öztunalı, 1985)

TEXTURE

It is observed that laminated sepiolite clay is formed by sepiolite fibers under scanning electron microscope. Occasionally undulated fibers are suited for bedding plane, are stacked as parallel or almost parallel to each other. They cause the lamination at this type of sepiolite. Round, having diameters of less than 0,5 mm. sepiolite grains of eolian origin are sparsely located in sepiolite groundmass of laminated sepiolite clay in some cases. Sparse or intensive intraclasts are located in sepiolite groundmass in some beds and in some places. They are in varying size and their maximum diameters 1-2 cm. in some cases. Primary laminar structures at sepiolite composition are kept in intraclasts. The shapes of intraclasts are flat or round and their corners are rounded. It is observed that intraclasts are made up of dolomite in some cases. Furthermore, muscovite, vermicular biotite and volcanic material such as volcanic glass and tuff grains are situated in sepiolite groundmass. They form sharp boundary with sepiolite groundmass in some cases.

Massive sepiolite clay consists of intraclasts and groundmass. Volumes of intraclasts are irregularly dispersed. They may up to 2-3 cm. in size, but generally are in sand size or smaller. These laminated, subrounded and flat intraclasts are in sepiolite composition. Their corners are also rounded. Detrital texture is clear under microscope. It is observed under SEM that the material consists of grains in 2 μ m-15 μ m size and sepiolite in fiber structure which fills the intergranular space. After the grains have been deposited and during the diagenesis period, the sepiolite has been lined up parallel to grains, later has laterally become larger from grain surfaces, and has covered the volume. The length of sepiolite fibers is 0.5-1 m. Over 15m. long fibers which are grown up in later period can occasionally be observed (Plate I, fig. 1).

Some dolomitic sepiolites in detrital character have textural features similar to massive sepiolite clay. However, intraclasts may be sepiolite and groundmass is sepiolite or intraclasts may be dolomite and groundmass is sepiolite. In some cases, intraclasts comprise of both sepiolite and dolomite at varying rates. As a result of these variations, material has a gross composition of dolomitic sepiolite character in any case.

Dolomitic sepiolites which are products of chemical precipitation consists of dolomite and sepiolite minerals that are smaller than 1m. Homogenous structure of dolomitic sepiolites which can be observed both by microscope and naked eye, due to different crystal morphologies, mixed dispersion at volume of two minerals and their flocculation after precipitation in electronic environment.

Sepiolite in meerschaum character is fine-grained and has detrital texture. Grain size varies from very fine sand to 2m. Sepiolite fibers which have reciprocally become larger and have clamped as vertical to grain surfaces in the intergranular space, probably have caused that the material does not disperse in water (Plate I, fig. 2). Occasionally observed calcite formations which have been occurred in intergranular space after forming of sepiolite, also probably have caused that the material does not disperse in water and has a white colour.

MINERALOGY

Clay mineral component in all kinds of sepiolite-rich materials is the sepiolite mineral which is pretty well crystallized in some cases (Fig. 6). The sepiolite mineral exists over 90 % in composition of laminated sepiolites. Organic matter is also located in composition of almost every sepiolite clay of this type. But the ratio of organic matter which causes the dark colour sepiolitic clay, is not over 10 %. Both intraclasts and groundmass in sepiolites with massive structure, are made up of the sepiolite mineral. This type of sepiolite does not contain organic matter. Its sepiolite content is over 90 %. Dolomite intraclasts, detrital quartz and sericite, feldspar and rounded volcanic glass grains may also be located in composition. Their total proportion in composition is not over 10 %.

Dolomitic sepiolites usually include 50 % or more sepiolite. Principal component except sepiolite is the dolomite mineral (Fig. 6). There are occasionally 5-10 % illite, very few detrital quartz and volcanic glass in dolomitic sepiolites at upper sections of main sepiolite bed. The material becomes sepiolite-rich dolomite where the sepiolite content decreases under 50 %. However, sepiolite is 10 % or more in almost every case at main sepiolite bed. Meerschaums include 50-70 % sepiolite, few dolomite and in some cases very few calcite.

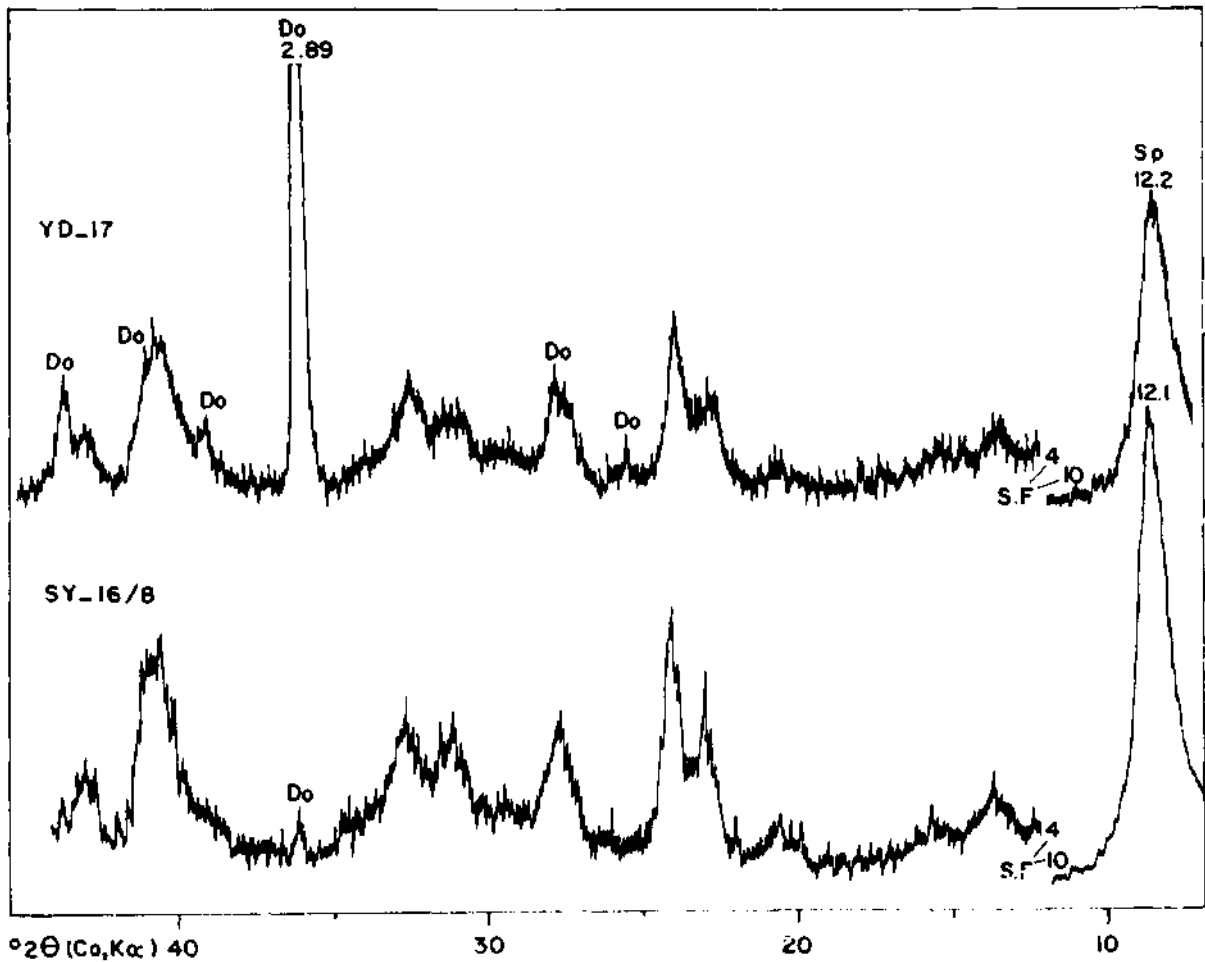


Fig. 6 - X-ray powder diffraction patterns. YD-17: dolomitic sepiolite, SY 16/8: sepiolite clay (SY-16/8 sample is taken from a trench opened between SY-3 and SY-17 trenches), DO: dolomite, SP: sepiolite, SF: scale factor.

ENVIRONMENT AND GENESIS OF SEPIOLITE

Sedimentation basin in which Neogene lithology deposited is an alkaline lake covers broad depression areas connected with each other in regional scale and shallow lakes and ponds which have been separated from the main mass during the arid periods caused that the lake became smaller and have been combined with main lake mass during the rainy periods. Sedimentation in this playa or similar to playa kinds of lakes have occurred under evaporite conditions and generally in chemical precipitation way. Limited detrital and volcanic material have also been deposited during in some periods.

Stratigraphic and lithologic features indicate that the seasonal rainy, arid or semi-arid climates have dominated in the region. Under these climatic conditions, pre-Neogene aged rimrocks have been subjected to chemical weathering, and the materials mainly in ion and gel state have been transported to basin by surface waters with low energy during the rainy periods. Recrystallized limestones which are the most regional widespread rimrocks are principal source of Ca^{2+} ions that have been transported to sedimentation basin. There is no other widespread rimrock which can be the source of this ion needed for dolomites which is the dominated lithology in the sequence. Ultramafics which are secondly most widespread rocks and their derivative rocks (serpentinites) are main sources of Mg^{2+} ions needed to dolomites and magnesium clays. Furthermore, Mg^{2+} presentation as at few rates from dolomitic sections of recrystallized limestones is probable. Ultramafics have provided Si^{4+} ions to-

gether with Mg^{2+} ions to basin. During these phases, additional silica has been also presented from devitrification of volcanic glass and ash which has fallen into water by volcanism that occasionally accompanied with sedimentation.

Slightly uplift of rimrocks by occasionally occurred vertical movements and slightly folding of the sediments by progressive subsidence of the basin caused that the detrital materials together with ions have been transported from rimrock to basin. However, this detrital material have reached to inner sections of the basin at limited rate and during the periods in which the surface waters have had high energy. Another source of clastic material is acidic volcanism. Volcanoclastic materials such as thin tuff, ash and glass (pumice) have been added to sedimentation environment by volcanic activity. The sediments have come up to atmosphere and have got dry due to narrowing of the lake area during arid periods. They have been eroded during the following wet periods, and have been transported by winds and waters. They have deposited again, so clastic materials have been added to sediments.

Quartz, feldspar, biotite, sericite and illite are the minerals which have been transported from rimrocks or have been added with volcanic activity. Calcite, dolomite, magnesite, celestite, gypsum, corrensite, chlorite, talc and sepiolite are authigenically formed. The formation of these authigenic minerals have been controlled by Ca^{2+} , Mg^{2+} , Si^{4+} , SO_4^{2-} ions and their abundance, partial press of CO_2 , temperature of environment, evaporation, organic catalytic and the other environmental conditions.

The formation of dolomite is still discussible. It has been formed during arid periods with chemical precipitation owing to increasing of Mg^{2+}/Ca^{2+} activity in lake water by precipitation of magnesium silicates. Dominating climate and other conditions at basin were generally convenient for dolomite formation. Gypsum, corrensite-bearing clays, magnesite and sepiolite have been formed in extreme climate conditions.

Lithologic features at middle section of the sequence indicate that the lake water occasionally has become brackish by adding SO_4^{2-} ions. Chlorite-corrensite clays and gypsum formations have occurred under hypersaline environment conditions during very arid periods owing to extreme evaporation (Weaver, 1984). During very extreme evaporation periods which the lake has nearly got dry, magnesite with over 10 pH values has been precipitated due to decreasing the other cations and increasing Mg^{2+} concentration in environment (Alderman, 1965). Magnesite may also have formed owing to high hidrate character of Mg^{2+} ion. In this way, magnesium probably has been formed at first as an hydrous magnesium mineral such as hydromagnesite or nesquehonite, later by dehydration of them (Langmuir, 1965). Calcite has been occurred during the post-diagenesis phase which was convenient to form calcite, probably by ground water that was in about 8 pH value needed for sepiolite forming, in the intergranular space and cracks (Galan and Ferrero, 1982).

Formation of sepiolite which is an indicator of paleoclimate, have taken place under the seasonal rainy, arid or semi-arid climate conditions (Gallon, 1984), but during the rainy periods as clearly observed with field data. The environments in which sepiolite has been precipitated are the marginal sections of lake basin which its pH has decreased by feeding of surface waters, short-lived ponds which have located at the edges of main water mass and their mixture zones which have exchanged water with main lake mass and the marshlands in which short-lived plants could have lived.

The pH value must be between 8-8.5 in order to form sepiolite according to works related to sepiolite and the investigations purposed synthesis of this mineral (Siffert, 1962; Wollast et al., 1968; Hegelson et al., 1969; Singer and Norrish, 1974; Khoury et al., 1982; Galan and Castillo, 1984; Abtahi, 1985; et al.). The low rates of Al^{3+} in the environment have made the sepiolite formation possible as a stable mineral phase instead of palygorskite which occurs under the same environmental conditions.

The Ca+Mg/Si ratio has decreased owing to dolomite precipitation. Sepiolite with about 8-8.5 pH values has been formed by convenient saturation index which have provided with Mg^{2+} and Si^{4+} ions that have been added to lake water by surface waters during rainy periods (Khoury et al., 1982). Field and laboratory investigations are demonstrated that there is not a direct relationship between sepiolite formation and volcanism. However, devitrification of volcanic glass might have provided an indirect aid in order to increase the Si^{4+} proportion

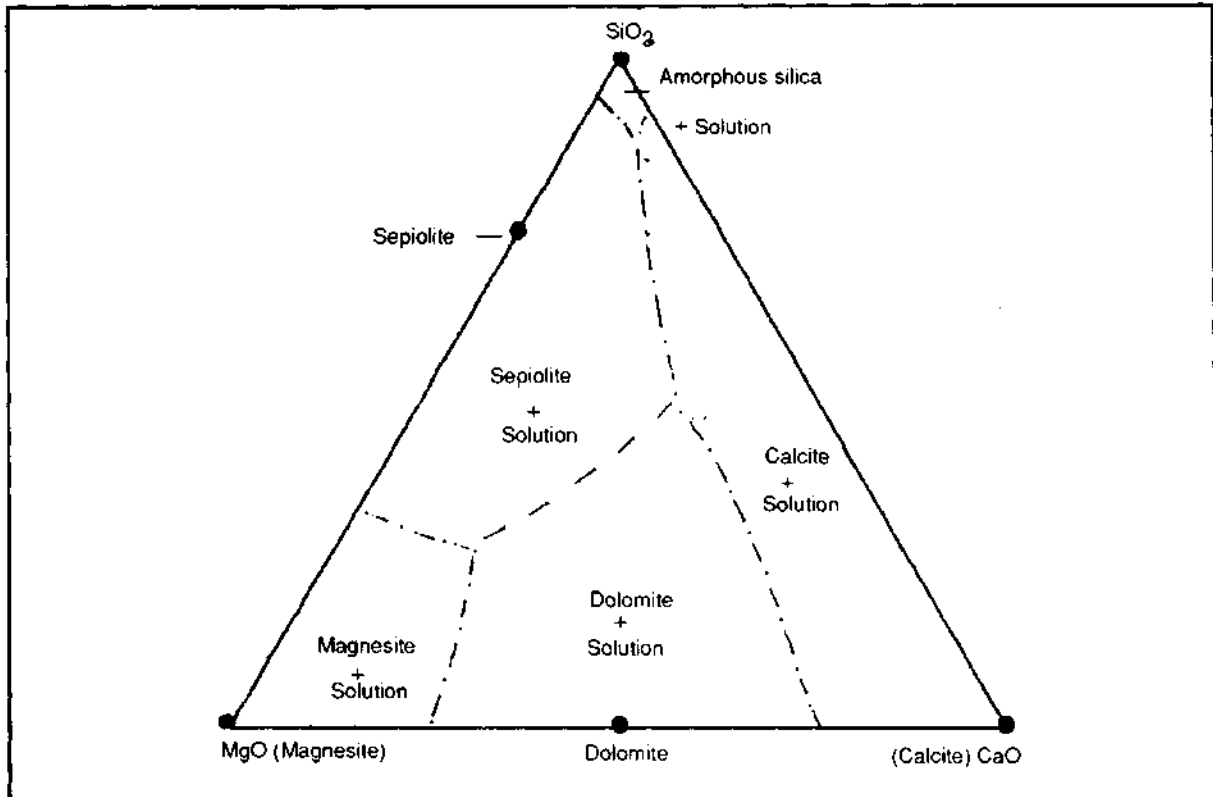


Fig. 7 - Saturation diagram for CaO-MgO CO_2 - SiO_2 - H_2O system at 25°C and 1 atmosphere (Hegelson et al., 1969).

needed for sepiolite formation. Therefore, sepiolite has been formed under appropriate environmental conditions in three different ways and phases; 1) direct chemical precipitation from lake water, 2) precipitation from intergranular solutions during diagenesis phase, 3) precipitation as crack filling during post-diagenesis phase.

In small ponds and marshlads which are fed with fresh surface waters, sepiolite has been formed with direct crystallization and precipitation defined as chemical precipitation. In the environments which the electrolytic concentration was low so flocculation was not effective, the sepiolite fibers have lined up as their long axis parallel to base, and caused the sepiolite clay has had a laminated structure. Under the conditions which fresh water has mixed with lake water, sepiolite and dolomite have together been formed by chemical precipitation with the solutions which their compositions are seen between dolomite and sepiolite areas on the Hegelson et al. saturation diagram (1969) (Fig. 7). Because of the different crystal morphologies of these two minerals, flocculation effect of the electrolytes in environment and stable precipitation conditions, a massive structure is observed in this type of sepiolite material.

Formed sepiolite and related sediments have occasionally got dry when they have outcropped by shrinking of lake area during arid periods. These sediments have been eroded, transported by surface waters and deposited again during the following rainy periods. The material has rapidly been deposited in this way, and has formed detrital "dolomitic sepiolites" which have varying dolomite/sepiolite ratios according to kind and spreading of the outcropped sediments.

During diagenesis phase which represents the second formation way, sepiolite has been formed in the intergranular spaces of the detrital sepiolites and the sediments composed of sepiolite and dolomite. Sepiolite has occurred with appropriate pore solutions by growing up from grain surfaces and vertical to these surfaces as fibers. Growing fibers in this way have reciprocally been clamped, and have caused dolomitic sepiolites do not disperse in water and have meerscham character in some cases.

Besides two formation ways considered above, sepiolite has also been formed during post-diagenesis phase or later phases. In these phases, sepiolite has produced thin veins as filling of desiccation cracks by precipitation from ground waters.

ACKNOWLEDGEMENTS

The author is thankful to Bülent Arman, Research Center of Turkey Bottle and Glass Factories Company; Prof. Dr. Adnan Tekin, Turgay Gönül and Hüseyin Sezer, Istanbul Technical University Chemistry Metallurgy Faculty for their kindly help on electron microscope studies.

Manuscript received January 21, 1991

REFERENCES

- Abtahi, A., 1985, Synthesis of sepiolite at room temperature from SiO_2 and MgCl_2 solution: *Clays and Clay Minerals*, 20, 521-523.
- Alderman, A.R., 1965, Dolomitic sediments and their environment in the South-East of South Australia: *Geochim. Cosmochim. Acta*, 29, 1355-1365.
- Akıncı, Ö., 1967, Geology of Eskişehir I24 quadrangle and layered meerschaum occurrences: *MTA Bull.* 68, 82-97 (in Turkish).
- Callen, R.A., 1984, Clay of the palygorskite-sepiolite group; depositional environments age and distribution: Singer, A. and Galan, E., ed., *Palygorskite-Sepiolite Occurrences, Genesis and Uses, Developments in Sedimentology*, 37, 1-37.
- Erentöz, C., 1975, Explanatory Text of 1: 500 000 scale Geological Map of Turkey Erentöz, C. comp MTA Publ., Ankara.
- Galan, E. and Castillo, A., 1984, Sepiolite-Palygorskite in Spanish Tertiary Basins; genetical patterns in continental environments: Singer, A. and Galan, E., ed., *Palygorskite-Sepiolite Occurrences, Genesis and Uses, Developments in Sedimentology*, 87-124.
- _____and Ferrero, A., 1982, Palygorskite-sepiolite clays of Lebrija, Southern Spain: *Clays and Clay Minerals*, 30, 191-199.
- Hegelson, H.C.; Garrels, R.M. and Mackenzie, FT., 1969, Evaluation of irreversible reactions in geochemical processes involving minerals and aqueous solutions-II. Applications: *Geochim Cosmochim Acta*, 33, 455-481
- Isphording, W.C., 1984, The clays of Yucatan, Mexico; a contrast in genesis: Singer, A and Galan, E , ed., *Palygorskite-Sepiolite Occurrences, Genesis and Uses, Developments in Sedimentology*, 59 73
- Khoury, H.N.; Eberl, D.D. and Jones, F.B., 1982, Origin of magnesium clays from the Amargosa Desert, Nevada; *Clays and Clay Minerals*, 30, 327-336.
- Langmuir, D., 1965, Stability of carbonates in the system $\text{MgO-CO}_2\text{-H}_2\text{O}$: *Jour. Geol.*, 73, 730-754
- Niehoff, W., 1964, Bericht über die Ergebnisse der Revisions-Kartierung 1:100 000 der Blätter Akşehir, Pafta 90/2, und Ilgın, Pafta 91/1; 91/3 und 91/4 im Sommer 1961: *MTA Rep.*, 3387 (unpublished), Ankara
- Sitfert, B., 1962, Quelques reactions de la silice en solution; La formation des argiles: *Mem Serv Carte Geol. Alsace-Lorraine*, 21, 100p.
- Singer, A. and Norrish, K., 1974, Pedogenic palygorskite occurrences in Australia: *Am Mineral* 59, 508-517
- Weaver, C.E., 1984, Origin and geologic implications of the palygorskite of the S.E. United States: Singer, A and Galan, E , ed., *Palygorskite-Sepiolite Occurrences, Genesis and Uses, Developments in Sedimentology*, 39-58.

Wollast, R., Mackenzie, FT. and Bricker, D.P., 1968, Experimental precipitation and genesis of sepiolite at earth surface conditions: Am. Mineral., 53, 1645-1661.

Yenirol, M., 1982, The problems of the genesis of the Yunak (Konya) magnesites, their evaluation and the petrogenesis of the surrounding rocks, Istanbul Earth Sciences Review, 3, 21-51 (in Turkish).

_____and Öztunalı, Ö., 1985, Mineralogy and formation of the Yunak sepiolite: Gündoğdu, M.N. and Aksoy, H., ed., II. National clay Symposium book, Bizim Büro Basımevi, 171-186, Ankara (in Turkish).

PLATE

PLATE -I

Fig. 1 - Scanning electron micrograph of massive sepiol
Linear scale = 10 micron.

Fig. 2 - Scanning electron micrograph of meerschaum.
Linear scale = 10 micron.



PYRITE OCCURRENCES NEXT TO THE ATTEPE IRON DEPOSITS, FEKE-ADANA, TURKEY

Ahmet AYHAN*, Şuayip KÜPELİ* and G.C. AMSTUTZ**

ABSTRACT. _ The pyrite occurrences described in this paper are located in the lowest section of Infracambrian sequences situated along the eastern border of the Attepe iron ore deposit in the Mansurlu District of Adana. The pyritic formations represent two different mineral parageneses. The dominant group is represented by thin pyrite layers and pyrite-bearing carbonate layers alternating with dark gray to black colored carbonaceous shales and phyllites, whereas the second group is found in siderite veins associated with fahlore. Sedimentary pyrites occurring mostly as small massive layers, lenses, isolated single crystals, diagenetic injection drops, defined in this study, and veins exhibit typical sedimentary and some distinctive geochemical features compared with the other. Their depositional and diagenetic features indicate a mode of sedimentary formation of pyrites under reducing conditions during the Infracambrian. On the contrary, pyrites in siderite veins having quite varying amounts of minor elements such as Cu, As, Sb, Co, Se and Hg when compared to the sedimentary pyrites, must have formed as a younger generation by an epigenetic process between post Cretaceous and Paleocene.

Key words: Pyrite occurrences, sedimentary and hydrothermal origin, geochemistry, Eastern Taurus, Turkey.

INTRODUCTION

The Attepe iron ore deposit, situated in the northern part of Mansurlu Village near Feke, Adana, is the second biggest mineable iron deposit in Turkey (Fig. 1). The pyritic rocks of Infracambrian age occurring along the eastern boundary of this deposit have been studied in detail.

The aim of this study is to examine the pyritic formations appearing either stratiform or as veins and to elucidate the occurrence of sedimentary pyrites. For this purpose, first of all, a geological map of the Attepe District was prepared, and later hand specimens taken from the pyrite-bearing rocks and their hostrocks were analysed geochemically and studied mineralogically.

GEOLOGICAL SETTING

The Attepe District, situated in the western part of the Eastern Taurus belt, is represented by rocks of the lower section of the autochthonous Geyikdağı tectonic unit. The exposed rocks of this unit ranging from Infracambrian to Middle Cambrian in age have been subdivided into three lithostratigraphic units, the Kandilcikdere, Attepe and Çaltepe formations (Fig. 1).

Horst and graben structures along two main faults striking in a NW-SE direction were developed in a tensional regime, most likely during Mesozoic time. On the other hand, all rocks were subjected to the low grade metamorphism of the greenschist fades.

The Kandilcikdere Formation has been described here, as the pyritic levels are confined only to this formation. It is composed mainly of dark gray and black shales and phyllites. It is now almost entirely exposed due to a mining operation carried out in the eastern section of the Attepe iron deposit, and the best exposures lie along the edge of the northern horst block (Fig. 1). Because of faulting, its base is unknown. It displays a limited lateral extension with a thickness of 80 m., and is overlain conformably by the Attepe Formation.

Shales and phyllites were partly folded and, in places, faulted and fractured. In these pelitic rocks, typical samples of syndimentary and diagenetic structures such as lamination, loadcast and geopetal structures are common. Some of the lenses, boudinage and flow structures are related to the late diagenetic and subsequent metamorphic processes. Pelitic rocks composed of mainly sericite, quartz, feldspar, chlorite and opaque minerals have been described as shale, phyllite, quartz phyllite and sericite-quartz phyllite.

No fossils have been found in Kandilcikdere and Attepe formations yet. Consequently, a relative age of Infracambrian is given for these formations, which are unconformably overlain by the Lower-Middle Cambrian Çaltepe Formation.

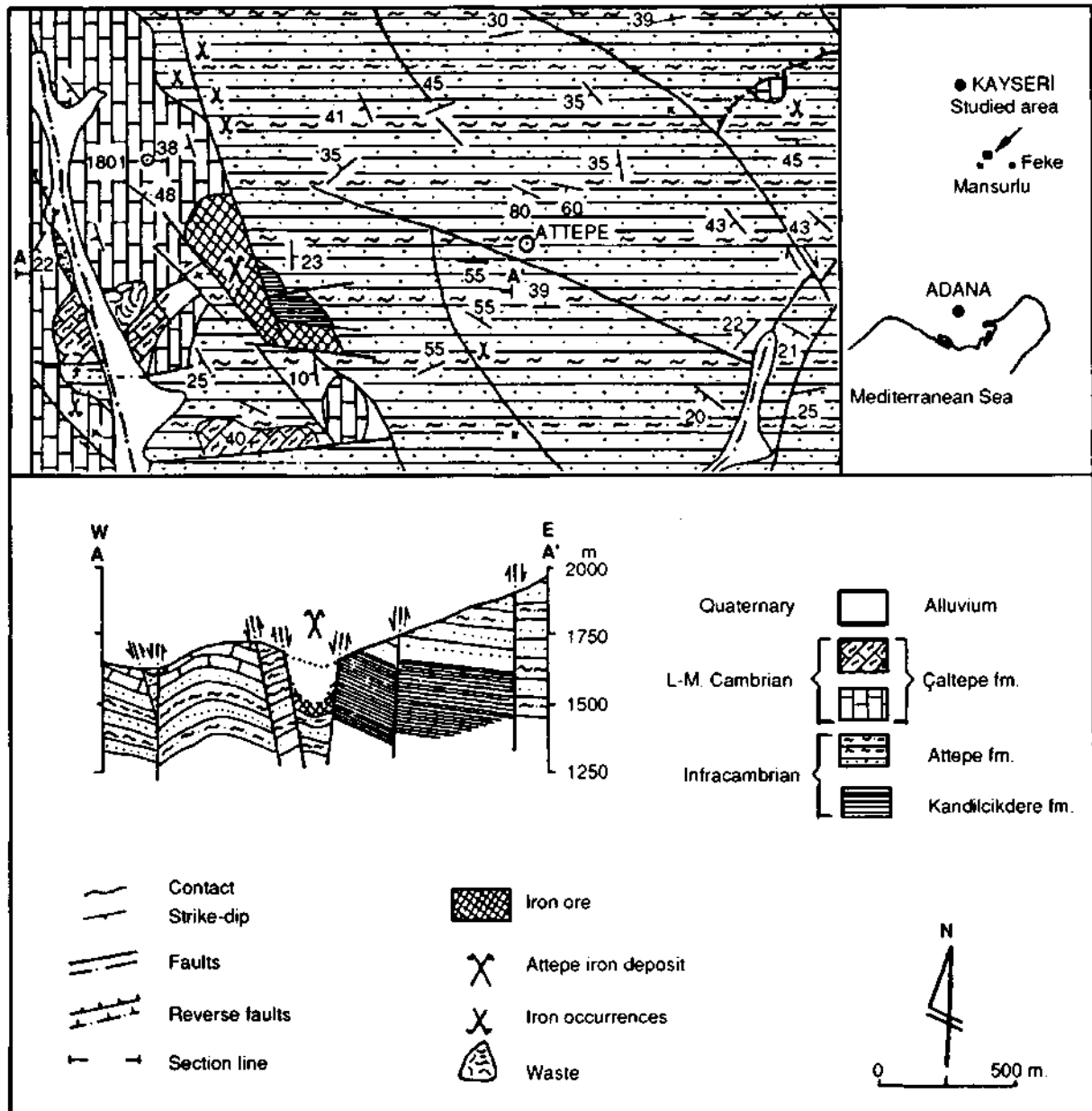


Fig. 1 - Geological map and cross-section of the study area. Scale is the same for both.

FIELD OBSERVATIONS

In the study area, there are two groups of pyrite occurrences in the shales and phyllites of the Kandilcikdere formation: Sedimentary pyrites, and pyrites in the siderite veins. These are differentiated on the basis of ore geometry, relationship to hostrock, mineral paragenesis and some syngedimentary features.

Sedimentary pyrites occur mostly as layers, groups of laminae, lenses, diagenetic injection drops and veins, individual grains in "disseminated" patterns (Fig. 2). Almost all pyrite-bearing layers and laminae of a few mm to 5 cm. in thickness alternate with the hostrocks. Black layers with high amounts of organic material contain, in most cases, fine-grained, disseminated pyrite crystals. On the other hand, light gray layers composed of mostly calcite have more coarse-grained pyrite.

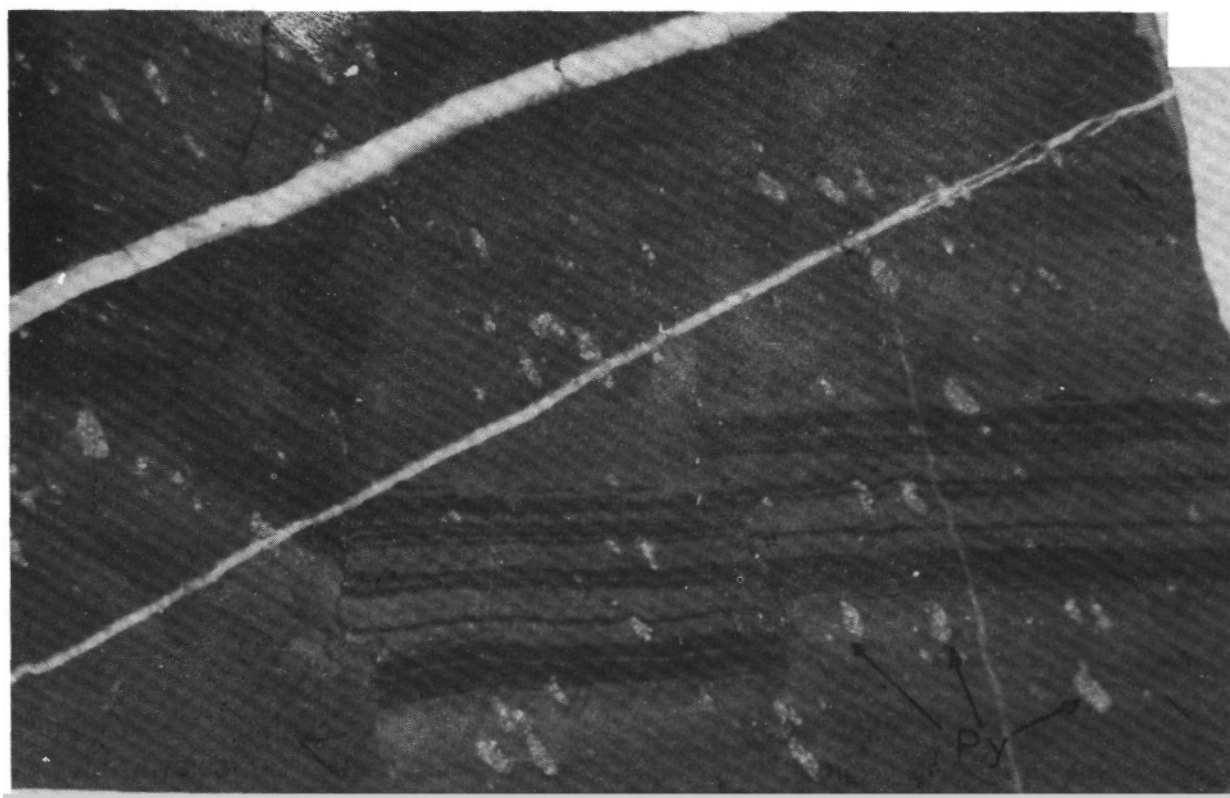


Fig. 2 - Relations between pyrite-bearing laminae and injection drops in shale.

Although some of the pyrite-bearing layers or groups of laminae show bedding, others appear disturbed so that the bedding is partly obliterated by the syndepositional and syndiagenetic deformation processes. In addition, all of the rocks have undergone low grade metamorphism and tectonism.

The pyrite-bearing rocks display many sedimentary features such as bottom to top features, rhythmicity, microcross-lamination, slump folding, diagenetic load casts, lenticular bedding, various other geopetal fabrics, plastic deformation fabric and diagenetic fissure fillings.

A typical feature of all pyrite-bearing layers is their distinctively shaped lower and upper surfaces. Most of the lower surfaces of most layers or groups of laminae are irregular. These are the result of submarine currents and load cast formation. Continuous or occasional submarine currents and compaction periods must have caused mechanical and partly chemical erosion on the yet hydroplastic mud like beds and laminae. This may be the reason of the irregular nature of their lower surfaces. Such curved surfaces were progressively deepened through the loading effects of the overlying sediments such as intensive pyrite accumulations. The overlying laminae were placed both unconformably and conformably on the underlying pelitic constituents, where some pyrite assemblages have a lateral and vertical graded bedding through carbonaceous pelitic and carbonate materials.

Laminated portions of pelitic rocks containing pyrite grains of variable size show differently shaped microfolds. These microfolded laminae imply a deformation stage connected with lateral gravity vectors and horizontal compression (Zimmermann and Amstutz, 1964). All primary depositional structures have undergone, to a certain degree, some diagenetic-tectonic processes.

Late calcite veins crosscutting the earlier structures indicate two stages of tectonic activities and calcite fillings. Diagenetic vein fillings are easily distinguishable from post diagenetic cracks and fillings, which cut earlier structures and layers over considerable distances.

PETROGRAPHICAL STUDIES

Sedimentary pyrites

Individual euhedral pyrite grains are widespread especially, in black shales, but in most cases they form coarse-grained crystals in calcite-rich portions of shales, diagenetic injection drops and vein fillings. Most of the pyrites are euhedral to subhedral. They appear dominantly as cubes and, to a lesser degree as pyritohedral and octahedral forms illustrated by Love and Amstutz (1966), and, Zimmermann and Amstutz (1973). Their grain size ranges from 20 μ m to 2 mm. Some of the large euhedral pyrite grains were replaced by calcite along crystal surfaces and show a remarkable zonation. The etching tests and different reflectivity values of pyrites reveal such zonation, being a result of overgrowth on the previously formed pyrite grains (Fig. 3). Their central parts contain numerous inclusions and replacement products of gangue materials and opaque minerals such as pyrrhotite, chalcopyrite and sphalerite, whereas most of their zoned peripheral portions are quite pure. This case indicates the presence of different stages taking place during diagenesis. These are more likely diagenetical overgrowths. However, they could also form by the gradual transformation of depositional pyrites to euhedral pyrite grains. A similar formation mechanism of pyrites was described by Udubasa (1984) for the iron sulfides in the black shales from Romania.

Framboidal or ring-like pyrites were observed either in the voids of massive pyrite populations or in very few laminae including populations of carbonate intraclasts, tiny individual pyrite grains, detritic quartz, zircon and tourmaline grains. The nuclei of these spheres are represented mainly by fragments of quartz and pelitic rocks as well as by leucoxene. Pyrite rings are composed of tiny, euhedral pyrite crystals with a grain size of 0.1 mm. Their crystal habit is more frequently cubic. Since the aforementioned-spherical forms occur in the same horizon with detritic minerals such as quartz and zircon, they could be related to the submarine currents caused to develop an envelope of pyrites around nonpyritic materials by rotational movements. The pyritic portions have undergone subsequently a diagenetic recrystallization which is connected with the burial grade varying from shallow to deep.

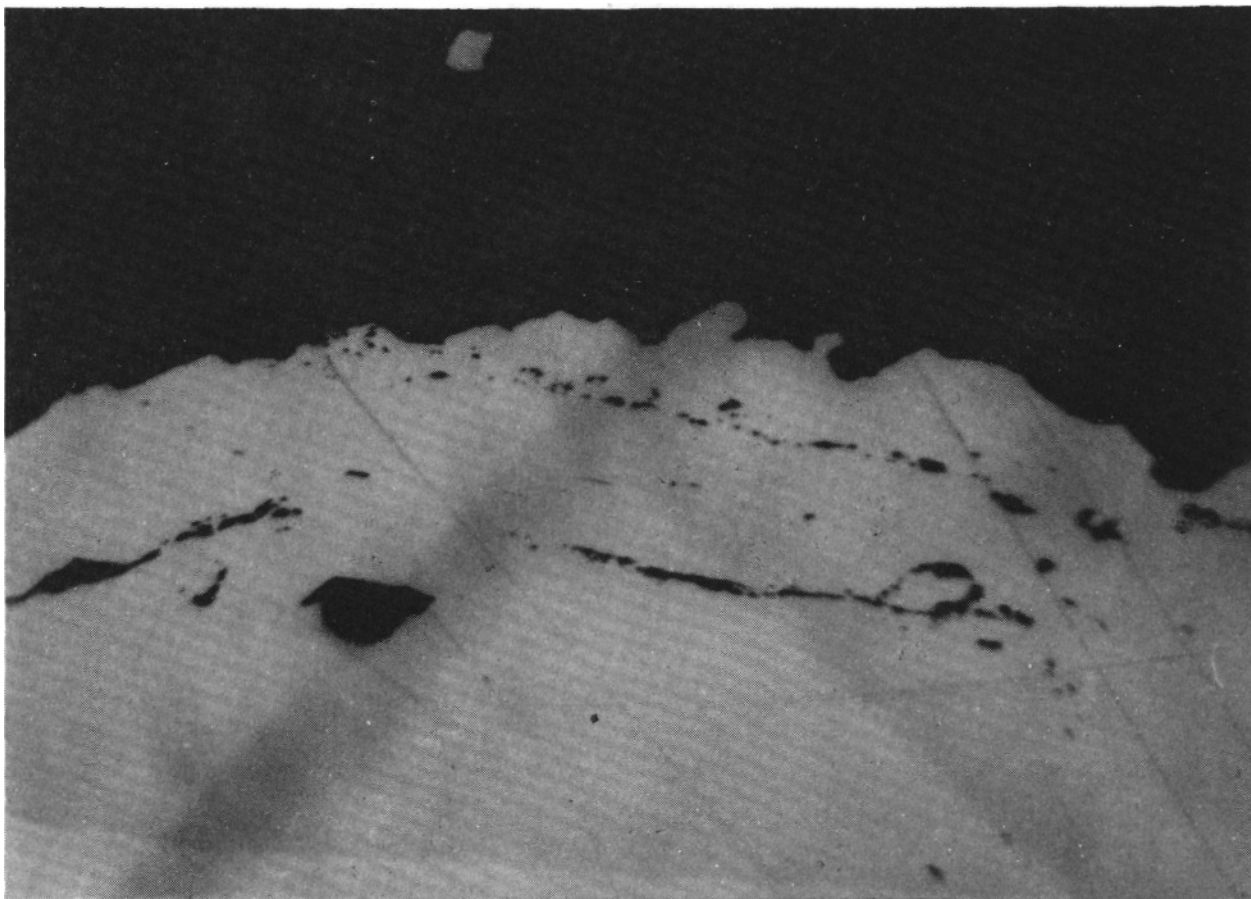


Fig. 3 - Zonation of pyrite crystals. Polished Section, //N, 32 X, in immersion oil.

The great amounts of framboidal pyrites formed between densely packed large euhedral pyrite grains, which grew during diagenetic recrystallization (Fig. 4). Pyrite spheres range from 50 to 200 μm . Their external outlines are relatively even. Microcrystals of pyrite spheres are euhedral to subhedral in habit. They are mostly loosely packed and originated through progressive modification of a colloid of iron monosulphide associated with an organic component into a sized sphere (Kalliokoski, 1965; Love and Amstutz, 1966; Chauhan, 1974).

Pyrite veins and diagenetic injection drops associated with calcite exhibit some explicit characteristics. Pyrites found near the wallrock occur not only as large single euhedral crystals, (Fig. 5) but also as twins and polycrystals packed closely in the sense of Love and Amstutz (1966). They are oriented partly parallel to the long axes of veins. But some euhedral pyrites are irregularly grown on the wallrocks.

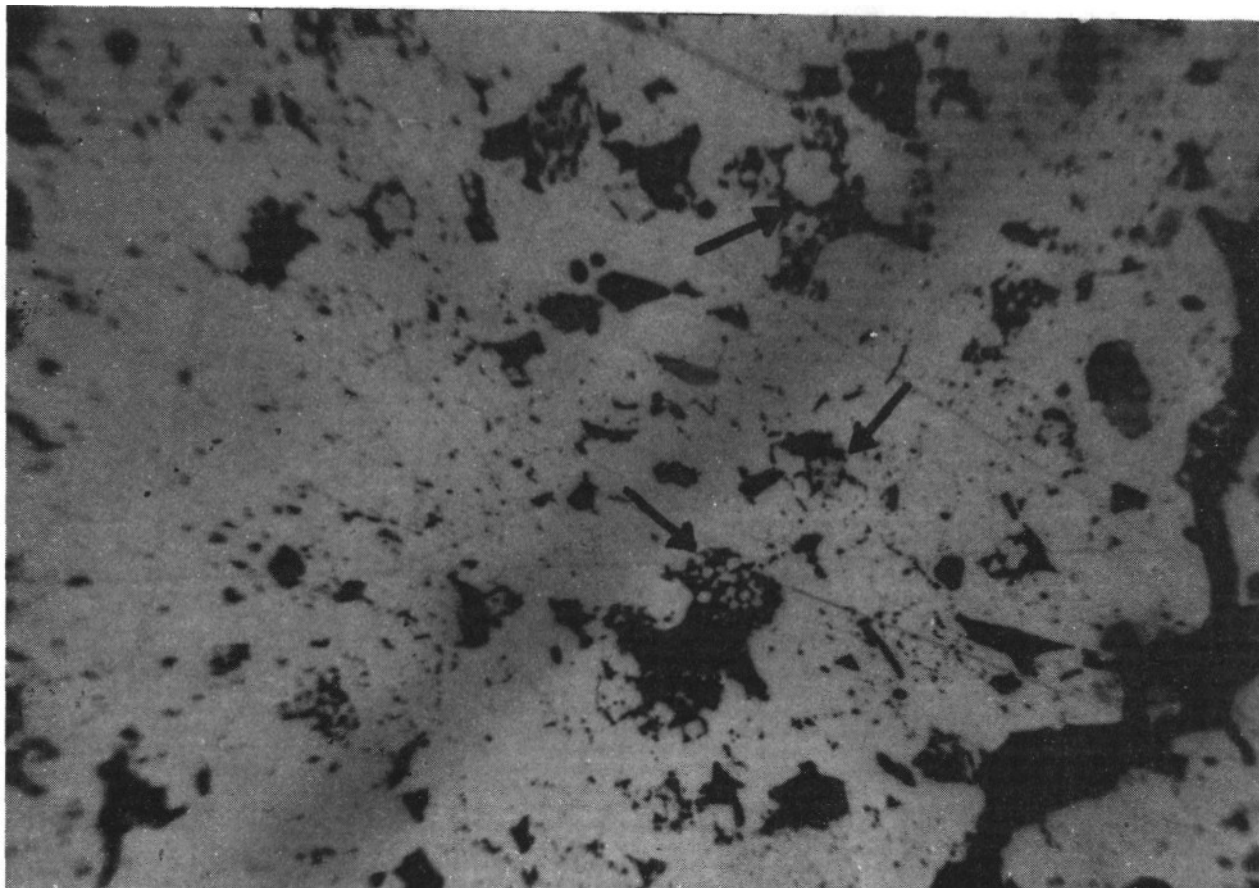


Fig. 4 - Framboidal pyrites (mostly at the center) in the gangue minerals between euhedral pyrite crystals. Polished section, //N, 32 X, in immersion oil.

Drop-like forms defined for the first time in this study are essentially precompactional features, because they do not cut cross shale laminae, and laminated carbonaceous shales found above or below these injection drops give rise to a geopetal fabric. Thus, it is considered that iron-bearing solutions migrated into syntectonically formed deformation places during an early stage of compaction. In contrast to these, pyrite veins cut across all laminae during the postcompactional stage.

Although this region has undergone low grade metamorphism, possibly during the Mesozoic (Küveli, 1991), numerous examples of depositional or early micro-structures were preserved in the pyrite occurrences. According to McClay and Ellis (1983), such structures can be preserved during metamorphic grades up to the mid-upper greenschist facies.

Carbonaceous laminae contain very frequently tiny dispersed pyrite grains arranged conformably to the general strike direction of laminations and foldings. There is a close relation between the above-mentioned laminae and overlying large individual pyrite crystals creating load cast structures (Fig. 6). According to Chauhan (1974), these are diagenetic load casts in which the underlying still hydro-plastic laminations are pressed down due to the force of growing crystals and their higher specific gravity. Fine pyrite crystals in the shales are thought to have formed post depositionally during early diagenesis (Schieber, 1985).

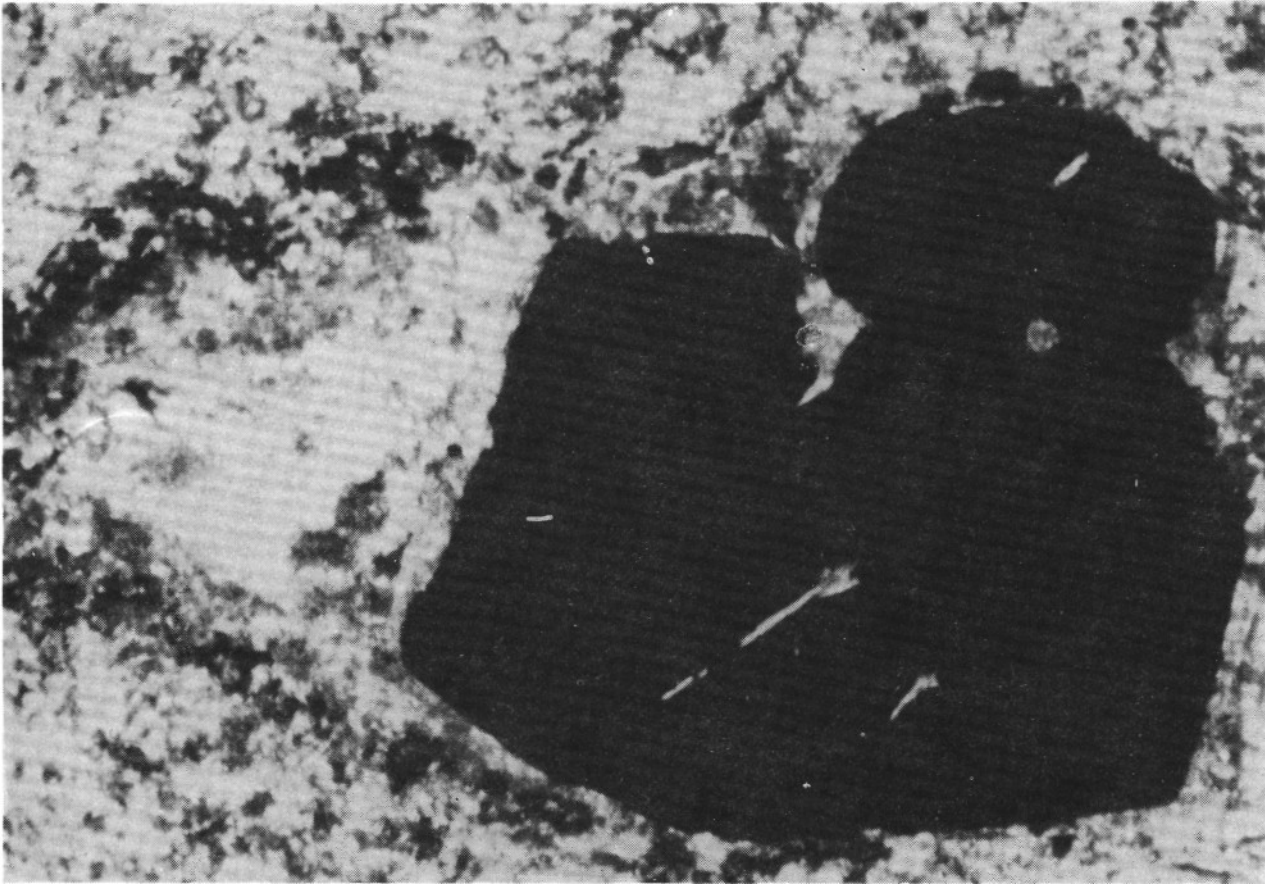


Fig. 5 - A view of a diagenetic injection drop, Pyrites (Black, at the right half) and calcite in fillings (White, in the left half). Thin Section, //N, 6 X.

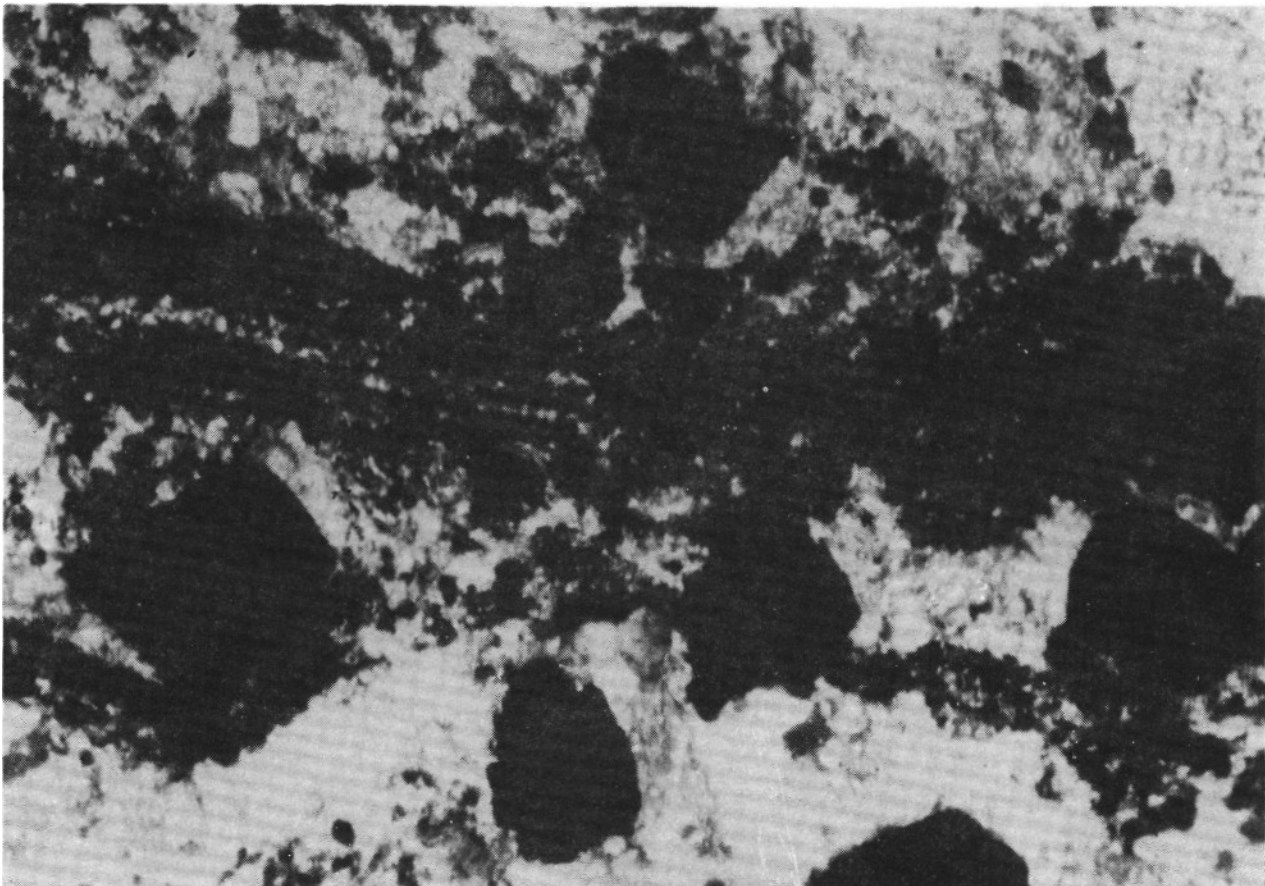


Fig. 6 - Load cast structure between a large pyrite crystal (Black) and an underlying pyrite-bearing lamina (Black, near left corner). Thin section, //N, 32 X, in immersion oil.

Some lenses are composed of rhythmic pyrite and calcite bands. Calcite and, in part, quartz crystals, have grown vertically to the pyrite bands. This rhythmicity resembles that of diagenetic crystallization rhythmites described by Amstutz (1977), Fontbote et al. (1981), Fontbote and Amstutz (1983).

Some large euhedral pyrites appear to be broken partly by intraformational brecciation, and partly to the compaction pressure. The latter were cemented with fibrous calcite.

Pyrites in siderite veins

Siderite veins contain massive pyrite and tetrahedrite bands fractured to varying degrees. Massive pyrite bands show perfectly grown euhedral crystals facing hostrocks and tetrahedrite bands (Fig. 7). Besides these,

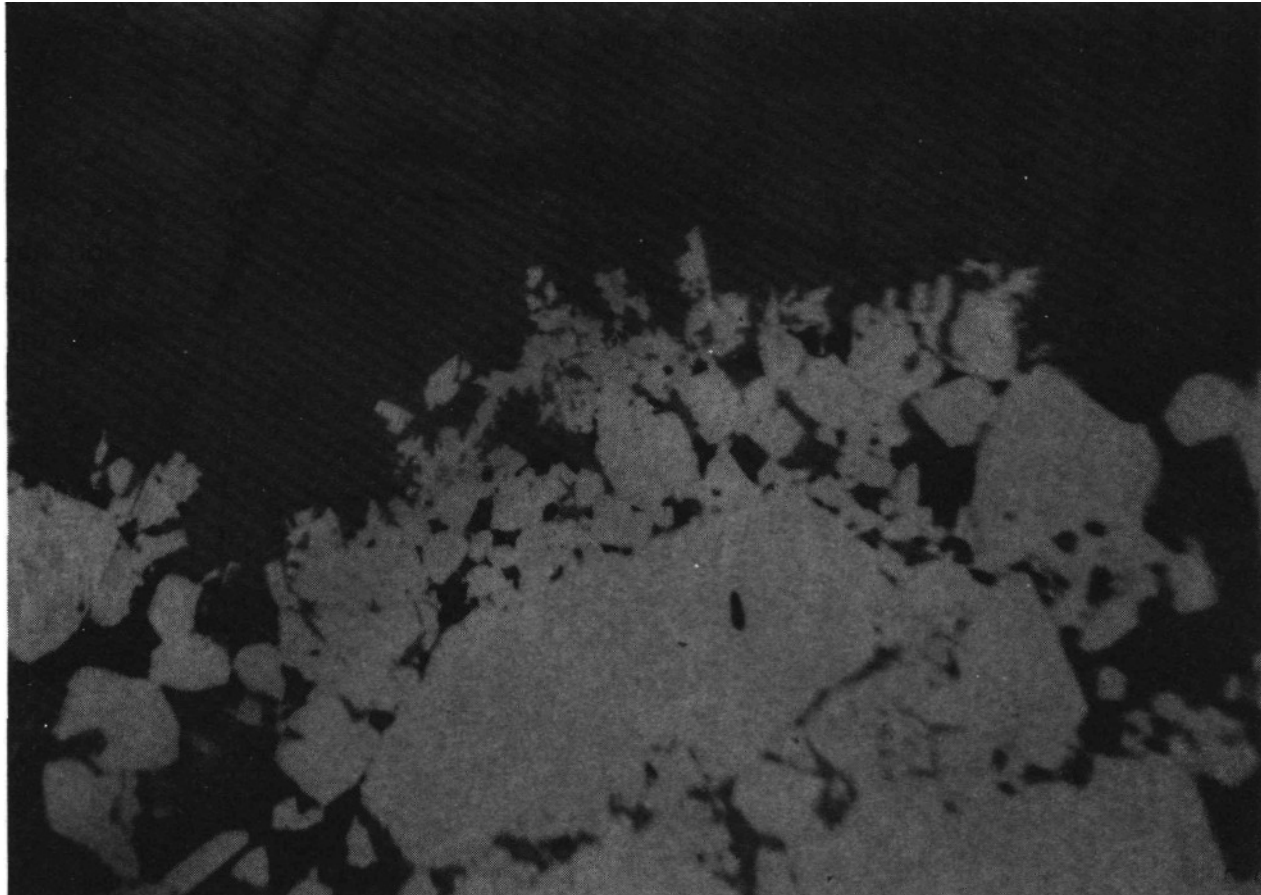


Fig. 7 - Some euhedral crystals of a massive pyrite band (Lower part) grown toward a tetrahedrite band (Upper part). Polished Section, //N. 32 X, in immersion oil.

single euhedral pyrites were observed in the gangue minerals found in the massive pyrite bands. Tetrahedrite, being of a younger generation than pyrite, is formed as bands and infillings between pyrite grains (Fig. 8).

Massive pyrites as well as siderites were fractured due to the brittle behavior of both minerals. This led in part to replacements by other constituents.

Chalcopyrite is very common among pyrite grains, along the boundaries of siderite and opaque minerals, and in the fissures of pyrite and tetrahedrite assemblages.

The second generation of pyrite was formed in the fractured portions of tetrahedrite as fine grains and in the colloform texture.

All siderites which exhibit coarse grains filled entire cavities and fractures. As a latest generation of deposition in siderite veins, small veins contain quartz, and the second generation of siderite cuts across previously formed minerals and features.

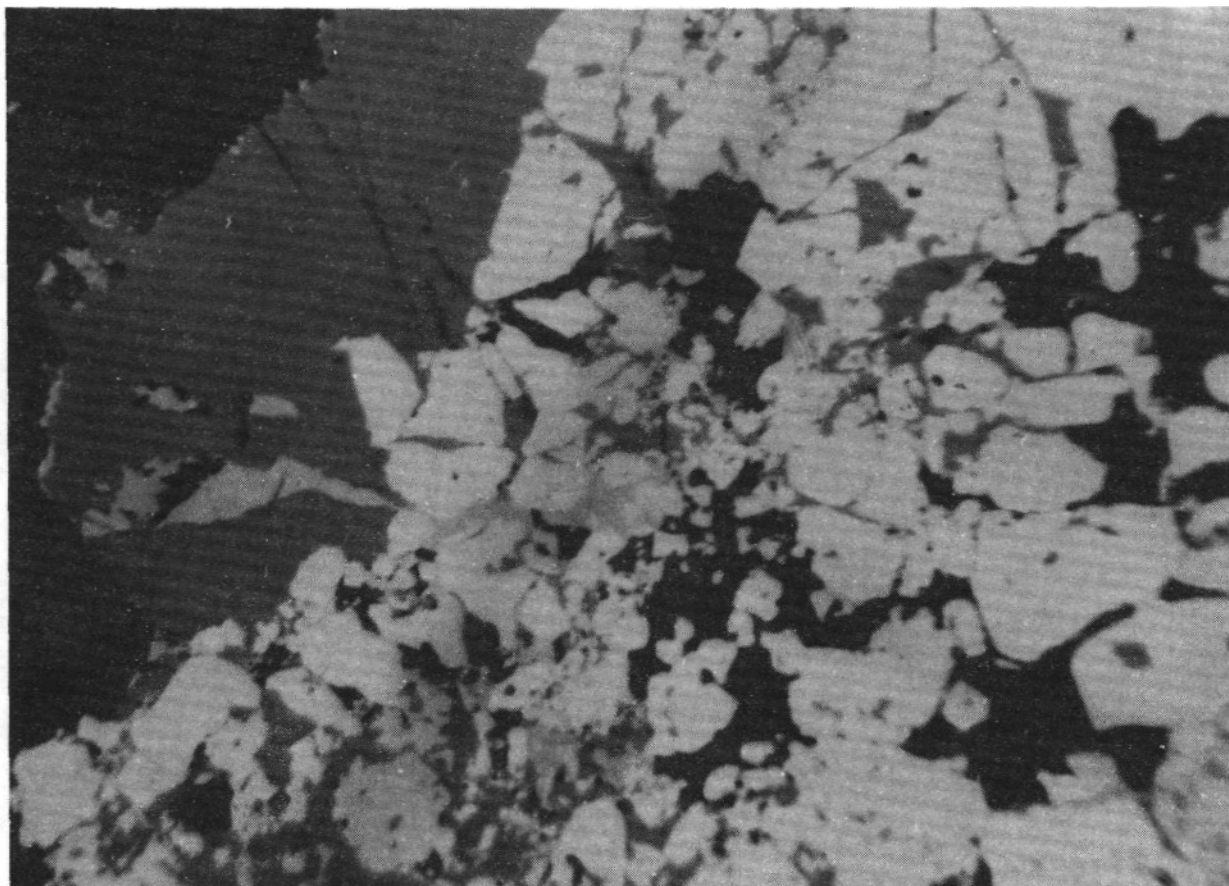


Fig. 8 - Infillings of tetrahedrite (dark gray) between pyrite grains (white). Siderite (black). Polished Section, //N, 32 X, in immersion oil.

GEOCHEMISTRY

Pyrite samples taken from massive pyrite layers, individual pyrites, pyrite populations and diagenetic injection drops of sedimentary pyrite occurrences and siderite veins were analyzed by a model ARL Sema-semq. Molybden microprobe in the Mineralogical-Petrographical Institute at the University of Heidelberg in Germany. The results of the minimum and maximum values of major and minor elements of pyrites are given in Table 1.

Table 1 - Microprobe results measured on different pyrites (%)

		<i>Fe</i>	<i>S</i>	<i>Cu</i>	<i>As</i>	<i>Sb</i>	<i>Co</i>	<i>Ni</i>	<i>Se</i>	<i>Hg</i>
1. Pyrites in siderite veins	max.	43.474	51.806	0.679	2.523	0.407	0.020	0.038	0.136	0.241
	min.	42.250	50.016	0.033	0.333	Tr	Tr	Tr	Tr	Tr
2. Massive pyrite layers	max.	46.382	54.051	0.123	0.157	Tr	Tr	0.060	0.040	Tr
	min.	45.537	52.355	Tr	Tr	Tr	Tr	Tr	Tr	Tr
3. Single euhedral pyrites	max.	45.172	53.578	0.074	0.094	Tr	0.465	0.079	0.067	-
	min.	43.881	51.108	Tr	Tr	Tr	Tr	Tr	Tr	-
4. Diagenetic injection drops	max.	44.299	53.304	0.049	0.115	Tr	Tr	0.121	0.043	0.138
	min.	41.160	51.845	Tr	Tr	Tr	Tr	0.022	Tr	Tr

1. Hydrothermal pyrites

2, 3, 4. Sedimentary pyrites

The results of pyrite analyses were evaluated within each group and were compared. As shown in Table 1, pyrites of siderite veins contain higher Cu, As, Sb, Hg and Se values, but lower Fe and Ni values than the sedimentary pyrite. However, Cu, As, Sb, Co, Se and Hg contents of most of the latter group samples were below detection limits.

High values of As, Sb and Cu in pyrites from siderite veins show a similar trend as the major element contents of associated tetrahedrite minerals. Therefore, it is proposed that pyrites and tetrahedrites in siderite veins may have been originated from similar sources.

The individual pyrite grains have distinctive As contents. Although this content increases up to 2.52 % around the pyrite cores, it decreases toward peripheral zones. This can be related to the character of ore-bearing solutions or a gradual change of physico-chemical conditions. On the other hand, there is a negative correlation between Fe and As. In these pyrites, As, Ni, Se values increase from the centre to the crystal edge; however, Fe and S contents decrease in the same direction. As and Ni contents of four sedimentary pyrite members have distinctive geochemical features. Massive pyrite layers among them contain a relatively high Fe value. But, they have low Se values.

Pyrites in diagenetic injection drops have a higher Ni content. This fact may indicate a mobilization and concentration of material, perhaps, derived from pelitic rocks and related to the zonation as described above.

The chemical composition of fahlore is shown in Table 2. This mineral has 8.8-11.5 % As and 14.6-15 % Sb. Based on the amounts present of both elements, it can be defined as tetrahedrite. This mineral, also includes considerable amounts of Bi, Se and Hg.

Table 2 - Chemical Composition of the tetrahedrite from siderite veins (%)

	S	Fe	As	Sb	Cu	Bi	Se	Hg
mm.	24.212	6.064	8.841	14.621	43.543	Tr	0.236	Tr
max.	26.925	7.207	11.571	15.026	38.728	0.481	0.269	0.301

The other main type of pyrite is represented by the occurrences in siderite veins. From the point of mineral paragenesis ore geometry, minor and trace element contents the origin of the pyrites associated with tetrahedrite may perhaps be called hydrothermal. But no magmatic activity is known in this area. The nearest volcanic center is found in the Erciyes Mountain, 80 km. from Attepe, and its volcanism began in late Miocene (Baş, 1986). The young Erciyes volcanism cannot have given rise to these sulfides and siderites. The conglomerates of the Zebil Formation in early Miocene contain some pebbles of sideritic formations in the neighboring area (Küpeli, 1991). Therefore, the ore-forming minerals may perhaps be deposited by other hydrothermal processes, between post Cretaceous and pre Miocene time.

After uplifting of the study area At the beginning of Miocene time, siderite veins were altered to the secondary iron minerals by the effects of multikarstification processes (Ayhan and Küpeli, 1991).

CONCLUSIONS

The present study of the pyrite occurrences showed that two basic genetic groups of pyrites can be distinguished; they are, the sedimentary pyrites, and the pyrite-bearing siderite veins.

Sedimentary pyrite occurrences formed syngenetically in shales and phyllites associated with carbonaceous matter, exhibiting various depositional and diagenetic features. Pyrites having different crystal habits are related to the various stages of sedimentary processes. Small isolated euhedral to subhedral pyrite grains must have occurred during precipitation and early diagenetic stage. However, the largest crystals found, "in most cases, in calcite-rich portions have undergone diagenetic recrystallization. Diagenetic injection drops and small veins were created during the compaction stage by the migration of iron sulfide-bearing solutions upwards into syntectonically formed deformation places. Those can be termed diagenetic remobilization deposits. Subsequently the pyrites were cemented by sparry calcites. Calcium carbonate was derived primarily from dissolution of marine organisms.

In most cases, pyrite layers and laminae occur for the most part, conformably in pelitic rocks; however, they sometimes show discontinuity. In addition, there are some layers containing ring-shaped pyrites and detritic constituents. All these data imply the effects of subaqueous currents and mechanical erosion.

All field and laboratory investigations showed that alldepositional features were produced by the repetitive precipitation under calm, but occasionally active regimes With the availability of reactive iron minerals, dissolved sulphate, organic matter and H₂S (Berner, 1970; 1979; 1984).

The sedimentary pyrites discussed in this paper are Precambrian in age. With this age, it is the oldest sedimentary ore deposit of Turkey.

ACKNOWLEDGEMENTS

The authors are grateful to Yurdal Genç, of the Mineralogic-Petrographic Institute of Heidelberg, for the help in performing the microprobe analyses.

Manuscript received January 15, 1992

REFERENCES

- Amstutz, G.C., 1977, Ore rhythmities: Process report-Ilrd ISMIDA, Leoben, Abstract, 43-44.
- Ayhan, A. and Küpeli, Ş., 1991, Batı Zamanı (Aladağlar) kurşun-çinko yatakları ile Mansurlu (Feke-Adana) demir yataklarının karşılaşmaları: Ahmet Acar Geology Symposium, Yetiş., C., Ed., 43-54, Adana.
- Baş, H., 1986, Erciyes Dağı volkanitlerinin özellikleri: SÜ Müh.-Mim.Fak. Derg., .1,1, 29-44.
- Berner, R.A., 1970, Sedimentary pyrite formation: Amer. J. Sci., 268, 1-23.
- _____, 1979, Authigenic iron sulfides as paleosalinity indicators: J. Sed. Petrol, 49, 4, 1345-1350.
- _____, 1984, Sedimentary pyrite formation: An update Geochem. Cosmochim. Acta, 48, 605-615.
- Chauhan, D.S., 1974, Diagenetic pyrite from the Lead-Zinc deposits of Zawar, India: Mineral Deposita, 9, 69-73.
- Fontbote, L; Amstutz, G.C. and Samaniego, A., 1981, Zur faziellen Stellung und zum diagenetischen Kristallisations-Prozess von Erzmineralien in schichtgebundenen Zn-Pb Lagerstätten (am Beispiel von San Vicente, im zentralen Peru): Proc. 7. Geowiss-Lateinamerika Koll., Heidelberg, 1980, Zbl. Geol. Palaont., Jg. 1981, 1, 465-477.
- and, 1983, Analyses of diagenetic crystallization rhythmities in strata-bound Pb-Zn-(Ba-F) deposits in the Triassic of Central and Southern Europe: Schneider, H.G. and Klemm, U.D.. Eds, Mineral deposits of the Alps and of the Alpine Epoch in Europe, Springer, 347-358.
- Kalliokoski, J., 1965, Framboids-macrocrystals of colloidal pyrite Abstract in Econ. Geol , 60, 1562.
- Küpeli, Ş., 1991, Attepe (Mansurlu-Feke) yöresi demir yataklarının jeolojik, petrografik ve jenetik incelemesi: Ph. D. Thesis, University of Selçuk department of Branch of Science Institute, 227, (unpublished), Konya.
- Love, L.G. and Amstutz, G.C., 1966, Review of microscopic pyrite from the Devonian Chattanooga shale and Rammelsberg Banderz: Fortschr. Miner. 43, 2, 273-309
- McClay, K.R. and Ellis, P.G., 1983, Deformation and recrystallization of pyrite: Mineralog. Mag. 47, 527-538.
- Schieber, J., 1985, The relationship between basin evolution and genesis of stratiform sulfide horizons in Mid-Proterozoic sediments of Central Montana: Ph. D. Thesis, Univ of Oregon.
- Udubaşı, G., 1984, Iron sulfides in sedimentary rocks, Some occurrences in Romania: Wauschkuhn, A., Kluth, C. Zimmermann, R.A., Eds, Syngeneses and epigenesis, Springer, Berlin-Heidelberg, 28-35
- Zimmerman, R.A. and Amstutz, G.C., 1964, Small scale sedimentary features in the Arkansas barite district: Amstutz, G.C. and Bernard, A., Eds. Sedimentology and Ore Genesis: Developments in Sedimentology, Elsevier, Amsterdam, 3, 157-163.
- _____and_____, 1973, Relations of sections of cubes, octahedra and pyritohedra N Jb Mineral Abh 120, 15-30.

GEOCHEMICAL DATA OF PAYAS (HATAY) KARSTIC MINERALIZATION ON THE ASPECTS OF THEIR SOURCES

Şükrü KOÇ** and M. Ali DEĞER***

ABSTRACT.- On the bases of geochemical properties and lithostragraphic location of the Payas mineralization region can be differentiated into three groups: 1- Limestone wall rock represents by Paşanın Eğreği plateau, Saryokuş Mağarabaşı site and Kozlu dere appearances. 2- Sandstone wall rock represents by Findik plateau-I appearances. 3- Iron enrichment serpentinite wall rock represents by Findik plateau-II appearances. According to the results of chemical analyses of these three groups Fe, Ca, and P elements are behaviour together, Al, Si, Ti and K elements group behave parallel to other group formation. The elements which have parallel behaviour distribute reversibly with each other. This situation indicates two different genesis. The enrichment of iron in the mineralization is derived from ultrabasic rocks. The lateritic iron which is formed due to of ultrabasic rocks lateritization is transported and precipitated in karstic cavity forming the mineralization. The sources of aluminium can also be explained by the same way. However in order to give sufficient explanation more data is required.

DISTRIBUTION AND CHARACTERISTICS OF THE UPPER CRETACEOUS-TERTIARY AGED SMECTITES AROUND BURDUR

Emel BAYHAN*

ABSTRACT.- Clay fraction is extracted and clay minerals are examined in Upper Cretaceous-Tertiary aged sediments around of Burdur Lake. illite, chlorite, smectite and 14s-14_c mixed layer are identified. Major element analyses made and structural formulas are calculated belonging to monomineralic smectites. According to these results the present day minerals are octahedral (beidellite) and trioctahedral (Al-Fe saponite).

DISTRIBUTION AND CHARACTERISTICS OF THE UPPER CRETACEOUS-TERTIARY AGED SMECTITES AROUND BURDUR

Emel BAYHAN*

ABSTRACT.- Clay fraction is extracted and clay minerals are examined in Upper Cretaceous-Tertiary aged sediments around of Burdur Lake. illite, chlorite, smectite and 14s-14_c mixed layer are identified. Major element analyses made and structural formulas are calculated belonging to monomineralic smectites. According to these results the present day minerals are octahedral (beidellite) and trioctahedral (Al-Fe saponite).

PALEOGENE BENTONIC FORAMINIFERS OF NAMRUN (İÇEL) AREA

Niyazi AVŞAR**

ABSTRACT.- Systematic descriptions of the benthonic foraminifers of the Paleogene sediments around Namrun (İçel) area have been investigated and general stratigraphical records of the area have been given. The rock units of Upper Cretaceous, Paleogene and Neogene ages crop out in the study area. Upper Cretaceous sequence comprises ophiolitic materials which includes radiolarite, limestone blocks and flysch. Upper Paleocene (Ilerdian) sequence discordantly overlies the Upper Cretaceous unit, and it is composed of sandstone, marl and sandy-clayey limestones. The sandy-clayey limestones contain species of the foraminifera such as *Alveolina subpyrenaica* Leymerie, *Alveolina moussoulensis* Hottinger and *Alveolina varians* Hottinger. Lower Eocene (Cuisian) sediments conformably overlie the Ilerdian, and it is composed of sandstone, marl and clayey limestones. The clayey limestones of the Cuisian sequence comprise foraminifers such as *Alveolina* cf. *levantina* Hottinger, *Alveolina* cf. *violea* Checchia-Rispoli, *Alveolina multicanalifera* Drobne, *Nummulites globulus* Leymerie, *Nummulites partschi* de la Harpe, *Nummulites burdigalensis* (de la Harpe), *Lockhartia conditi* (Nuttall), and *Lockhartia hunt* Ovey. Middle Eocene (Lutetian) sequence overlies conformably the Cuisian sediments, and it is composed of clayey limestones which are soiled white, yellow and cream colored, and well bedded. In addition, the Lutetian sediments are represented by *Alveolina tenuis* Hottinger, *Alveolina frumentiformis* Schwager, *Alveolina stipes* Hottinger, *Alveolina munieri* Hottinger, *Nummulites uranensis* (de la Harpe), *Nummulites lehneri* Schaub, *Assilina exponens* (Sowerby), and *Sphzerogypsina globulus* (Reuss). The Lutetian sequence is discordantly overlain by the Neogene clayey limestone and conglomerates.

NEW RHINOCEROTIDAE FOSSILS IN BAYRAKTEPE (ÇANAKKALE)

Tanju KAYA***

ABSTRACT.- In the Bayraktepe area (Çanakkale) *Begertherium grimmii* (Heissig) and *Aceratherium* aff. *simorreense* (Lartet) are found in Sarpdere, and *Aceratherium* aff. *simorreense* (Lartet) and *Aceratherium* sp. are found in Dutiudere. On the basis of correlations with the Turkish and Eurasian forms, it seems that the Sarpdere forms are late Astaracian (late Middle Miocene) MN 8 (upper) in age, and the Dutiudere forms are late Vallesian (early Late Miocene) MN 10 in age. The paleoecological characteristics of the transported fossils indicate an open humid and warm forest with patches of bushes.

GEOLOGY OF THE ULUKIŞLA-ÇAMARDI (NİĞDE) BASIN

Ali ÇEVİKBAŞ* and Önder ÖZTUNALI

ABSTRACT.- The studied area is restricted by the Niğde group at the north, Bolkar group at the south and Ecemiş fault zone at the east. The Niğde group is composed of Aşığediği and Çamardı formations in the studied area. Üçkapılı granodiorite is intruded into all of these rock units. Yeniköy formation which consists of sedimentary rocks, overlies the Niğde group. The Bolkar group is made of Permian aged marbles and schists. The Alihoca ophiolite complex overlies this group with a tectonic contact. The Horoz granodiorite intrudes into the Bolkardağı marbles and quartz-porphyr dykes cut the ophiolitic rocks. The Aladağ group, which is located at the eastern part of Ecemiş fault, is composed of Akdağ and Gökbel formations. The Aladağ ophiolitic melange has a sedimentary contact with the carbonaceous rocks that forms the basement. The Aladağ ophiolitic nappe overlies the former with a tectonic contact. The Ulukışla-Çamardı Tertiary basin overlies many different tectonic units. The volcano-sedimentary and plutonic rocks which crop out at the north are developed on the Niğde massif sedimentary rocks cropping out at the south are developed on the Bolkardağı marbles and the volcano-sedimentary rocks of the central part, are developed on the Alihoca ophiolite complex. All the three sections came in conjunction with the Upper Eocene tectonic movements. The basement of the Tertiary basins starts with Bolkardağı marbles and Kalkankaya formation, which overlie the ophiolite complex with angular unconformity, at the southern section. It ends with Yağbağ and Kırkpınar formations. The Plio-Quaternary actual sediments cover these units. The rock units of Cretaceous to Middle Eocene are observed in the central section. This section is made of Kırkgeçit, Tabaklı, Ardıçlı, Hasangazi formations and their members. The Zeyvegediği anhydrite, which is diagenetic, overlies these units with angular unconformity. The Kurtulmuş, and Kızılöz formations, Ilıcadere basalt and actual sediments cover all the former units. North section also consists of Cretaceous to Middle Eocene rock units. This section is composed of Ömerli, Yeniköy, and Unlukaya formations, Başmakçı limestone, Karlık basalt, Alıçlı andesite, South and Çaykavak formations, Elmalı syenite-Porphyr, diabase dyke and Kaletepe trachyte. Finally, the Kaletepe trachyte cuts all of these units. Oligo-Miocene aged Fındıklı formation covers them with an angular unconformity and proceeds with Miocene Burç formation. It ends up with Çanaktepe formation. Havuzlu tuffite, Gökbez formation, İkiztepe ignimbrite and actual sediments at the top. The basin has experienced three different compression stages, which occurred in Upper Eocene-Lower Oligocene, Upper Miocene and Upper Pliocene.